



TECHNICAL UNIVERSITY OF CRETE
SCHOOL OF MINERAL RESOURCES ENGINEERING
PETROLEUM ENGINEERING MASTER COURSE

**Gas Hydrate Formation in Oil/Gas Pipelines:
Computer Implementation of
Hand Calculation Methods with MATLAB**

MASTER THESIS
Niki Dimou

SCIENTIFIC ADVISOR
Prof. Nikos Pasadakis
Dr. Dimitris Marinakis

CHANIA
FEBRUARY 2020

*A thesis submitted in fulfillment of the requirements for the
Master degree of Petroleum Engineering in the
School of Mineral Resources Engineering
Technical University of Crete*

*The MSc Program in Petroleum Engineering of the Technical University of Crete,
was attended and completed by Ms. Niki Dimou, in the context of
the Hellenic Petroleum Group Scholarship award.*

ACKNOWLEDGEMENTS

The present thesis was prepared at the School of Mineral Resources Engineering of the Technical University of Crete under the supervision of Prof. Nikos Pasadakis and Dr. Dimitris Marinakis. With this thesis, my studies in the field of Petroleum Engineering are completed, so I would like to express my thanks to the people who supported me in this endeavor.

First of all, many thanks to my supervisor, Prof. Nikos Pasadakis, Petroleum Engineering MSc Course coordinator, for the opportunity he gave me to participate in the specific postgraduate programme, as well as for the provision of the Multiflash KBC's simulation software. I would also like to thank my scientific advisor, Dr. Dimitris Marinakis, Laboratory Teaching Staff, for his support both during the postgraduate studies as well as during the compilation of the thesis. I would like to thank him for the trust he showed in me and for recommending Mr. Konstantinos Roussis, Process Engineer of ASPROFOS S.A. assist me on technical and practical issues regarding my thesis. Many thanks to Mr. Roussis for his time and scientific guidance.

Many thanks are also due to the staff at MOTOR OIL (Hellas) Corinth Refineries S.A., for the provision of the data necessary which were used as case studies for the solution of the mathematical model, as well as for the time they spent. It was a great pleasure and honor that I worked again with the specific company in the context of my present thesis, after my internship in the Lubricants and Utilities Unit department in the summer of 2017. More specifically, I would like to thank Mr. Athanasios Theodorou, Lubricants Production and Utilities Section Head and Dr. Vangelis Oikonomopoulos, Chemical Engineer of the Technical Service department in MOTOR OIL.

I cannot thank enough Mr. Stergios Yiantsios, an excellent person and scientist, Professor of Transport Phenomena with an emphasis on Computational Fluid Dynamics, at the department of Chemical Engineering of Aristotle University of Thessaloniki. I am gratefully indebted for the time and advice on the part of modeling. I really appreciated his showing concern and providing an open and friendly environment required for the research, although I am a graduate of the department.

In the end, I would like to thank my family, and my friends, for their understanding and encouragement during the compilation of my thesis, which I wholeheartedly dedicate to my mother.

ABSTRACT

The present diploma thesis aims at the development and assessment of a computer program, based on the MATLAB programming language, implementing the "hand calculation methods" for gas hydrate formation conditions in oil and gas pipelines. The hand calculation methods examined in this project are the "gas gravity method" and the "distribution coefficient method" or the "K-factor method". The computer program predicts the hydrate formation conditions, having as input data the composition (or the specific gravity) of the mixture and an operating condition (pressure or temperature). In the gas gravity method the available charts were interpolated and reproduced numerically and the solution was obtained on basis of the bisection method. For the K-factor method the Newton-Raphson method was employed to obtain the solution. The hydrate deposits in oil and gas pipelines are a common problem in the upstreaming, midstreaming, and downstreaming processes of the oil and gas industry. In the present diploma thesis, Fuel Gas and LPG (Liquefied Petroleum Gas) streams from MOTOR OIL (Hellas) Corinth Refineries S.A. were examined to determine the hydrate formation conditions in transport pipelines within the refinery. The results, which were compared with commercial software such as KBC's Multiflash and CSMGem (CSM: Colorado School of Mines), showed that neither of the streams are at risk of forming solid hydrate crystals in the oil and gas pipelines.

ΠΕΡΙΛΗΨΗ

Η παρούσα διπλωματική εργασία στοχεύει στην ανάπτυξη και αξιολόγηση ενός υπολογιστικού προγράμματος, στη γλώσσα προγραμματισμού MATLAB, το οποίο υλοποιεί τις μεθόδους προσδιορισμού «με το χέρι» (hand calculation methods) των συνθηκών σχηματισμού υδριτών σε αγωγούς μεταφοράς πετρελαίου και φυσικού αερίου. Οι μέθοδοι που εξετάστηκαν στην παρούσα εργασία είναι η μέθοδος ειδικού βάρους (gas gravity) και η μέθοδος συντελεστών κατανομής (distribution coefficient) ή μέθοδος του K-παράγοντα (K-factor). Το πρόγραμμα προβλέπει τις συνθήκες σχηματισμού υδριτών έχοντας ως δεδομένα εισόδου τη σύσταση (ή το ειδικό βάρος) του μείγματος και μία συνθήκη λειτουργίας (πίεση ή θερμοκρασία). Στη μέθοδο ειδικού βάρους τα διαθέσιμα διαγράμματα αναπαρίστανται και αναπαράγονται αριθμητικά, και η λύση επιτυγχάνεται με τη μέθοδο διχοτόμησης του διαστήματος (bisection method). Για τη μέθοδο του K-παράγοντα χρησιμοποιείται η μέθοδος Newton-Raphson για την αριθμητική επίλυση. Οι επικαθίσεις υδριτών σε αγωγούς μεταφοράς πετρελαίου και φυσικού αερίου αποτελούν κοινό πρόβλημα των διεργασιών παραγωγής-εξόρυξης, μεταφοράς-αποθήκευσης, καθώς και διύλισης του πετρελαίου. Στην παρούσα διπλωματική εργασία εξετάστηκαν ρεύματα αέριων καυσίμων (Fuel Gas) και υγραερίου (LPG: Liquefied Petroleum Gas) της εταιρείας MOTOR OIL (Ελλάς) Διυλιστήρια Κορίνθου Α.Ε., για τον προσδιορισμό των συνθηκών σχηματισμού υδριτών σε αγωγούς μεταφοράς εντός του διυλιστηρίου. Τα αποτελέσματα, τα οποία συγκρίθηκαν με λογισμικά του εμπορίου, όπως το Multiflash της εταιρείας KBC και το CSMGem (CSM: Colorado School of Mines), έδειξαν ότι κανένα από τα ρεύματα δεν ενέχει τον κίνδυνο σχηματισμού στερεών κρυστάλλων υδρίτη.

CONTENTS

1. INTRODUCTION.....	1
1.1. Upstream, Midstream, and Downstream Activities.....	2
1.2. Transportation of Oil and Gas, and their respective Products.....	3
1.2.1. Oil and Gas Pipeline transportation: Classification and Current state.....	7
1.3. Flow Assurance.....	9
1.3.1. Organic and Inorganic Deposits.....	11
1.4. Hydrates.....	13
1.4.1. Hydrate Definition and Structure.....	13
1.4.2. Location of Hydrate Formation.....	16
1.4.3. Phase Behavior of Hydrocarbon Systems and Hydrates.....	17
1.4.4. Thermodynamic Equilibrium and Kinetics during Hydrates Formation.....	20
1.4.5. Prevention Methods.....	23
1.4.5.1. Heating.....	24
1.4.5.2. Pressure reduction.....	24
1.4.5.3. Inhibitors.....	25
1.4.5.4. Pigging.....	27
2. MATHEMATICAL MODELING.....	29
2.1. Hydrate Formation.....	29
2.1.1. The Gas Gravity Method.....	30
2.1.2. Joule-Thomson Charts - Hydrate Limits to Gas Expansion through a Valve.....	38
2.1.3. The Distribution Coefficient Method (The K-factor Method).....	43
2.2. Injection of Inhibitors.....	48
3. SIMULATION RESULTS.....	50
3.1. Assessment of the "Hand Calculation Methods" with Artificial Hydrocarbon Feeds..	51
3.2. Assessment of Motor Oil Streams.....	54
3.2.1. Fuel Gas.....	54
3.2.2. Liquefied Petroleum Gas (LPG).....	58
4. CONCLUSIONS.....	64
5. BIBLIOGRAPHY.....	66
6. APPENDIX.....	69
6.1. MATLAB Code - The Gas Gravity Method.....	69
6.2. MATLAB Code - The Distribution Coefficient Method (The K-factor Method).....	79

LIST OF FIGURES

Figure 1.1: <i>A four axis tank - wagon ((a): Gerding, 1986; (b): LLC «Express Logistics», 2020)</i>	3
Figure 1.2: <i>(a) CNG ship (Tractebel Engineering, 2015), and (b) LNG carrier (International Gas Union, 2018)</i>	4
Figure 1.3: <i>Tank tractor-trailers ((a): Gerding, 1986; (b): O'Connell, 2018)</i>	5
Figure 1.4: <i>Installation of underground pipelines (Natural Gas, 2013)</i>	6
Figure 1.5: <i>Trade flows worldwide in billion cubic meters (BP, 2016)</i>	8
Figure 1.6: <i>Pipelines in Europe (Information Technology Associates, 2017)</i>	8
Figure 1.7: <i>Natural Gas Pipeline System - Geophysical Map of Greece (Modification by DESFA, 2018)</i>	9
Figure 1.8: <i>Various organic and inorganic solids (Modification by Mullins et al., 2006)</i>	11
Figure 1.9: <i>Depiction of scale-blocking formation pores (Crabtree et al., 1999)</i>	12
Figure 1.10: <i>Form of methane hydrate ((a)&(b): Giavarini & Hester, 2011; (c): Mao et al., 2007)</i>	13
Figure 1.11: <i>(a) The inclusion or trapping of gas molecules in the gas hydrate lattice (Frenier et al., 2010), and (b) Gas molecules enclosed in the water cavities of the hydrate (Giavarini & Hester, 2011)</i>	14
Figure 1.12: <i>Various hydrate structures - clathrate polyhedral water cavities comprising sI, sII, and sH hydrates ((a): Frenier et al., 2010; (b): Mao et al., 2007)</i>	15
Figure 1.13: <i>Hydrate crystal unit structures: (a) sI, (b) sII, and (c) sH (Sloan & Koh, 2008)</i>	15
Figure 1.14: <i>A clathrate plug recovered from an offshore gas flowline of Petrobras Company (Mao et al., 2007)</i>	16
Figure 1.15: <i>(a) Precipitation regimes for hydrates, waxes, and asphaltenes (Frenier et al., 2010), and (b) Thermodynamic conditions of the flow assurance elements (Ahmed, 2007)</i>	18
Figure 1.16: <i>Precipitation regimes for hydrates formation (Tohidi, 2018)</i>	19
Figure 1.17: <i>(a) A typical phase diagram for a pure hydrocarbon - larger than methane (Modification by Giavarini & Hester, 2011), and (b) The hydrate formation regions for C₁ to C₄ paraffins (Sloan & Koh, 2008)</i>	20
Figure 1.18: <i>Lowering of the hydrate formation temperature by different inhibitors (Giavarini & Hester, 2011)</i>	27
Figure 1.19: <i>(a) Pipeline inspection tool (Natural Gas, 2013), and (b) Various types of pigs used in pipeline pigging operations (T.D. Williamson, 2020)</i>	28
Figure 2.1: <i>Gas gravity chart for prediction of three-phase (L_w-H-V) pressure and temperature (Sloan & Koh, 2008)</i>	30
Figure 2.2: <i>Gas gravity chart - Definition of turning points</i>	32
Figure 2.3: <i>Logarithm of pressure versus specific gravity for turning point A₁</i>	32
Figure 2.4: <i>Logarithm of pressure versus specific gravity for turning point A₂</i>	32
Figure 2.5: <i>Logarithm of pressure versus specific gravity for turning point A₃</i>	33
Figure 2.6: <i>Temperature versus specific gravity for turning point TA₃</i>	33

Figure 2.7: <i>Logarithm of pressure versus specific gravity for turning point A_4</i>	33
Figure 2.8: <i>Representation of Figure 2.1 - Hydrate locus using the gas gravity method</i>	36
Figure 2.9: <i>Conditions for hydrate formation for light gases (GPSA, 2004)</i>	36
Figure 2.10: <i>Representation of Figure 2.9 - Hydrate locus using the gas gravity method for light gases</i>	38
Figure 2.11: <i>Permissible expansion of (a) a 0.6, and (b) a 0.7 gravity natural gas without hydrate formation (Ahmed & McKinney, 2005)</i>	39
Figure 2.12: <i>Permissible expansion of (a) a 0.8, and (b) a 0.9 gravity natural gas without hydrate formation (Ahmed & McKinney, 2005)</i>	40
Figure 2.13: <i>Permissible expansion of a 1.0 gravity natural gas without hydrate formation (Ahmed & McKinney, 2005)</i>	40
Figure 2.14: <i>Vapor-solid equilibrium constants for (a) ethane, and (b) isobutane (Sloan & Koh, 2008)</i>	43
Figure 2.15: <i>Vapor-solid equilibrium constants for (a) methane, and (b) nitrogen (Sloan & Koh, 2008)</i>	43
Figure 2.16: <i>Vapor-solid equilibrium constants for (a) propane, and (b) n-butane (Sloan & Koh, 2008)</i>	44
Figure 2.17: <i>Vapor-solid equilibrium constants for (a) carbon dioxide, and (b) hydrogen sulfide (Sloan & Koh, 2008)</i>	44
Figure 3.1: <i>Results for methane - ethane mixtures</i>	52
Figure 3.2: <i>Results for methane - ethane - hydrogen sulfide mixtures</i>	53
Figure 3.3: <i>Average of mol rate of Fuel Gas composition</i>	55
Figure 3.4: <i>Fuel Gas hydrate formation conditions</i>	56
Figure 3.5: <i>Gas gravity method for operating pressure Fuel Gas $P=19.5\text{kg/cm}^2$</i>	56
Figure 3.6: <i>LPG composition of mass rate for Arabian Light and Arabian Medium distillation feeds</i>	59
Figure 3.7: <i>LPG hydrate formation temperature results for Arabian Light and Medium distillation feeds</i>	61
Figure 3.8: <i>LPG hydrate formation pressure results for Arabian Light and Medium distillation feeds</i>	61
Figure 3.9: <i>Gas gravity method for operating pressure LPG $P=2.96\text{kg/cm}^2$</i>	61
Figure 3.10: <i>Gas gravity chart for light gases for operating pressure LPG $P=2.96\text{kg/cm}^2$</i>	62

LIST OF TABLES

Table 1.1: <i>The advantages and disadvantages of railroad transport (Ilyeva & Andrianova, 2011)</i>	3
Table 1.2: <i>The advantages and disadvantages of water transport (Ilyeva & Andrianova, 2011)</i>	4
Table 1.3: <i>The advantages and disadvantages of automobile transport (Ilyeva & Andrianova, 2011)</i>	5
Table 1.4: <i>The advantages and disadvantages of pipeline transport (Ilyeva & Andrianova, 2011)</i>	6
Table 2.1: <i>The values of constants in equation (2.20) (Ahmed & McKinney, 2005)</i>	42
Table 2.2: <i>The values of coefficients A through S in equation (2.30) (Sloan & Koh, 2008)</i>	45
Table 2.3: <i>The constants of equation (2.34) for various inhibitors (Bai & Bai, 2010)</i>	49
Table 3.1: <i>Results for a mixture of 75% methane and 25% ethane ($\gamma=0.675$)</i>	51
Table 3.2: <i>Results for a mixture of 25% methane and 75% ethane ($\gamma=0.917$)</i>	52
Table 3.3: <i>Results for a mixture of 67.5% methane, 22.5% methane, and 10% hydrogen sulfide ($\gamma=0.725$)</i>	52
Table 3.4: <i>Results for a mixture of 22.5% methane, 67.5% methane, and 10% hydrogen sulfide ($\gamma=0.943$)</i>	53
Table 3.5: <i>Fuel Gas hydrate formation temperature results</i>	55
Table 3.6: <i>Fuel Gas hydrate formation pressure results</i>	56
Table 3.7: <i>LPG hydrate formation temperature results for Arabian Light distillation feed</i>	60
Table 3.8: <i>LPG hydrate formation pressure results for Arabian Light distillation feed</i>	60
Table 3.9: <i>LPG hydrate formation temperature results for Arabian Medium distillation feed</i>	60
Table 3.10: <i>LPG hydrate formation pressure results for Arabian Medium distillation feed</i>	60
Table 3.11: <i>LPG hydrate formation results of commercial software with (Case A) and without (Case B) the heavier components for Arabian Light distillation feed</i>	62
Table 3.12: <i>LPG hydrate formation results of commercial software with (Case A) and without (Case B) the heavier components for Arabian Medium distillation feed</i>	62

1. INTRODUCTION

The aim of the present diploma thesis is to develop a computational background for implementing the "hand calculation methods" for gas hydrate formation conditions estimation in oil and gas pipelines. Natural gas hydrates are solid, ice-like compounds of water and the light components of natural gas. They are organic scale deposits that develop in oil and gas pipelines and cause flow assurance problems.

In this project, initially the three major sectors of oil and gas industry are described, where the problem of hydrates deposits appear mostly. The methods of oil, oil products and gas transportation are outlined, with emphasis on pipeline transportation. The pipeline transportation is classified in oil and gas transportation. Maps from Greece, Europe and the world are provided to reflect the current state. In addition, the basic principles of flow assurance problems are analyzed, resulting from inorganic and organic scale deposits, such as asphaltenes, waxes, and hydrates. Furthermore, the problem of hydrate deposition is studied by presenting their chemical structure, phase behavior, conditions necessary for their formation, thermodynamic equilibrium and kinetics during hydrate formation. The phase behavior of other hydrocarbon systems is also highlighted, such as waxes and asphaltenes, in order to understand the complexity of these systems. Moreover, the locations where the problems of hydrates deposition appear, mainly in offshore drilling processes where the temperature is particularly low in combination with high pressure. Some prevention methods are listed for the elimination of hydrate deposits, such as the alteration of the operating conditions (where possible), or the use of an inhibitor, or the mechanical cleaning of the pipelines (e.g. pigging).

The mathematical modeling for predicting hydrate formation conditions was based on "hand calculation methods" and compared with thermodynamic models from well-established simulation software. More precisely, the "gas gravity method" and the "K-factor method" were used. For reasons of completeness, the Joule-Thomson charts are also mentioned, which mainly refer to hydrate limits to gas expansion through a valve. However, the latter method and the basic equation for calculating the amount of injection of inhibitors to avoid hydrate deposits are not applied in any case study in this work.

Finally, an assessment of the "hand calculation methods" with artificial hydrocarbon feeds and with Fuel Gas and LPG streams from the MOTOR OIL (Hellas) Corinth Refineries S.A. company was conducted. The results of the study are in accordance with commercially available software, such as KBC's Multiflash and CSMGem.

1.1. Upstream, Midstream, and Downstream Activities

Three major sectors comprise the oil and gas industry, which namely are: the upstream sector, the midstream sector and the downstream sector. The first one, the upstream sector, also referred to as the exploration or production (E&P) sector, represents the process through which the oil and natural gas is produced. It consists of searching the underground or underwater crude oil and natural gas fields, drilling of exploratory wells, and drilling and operating the wells that recover and bring to the surface the crude oil and/or natural gas. The processing of oil and gas, in addition to the upstream transport operations, all occur within this stage. The activities comprising the upstream offshore exploration and production are: exploration, reservoir engineering, drilling, field development, production, subsea pipe-laying, natural gas processing, and oil processing (Kassinis, 2015).

Midstream is the linking point where oil and gas produced from the upstream fields is processed and transported to the downstream markets. This sector encompasses natural gas liquefaction, oil and gas transport and shipping of LNG (Liquefied Natural Gas). Generally speaking, the midstream sector includes processes between the upstream and the downstream sector (namely transport and processing), and from the downstream sector to consumer markets (i.e. trading and shipping), including: natural gas liquefaction, LNG Plants, LNG shipping, pipeline transport of gas, and oil shipping and pipeline transport. Midstream processes comprise a separate and distinct branch of the petroleum industry, which includes processing, bulk storage, transportation (by pipeline, rail, or tanker vessel) as well as wholesale marketing/trading of hydrocarbon products. Midstream operations mainly involve storage, transportation, and trading (Kassinis, 2015).

Downstream relates to the point where processed oil and gas reach the final consumers, the industries and downstream markets, either directly or indirectly through the abundance of processed products. The downstream sector has to do with products and services, concentrating on fuels, lubricants and petrochemicals. The oil refinement and gas processing, the oil, gas, and petrochemical products manufacturing, the sales, marketing, and transportation of the products, in addition to the supply and trading of crude oil, petroleum, petrochemical products and connected services to wholesale and retail customers, all comprise the downstream sector. The downstream activities include: natural gas regasification process and plants, transmission and distribution, downstream utilization of natural gas (power generation, petrochemicals, gas to liquids), and oil refining and utilization (Kassinis, 2015).

1.2. Transportation of Oil and Gas, and their respective Products

An intricate transportation system is required to move oil and gas from a field to refining and processing plants and to move petroleum products from refineries to consumers. Inland waterway barges, railway tank cars, transport trucks, oceangoing tankers, crude oil and products pipelines, and gas transmission pipelines, all represent an integral part of the oil and gas transportation industry, which in its infancy utilized horse-drawn wagons to carry wooden barrels of oil to closeby streams. The more the industry grew, the more the transportation methods developed, and nowadays millions of barrels of crude oil, gasoline, fuel oils, and other petroleum products, in addition to billions of cubic feet of natural gas, are transported from the wellhead to the plant, from one refinery to another, from offshore to onshore, and from continent to continent to reach the final consumer (Gerding, 1986).

One of the first types of transportation was the one accomplished through railroads. Special tank-wagons or containers in covered wagons were and are still used for the transportation of oil, oil products and gases by rail. Table 1.1 lists the advantages and disadvantages of using railroad transport, and Figure 1.1 shows a tank - wagon for transportation of petroleum and light oil products.

Table 1.1: *The advantages and disadvantages of railroad transport (Ilyaeva & Andrianova, 2011)*

Advantages
1) The possibility of transportation all year round
2) Various loads (oil products) can be simultaneously transported in one train
3) Oil and oil products can be delivered to any point of the country, which has railway communication means
4) The speed of the loads delivery by rail is approximately two times higher than the river transportation speed
Disadvantages
1) High cost of the railway lining
2) The increase of loading of the existing railways and as a consequence the possible faults in transportation of other mass cargoes
3) Empty trips of the rail tank from the consumers back to the producers, which cause loss of profits and the senseless increase of road traffic

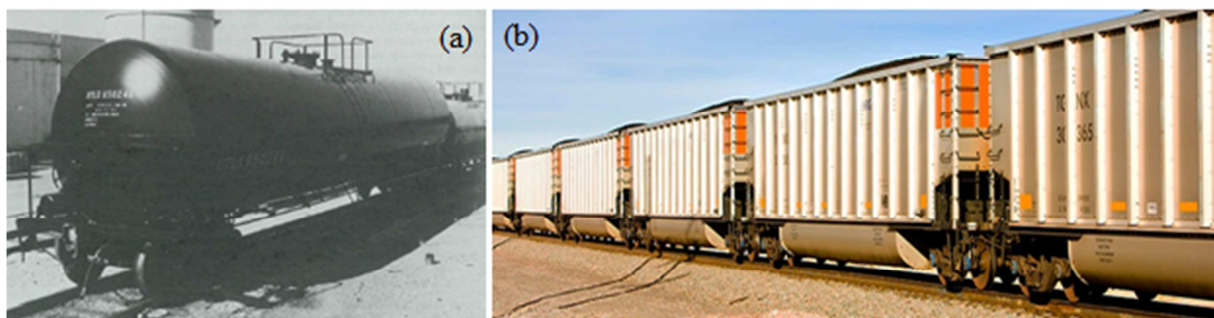


Figure 1.1: *A four axis tank - wagon ((a): Gerding, 1986; (b): LLC «Express Logistics», 2020)*

An alternative transportation method is through water. Water transportation is widely spread in countries with a long length of the coast marine line. Dry-cargo ships and cargo tanks transport oils and oil products. Table 1.2 lists the advantages and disadvantages of using water transport. A CNG (Compressed Natural Gas) vessel is illustrated in Figure 1.2.a, and a LNG (Liquefied Natural Gas) tanker carrier is illustrated in Figures 1.2.b.

Table 1.2: *The advantages and disadvantages of water transport (Ilyaeva & Andrianova, 2011)*

Advantages
1) Cost effective transportation
2) Unlimited throughput capacity of the waterways (especially marine)
3) The capability of oil products delivery to distant regions of countries without railways
Disadvantages
1) The seasonal prevalence of transportation on rivers and partly on marine paths, the necessity to make large reserves of oil loads
2) Slow travel of loads (especially upstream the rivers)
3) The impossibility to use the tonnage of ships completely if it is necessary to transport small amounts of special oil products
4) Empty backwards trips of the ships

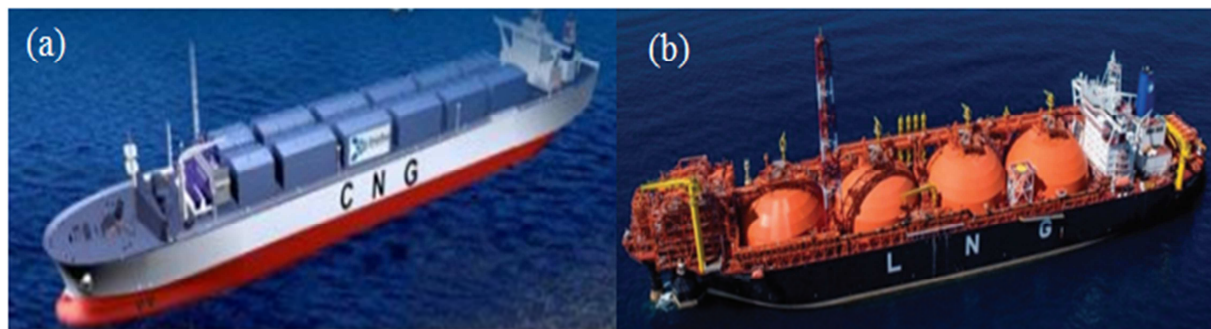


Figure 1.2: (a) CNG ship (Tractebel Engineering, 2015), and (b) LNG carrier (International Gas Union, 2018)

Another method of transportation is that of automobile. All types of hydrocarbon fluids can be transported by automobile transport. The automobile transport is used in cases, when there are no other means of transportation, for example, when a new field is being developed without any transportation infrastructure. Table 1.3 lists the advantages and disadvantages of using automobile transport. Figure 1.3 illustrates the different types of automobile tank trucks used in transportation, namely semi-trailer tank trucks and trailer tank trucks. This classification is essential, as we cannot afford using one and the same truck for different products, as their mixing cannot be allowed. Another classification is made according the loading capacity of the automobile tank trucks.

Table 1.3: *The advantages and disadvantages of automobile transport (Ilyaeva & Andrianova, 2011)*

Advantages
1) Large maneuverability
2) High speed of delivery
3) The capability to deliver loads to the points distant from water or railways
4) Transportation possibility all year round
Disadvantages
1) Limited tank trucks loading capacity
2) Rather high cost of transportation
3) Empty backwards run of the tank trucks
4) Significant consumption of fuel (transported oil products) for own needs



Figure 1.3: *Tank tractor-trailers ((a): Gerding, 1986; (b): O'Connell, 2018)*

Last but not least, transportation is also accomplished through pipelines. Pipelines or pipe lines are continuous large-diameter piping systems, usually buried underground where feasible, through which gases, liquids, or solids suspended in fluids are transported over considerable distances. They are used to move water, wastes, minerals, chemicals, and industrial gases, but primarily crude oil, petroleum products, and natural gas. In the oil and gas business, a pipeline system consists of a trunk-line, i.e., the large-diameter, high pressure, long-distance portion of the piping system through which crude oil is shipped to refineries, or natural gas and oil products, respectively, are transported to distribution points, and smaller low pressure gathering lines that transport oil or gas from wells to the trunk-line. Smaller lines used by natural gas distributors are not considered part of a gas pipeline system. Pipeline transport involves the application of force to the material being moved, either through the use of pumps to transport liquids, compressors to move gases, or flowing water to move solids (Barker et al., 2007). The transportation of crude oil from the point of extraction to the refining facilities takes place through pipelines. The shipment of gasoline, diesel fuel, home heating fuel, kerosene, and jet fuel from the refining facilities to the distribution ones is done through product pipelines. Pipelines are also used to transport the refined products, which are derived from the conversion of crude oil, to terminals and subsequently to gasoline stations.

Table 1.4 lists the advantages and disadvantages of using pipeline transport and Figure 1.4 displays the installation of underground pipelines.

Table 1.4: *The advantages and disadvantages of pipeline transport (Ilyaeva & Andrianova, 2011)*

Advantages
1) The capability of pipelines laying in any direction and at any distance; it is the shortest way between the initial and the final points
2) Uninterrupted operation and accordingly the guaranteed supply to customers, irrespectively of the weather, the season and the day
3) The greatest degree of automation
4) High reliability and simplicity in the operation and its smaller ecological footprint
5) The decrease of the load on the traditional means of transport
6) Pipelines are the safest method of transporting petroleum and natural gas (U.S. Department of Transportation, 2019)
Disadvantages
1) Large initial expenditures on the building of trunk pipelines
2) Definite limitations of the amount of the sorts of hydrocarbons transported through one pipeline
3) "Stiffness" of the pipeline, which causes additional investments for building new pipelines for delivering products to new customers

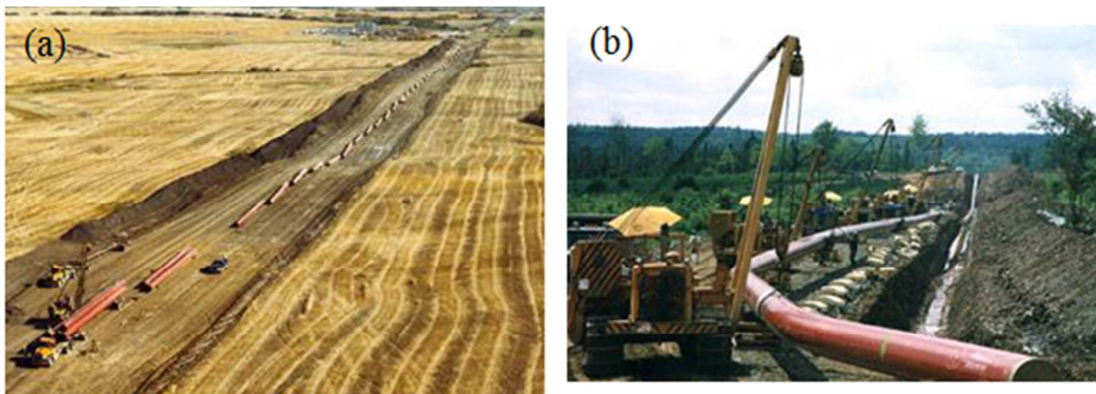


Figure 1.4: *Installation of underground pipelines (Natural Gas, 2013)*

Pipeline transportation of oil products is not the basic, it is the most progressive type of transportation and it has a large perspective for the further progressing. In some cases, pipeline transportation is a one-way street, such as during the drilling operations and during the refining process. Depending on the transported products, we distinguish the following types of specialized pipeline systems: oil pipelines, oil products pipelines, gas lines and pipelines for transportation of nontraditional loads (for example, condensate, methanol and so on) (Ilyaeva & Andrianova, 2011).

1.2.1. Oil and Gas Pipeline transportation: Classification and Current state

There are two general types of pipelines; the oil transportation and the gas transportation pipelines. There are three categories of both oil and gas pipelines depending on the area of work: 1) internal pipelines, 2) local pipelines and 3) trunk or main pipelines for oil transportation and gas-main pipelines for gas transportation.

Internal pipelines connect the various pieces of equipment used throughout the flow of crude oil and gas, i.e. from the extraction facilities to the refining ones. Local pipelines, which contrary to internal oil/gas pipelines have a larger length (reaching up to several tens of km), are used to connect oil/gas fields or oil/gas refining plants to the main stations from which the delivery to consumer begins. Finally, the transportation of oil/gas products from the storage regions to the final consumer is done through the main pipelines which are characterized by large length, high pressure, the presence of several pumping stations (in the case of oil transportation) or compressor stations (in the case of gas transportation), and relative operation continuity. The operating pressure in main oil pipelines usually varies from 5MPa to 7.5MPa, while the main gas pipelines are designed to stand pressure achieving 7.5MPa to 10MPa. According to the area of work, the diameter, the way of laying and building conditions gas mains and their parts are subdivided into five categories: higher (H-class with the conditional diameter more than 1200mm), I (I-st class with the conditional diameter changing from 1000mm up to 1200mm), II (II-nd class with the conditional diameter changing from 500mm up to 1000mm), III (III-rd class with the conditional diameter changing from 300mm up to 500mm), IV (IV-th class with the conditional diameter less than 300mm), as well as trunk oil pipelines. According to the operating pressure, gas mains are subdivided into two classes: class I pipelines have the operating pressure value varying from 2.5MPa up to 10MPa; for class II pipelines the operating pressure varies from 1.2MPa up to 2.5MPa (Ilyeva & Andrianova, 2011).

Transportation pipelines are used for moving products (oil or gas, and refined products) between regions, countries and even continents. Figure 1.5 shows trade flows worldwide in billion cubic meters using gas pipeline transportation and LNG carriers. Figure 1.6 shows the map illustrating the pipelines in Europe, including cross-border, international pipelines originating or ending in these countries. On the map, pipeline label codes are colored green for oil, red for gas and blue for products such as gasoline, propane and ethylene. Figure 1.7 illustrates the Greek national natural gas transmission system from the Greek-Bulgarian border and the Greek-Turkish border to consumers in continental Greece.

The current conditions of the gas and oil transportation systems are apparent in these three Figures. Pipe-work design standards that are relevant to LNG facilities are given in the installation and equipment for liquefied natural gas, design of onshore installations (BSI Standards Publication, 2007).

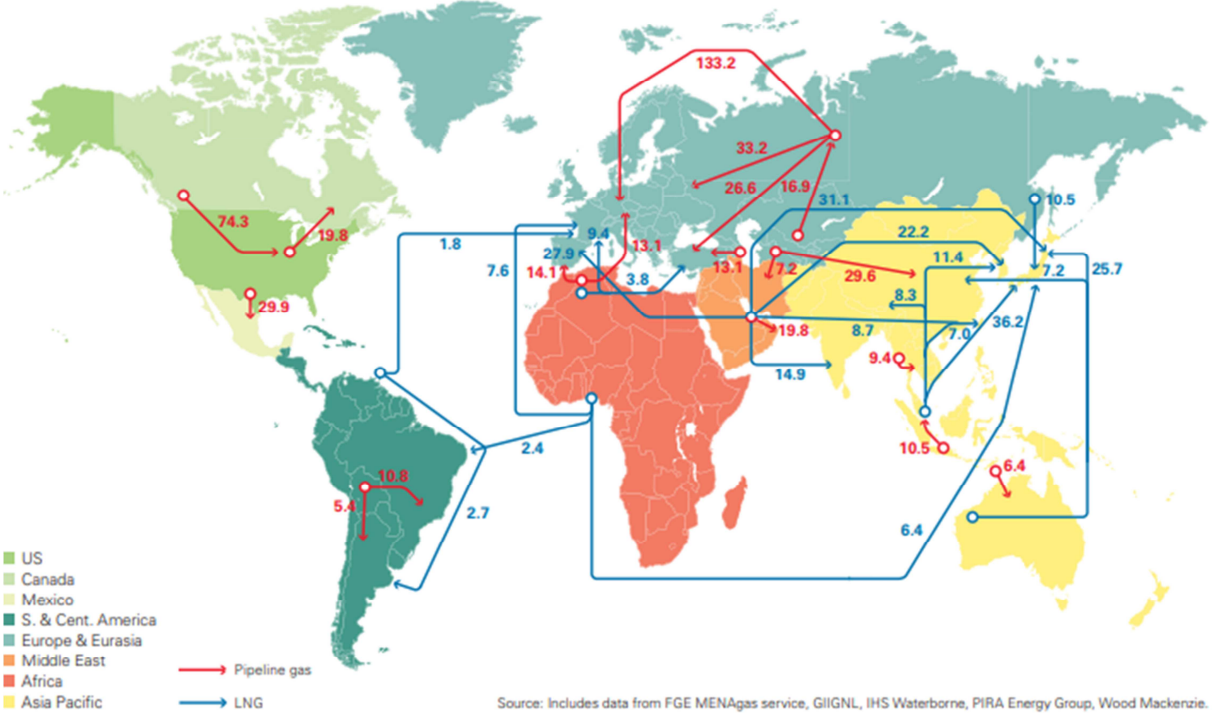


Figure 1.5: Trade flows worldwide in billion cubic meters (BP, 2016)

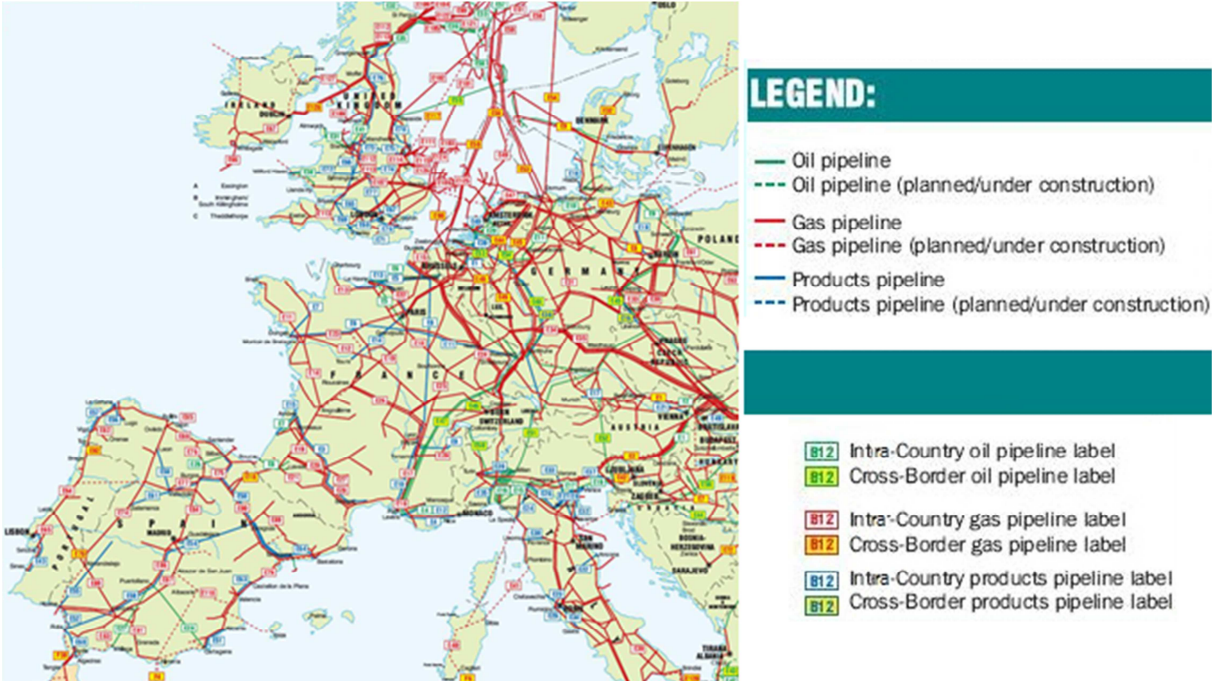


Figure 1.6: Pipelines in Europe (Information Technology Associates, 2017)

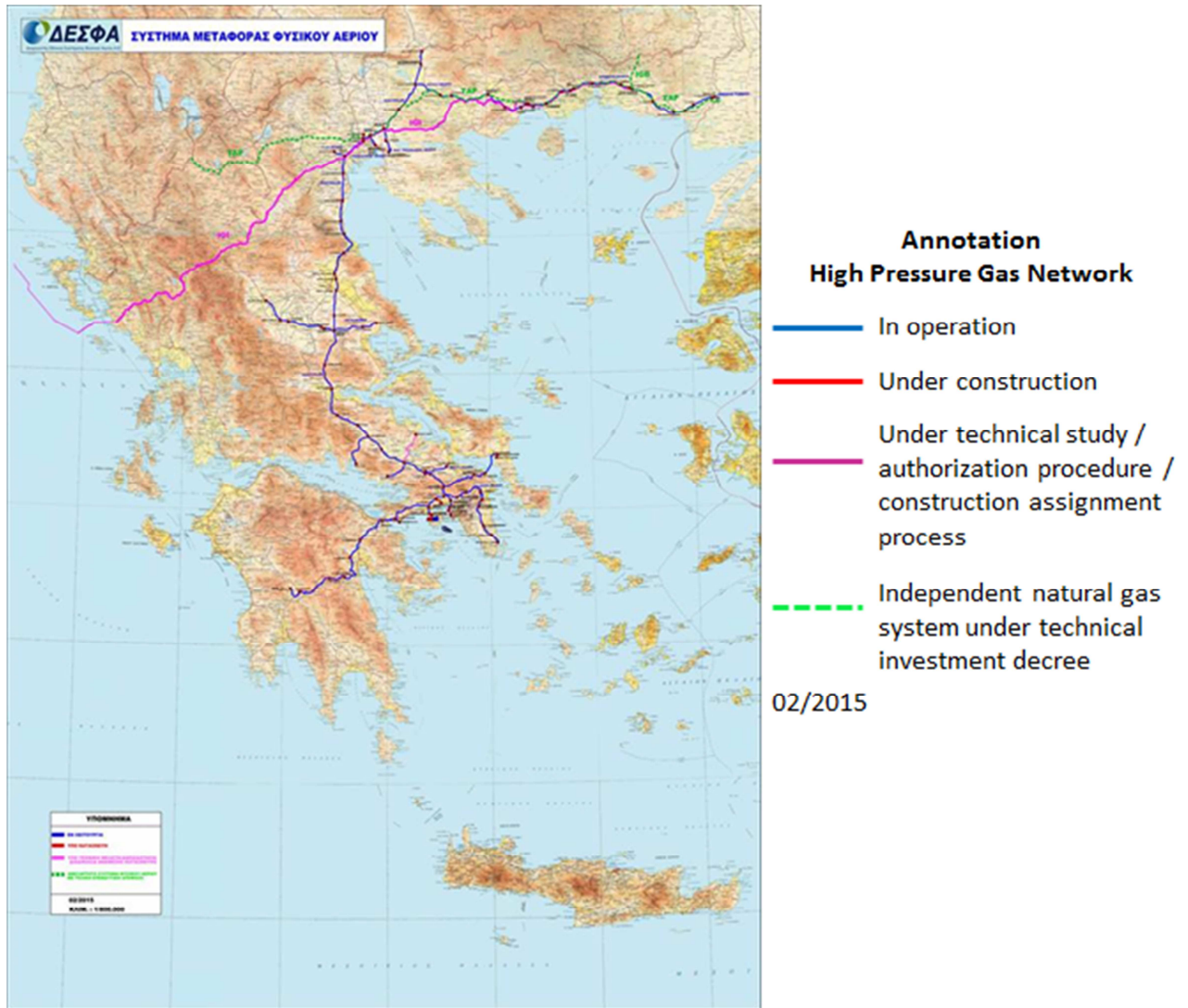


Figure 1.7: *Natural Gas Pipeline System - Geophysical Map of Greece (Modification by DESFA, 2018)*

1.3. Flow Assurance

The term "flow assurance" refers to the evaluation of the effects of fluid hydrocarbon solids (asphaltene, wax, and hydrate) and to their potentially disrupting the production because of the depositions in the flow system. It should be mentioned that the deposition of inorganic fluids coming from the aqueous phase (i.e. scale) also seriously threatens flow assurance. The current trend of deepwater developments means that future oil and gas production will be done through multiphase flow lines from isolated facilities in deepwater environments. A mixture of gas, oil, condensate, and water consist these multiphase fluids. These fluids together with sand and scales have the capability to create many problems; deposition of asphaltene, of wax, of hydrate formations, corrosion and erosion, emulsions, slugging are just some of them (Ahmed, 2007).

Field production can be seriously decreased if scale is accumulated anywhere in the tubulars which lead from the reservoir to the sales point. The accumulation of scale in the tubulars diminishes the tubular diameter available for flow and can, consequently, lead to the choking of the production from the reservoir (Frenier et al., 2010). The pressure also drops as a consequence of scale deposition, and this drop can be quite significant. The following equation (1.1) gives the relationship between pressure drop and flow rate for single-phase pipe flow.

$$\Delta P = \frac{2L}{D} f \rho u^2 \quad (1.1)$$

ΔP : the pressure drop

L & D: the pipe length & the pipe diameter

ρ & u : the fluid density & the average fluid velocity defined as: $u = \frac{4q}{(\pi D)^2}$

q: the volumetric flow rate

f: the friction factor, for laminar flow $f = \frac{64}{Re}$ and for turbulent flow in a smooth pipe $f = \frac{0.3164}{Re^{0.25}}$

Re: dimensional Reynolds number defined as: $Re = \frac{\rho u D}{\mu}$, where μ is the fluid viscosity

From the above equation (1.1) it can be seen that for a given flow rate the pressure drop is proportional to $1/D^4$ for laminar flow, and for turbulent flow in a smooth pipe, the pressure drop is proportional to $1/D^{4.75}$. Therefore, deposit accumulation can lead to reduction in the pipe diameter which in turn causes an increase of pressure drop, which consequently means a similar decrease in the reservoir production (Frenier et al., 2010).

When pressure drops excessively, the ability of the reservoir fluids to flow to the point of sale is dramatically inhibited. "Flow assurance" is the term used in the oil industry to refer to the description of such problems. So, flow assurance is described as the production operation which creates a reliable, manageable, and profitable fluid flow from the reservoir to the sales point. Flow assurance plays a vital role especially in deepwater assets. Due to the fact that access to the seafloor infrastructure is restricted in the case of deepwater assets, clogging of the tubular because of scale accumulation can result in expensive workovers that are occasionally prohibitively high in cost. The pressure-volume-temperature (PVT) characteristics (e.g. analysis of phase behavior of saturates, aromatics, resins, asphaltenes, paraffins, and naphthalene), water chemistry, and drilling-mud characteristics are vital in order for an asset to be developed (Frenier & Ziauddin, 2008).

1.3.1. Organic and Inorganic Deposits

Deposition of organic and inorganic solids is common in various facets of oil and gas production operations, including pipelines, wellbores, and reservoir and surface facilities. Precipitation is the formation of a solid phase out of a liquid phase and is the first step leading to deposition and is a necessary but not sufficient condition for deposits. Precipitation is a function of temperature, pressure, and composition. Deposition is the formation of a solid layer on a surface and is a function of shear, surface condition, and particle interaction as well as of pressure, temperature, and composition. Deposition depends on many factors, including oil, gas, and brine compositions, and the well environment (Frenier et al., 2010).

Organic scales, including waxes (paraffins), asphaltenes, gas hydrates and mixtures of these chemicals, as well as naphthenic acid salts, can cause the damage of the well. These substances come from the crude oil, gases, or reactions of the crude oil and may result in plugging of the formation or the various flowlines (Frenier et al., 2010). Inorganic scales are minerals which are formed on a surface due to the saturation of the local environment with an inorganic salt. The major categories of scales are carbonates [Ca(II), Mg(II), and Fe(II)]; sulfates [Ca(II), Ba(II), Sr(II), and Ra(II)]; oxides and hydroxides [Fe(II), Fe(III), Mg(II), and Cu(II)]; sulfides [Fe(II), Cu(II), and Zn(II)]; and silicates [Ca(II), Mg(II), Al(III), and Na(I)] (Frenier & Ziauddin, 2008).

Crude oils can be put through several phase transitions, generating gas, asphaltenes, wax, hydrate, and diamondoids. The numerous solids which are associated with hydrocarbon phase transitions can, apparently, cause numerous problems. Figure 1.8 shows some solids which can occur during the production of crude oil. These solids have a detrimental effect on flow assurance and have to be taken into consideration especially in deepwater extraction, due to the fact that in this case access to the seafloor pipelines and facilities is restricted, not to mention access to well completions (Mullins, 2008).

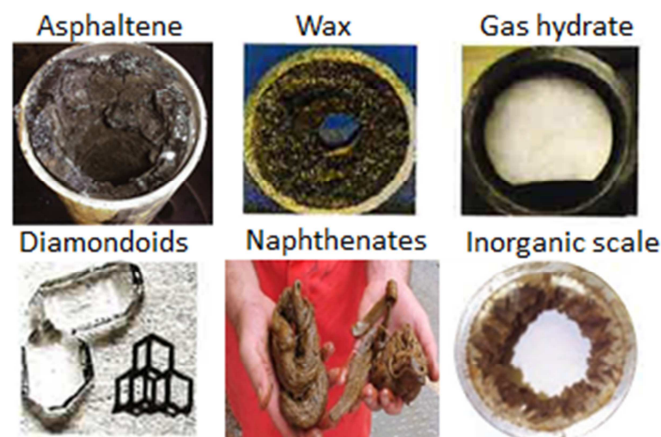


Figure 1.8: Various organic and inorganic solids (Modification by Mullins et al., 2006)

The generation of gas clathrate hydrates represents the most significant problem in offshore developments, from a flow assurance aspect. The second most serious problem is that of wax damage, followed by asphaltenes (Frenier et al., 2010). Naphthenates commonly cause problems on the topside, but these occurrences are rare. Inorganic scales in addition to mixed deposits can accumulate at any time when aqueous brines are present too (OILFIELD WIKI, 2016).

Before the drilling and completion of the well, the fluids in the formation are in equilibrium with their surroundings. Nevertheless, when the well is drilled and starts to flow, this balance is disrupted, and the precipitation of the solids may begin. In the upstream process, any of these substances may precipitate in the formation, in the near-wellbore region, in perforations, in tubulars, on downhole completion equipment, and in surface equipment such as gathering lines, separation equipment, and pipelines. In addition, corrosion is a significant source of scale which is often neglected. The iron generated by corrosion of tubular materials and surface equipment provides the cations for iron carbonate, iron oxide, and iron sulfide scales formation (Frenier et al., 2010).

Every time precipitation occurs, there is reduction in the flow of different degrees, which can even lead to the abandonment of the well. Figure 1.9 shows formation scale that is blocking the matrix. The conditions that enable scale or organic solids to form can be predicted, but the exact location where deposition will occur is more difficult to determine. The formation of such deposits can be minimized by chemical and mechanical methods (Frenier & Ziauddin, 2008).

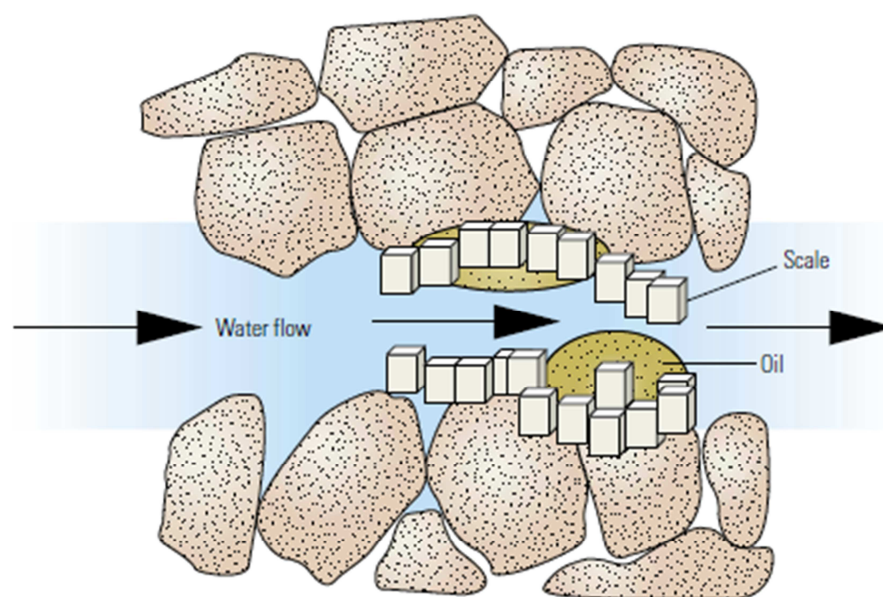


Figure 1.9: *Depiction of scale-blocking formation pores (Crabtree et al., 1999)*

1.4. Hydrates

1.4.1. Hydrate Definition and Structure

The formation of gas hydrates, which are crystalline compounds, happens when water (or ice) comes into contact with small molecules (called hydrate guests) under specific pressure and temperature conditions. The precise chemical name should be gas clathrate hydrates, because a clathrate is a compound which is formed when molecules of one kind are included in the crystal lattice of another (water in our case). In practice though, these compounds are known as gas hydrates, clathrate hydrates, or just hydrates. While distinct to the particular hydrate guest, gas hydrates are stable commonly at high pressures and low temperatures (as shown schematically in Figure 1.15). Natural gas hydrates are solid, ice-like compounds of water and the light components of natural gas. A number of heavier hydrocarbons existent in gas condensates and oils can also cause hydrate formation if smaller molecules, such as methane or nitrogen, are present to stabilize the structure. In Figure 1.10 we can see that methane hydrate looks like ice but, in contrast to ice, we can burn the methane in the hydrate and maintain a flame. While the compound melts, the gas that is released supports the flame and the ice in the framework leaks like water (Giavarini & Hester, 2011).

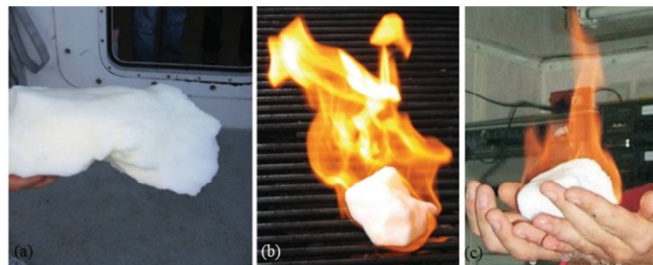


Figure 1.10: *Form of methane hydrate*
((a)&(b): Giavarini & Hester, 2011; (c): Mao et al., 2007)

Gas hydrates are formed by a wide variety of molecules. Light hydrocarbons such as methane, ethane, and propane are those which interest us most, in addition to carbon dioxide and hydrogen sulfide. When hydrate formation takes place, water crystallizes and creates a lattice of molecular-sized cages which entrap guest molecules but there is no chemical bonding between the host water and the guest molecules (Giavarini & Hester, 2011). In Figure 1.11, it can be seen that an oxygen atom occupies each vertex, and the midpoint of each edge consists a hydrogen atom. This atom is connected to an oxygen atom as component of a water molecule and hydrogen-bonded to the other. In Figure 1.11.a, we can see one cage with oxygen atoms in blue and hydrogen atoms in red. A methane molecule is illustrated inside one of the cage skeletons (Frenier et al., 2010).

Water turns into ice at 0°C. Under certain conditions, when other molecular species are present, this leads to the orientation of hydrogen-bonded H₂O molecules around these molecules and the formation of a solid crystal. The water behaves as the host structure, which is composed of cages which entrap and concentrate guest molecules (Figure 1.11.b). The solid hydrate stabilization is not because of the direct bonding of the guest molecule with the host water molecules. The guest molecules freely rotate in the molecular water cages. Rather, the hydrate stabilization occurs by an attractive van der Waals type force between the guest molecules and the water (Carroll, 2009).

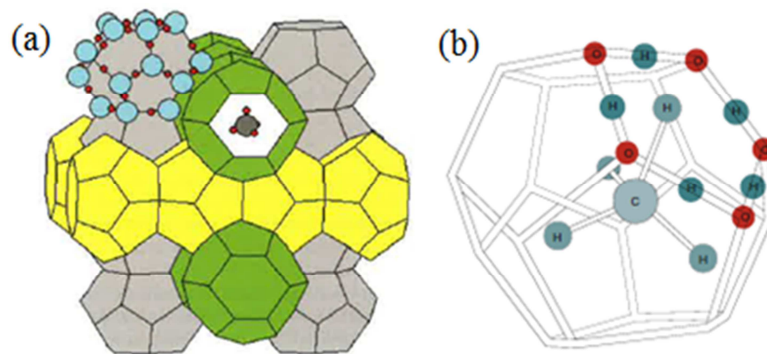


Figure 1.11: (a) *The inclusion or trapping of gas molecules in the gas hydrate lattice (Frenier et al., 2010),* and (b) *Gas molecules enclosed in the water cavities of the hydrate (Giavarini & Hester, 2011)*

Three conditions are necessary for the formation of hydrates (Cholet, 2000):

- Presence of water is essential. Hydrates are 80-90wt% water formed into a lattice structure similar to that of ice.
- Presence of hydrocarbons is essential. For the hydrate structure to stabilize, relatively high pressure is needed. Molecules such as methane, ethane, propane and butane, as well as nitrogen and carbon dioxide are vital for the stabilization of the structure.
- Temperatures of around 5-25°C are needed, according to the structure. In contrast to ice, when there is increase in pressure, the hydrate formation temperature also increases.

As it was mentioned above, gas hydrates are in essence clathrate compounds, i.e. ice-like, crystalline molecular complexes in a cage structure. Light gas molecules (guest molecules) go into this lattice and sit at the cavities, which are interstitial gaps between hydrogen-bonded H₂O molecules (host molecules). The structure is stabilized through physical bonding by van der Waals forces, when a gas or volatile liquid is present inside the water network. This structure differs greatly from that of salt hydrates, in that water is blended into the crystal lattice of a mineral such as gypsum (CaSO₄·2H₂O). A Type II natural-gas hydrate may contain 83mol% water, whereas gypsum only contains 20mol% water (Frenier et al., 2010).

Methane, ethane, propane, butanes, nitrogen, carbon dioxide, and hydrogen sulfide are conducive to hydrate formation. Only gases with the appropriate geometry and of the appropriate size can go into these cavities, which commonly have a diameter of 8-9Å. Hydrate formation takes place when, under certain conditions, they are more stable than pure water. These conditions are usually met at pressures higher than 30atm and near-seafloor temperatures. Three types of crystal structures have been determined. The first two structures (Structures I (sI) and II (sII)) were identified by X-ray techniques, and the third (Structure H (sH)) by NMR spectroscopy and by powder diffraction techniques. Figures 1.12, and 1.13 show the structure of the hydrates (Frenier et al., 2010).

Based on hydrogen bonding, molecules of water can form lattice structures. Natural gas clathrate hydrates usually develop either in the primitive cubic structure I, in the face-centered cubic structure II, or in the hexagonal structure H (Sloan & Koh, 2008). Hydrates of sI are mainly formed by pure methane; while hydrates of sII, will be formed by gas containing ethane or propane as low as 0.5mol%. Gas hydrates trouble the oil and gas industry because they can obstruct flowlines, valves, wellheads, and pipelines, thus resulting in loss of production when they form (Frenier et al., 2010).

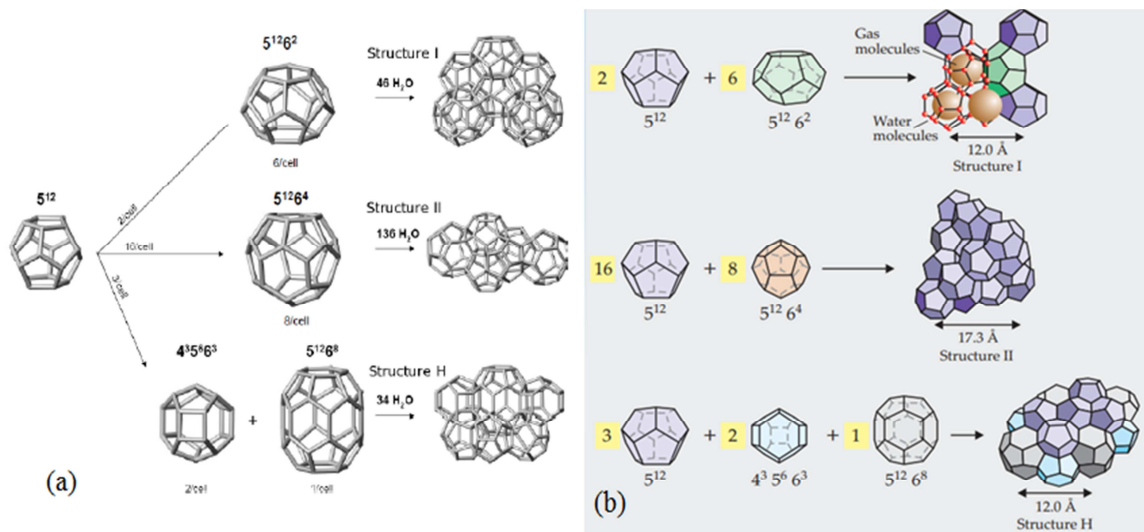


Figure 1.12: Various hydrate structures - clathrate polyhedral water cavities comprising sI, sII, and sH hydrates ((a): Frenier et al., 2010; (b): Mao et al., 2007)

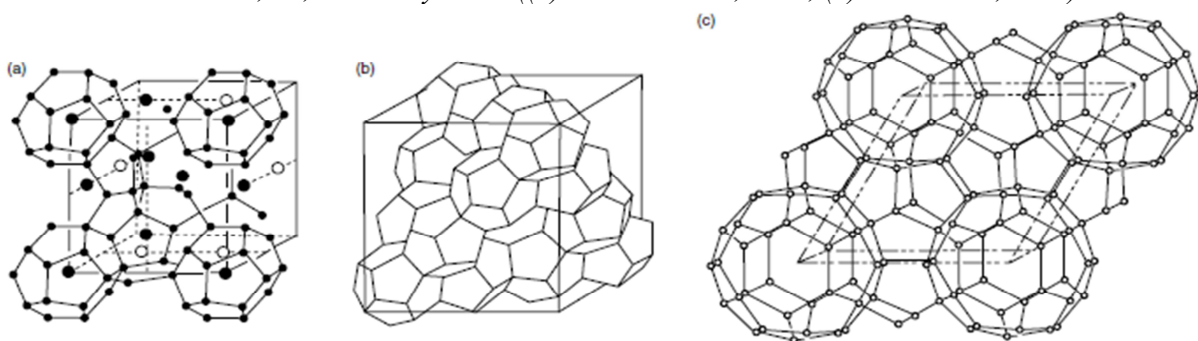


Figure 1.13: Hydrate crystal unit structures: (a) sI, (b) sII, and (c) sH (Sloan & Koh, 2008)

1.4.2. Location of Hydrate Formation

Gas hydrate formation may occur anywhere in space, on condition that a free gas, water, the suitable temperature and pressure exist; in the subsurface (gas hydrates make up over 50% of the world's organic carbon deposits and are considered a potential future energy source), in the technical production or transportation systems, in systems processing gases. Hydrate formation also occurs when the fluid temperature decreases below the equilibrium temperature resulting from big depressions, or while water is being pumped with a temperature less than that of the hydrate equilibrium into the well bottom zone of a gas or a gas-oil well (Makogon, 1997).

Hydrate formation can occur anywhere from pipelines (offshore and onshore), processing facilities (separators, valves), heat exchangers, sediments (permafrost regions and subsea sediments), to offshore drilling operations (Tohidi, 2018). Hydrate crystals, which look like ice or wet snow, are known to almost obstruct and stop the transmission of gas lines, as illustrated in Figure 1.14. Hydrates may also form inside equipment as a consequence of the cooling procedure resulting from decrease in pressure. This constitutes a problem, especially for pressure-control valves and pressure regulators, which can virtually freeze up. Moreover, hydrates can effortlessly form downstream of a choke where the temperature of the fluid can be reduced into the hydrate formation region because of Joule-Thomson cooling effects (Nayyar, 2000).



Figure 1.14: *A clathrate plug recovered from an offshore gas flowline of Petrobras Company (Mao et al., 2007)*

Two are the factors that enhance hydrate formation during drilling; the increase of drilling operations in the Arctic zones and deep seas, as well as the increasing employment of water-based drilling fluids, instead of oil-based fluids for ecological reasons. Hydrate presence in the reservoir and in offshore drilling poses a problem at a water depth above 300m. Because of the complexity of the drilling fluid composition, prediction of the specific conditions of hydrate formation becomes challenging (Rojey et al., 1997).

Hydrate formation may occur in the bottom of a well in a production pipes column, particularly if these pipes are equipped with throttle devices, in the annular space, and in the christmas-tree equipment. The most favorable period for hydrate formation is the startup period when the wellbore is cold. While the well is inactive, hydrates may totally clog the wellbore and under specific conditions they may even result in the destruction of the well, necessitating an emergency fountain. Any part of the technological line of gas collection and pretreatment can be a hydrate formation environment, as well as the long distance systems of transportation, and the underground storage and distribution of gases and a wide proportion of liquid hydrocarbons (Makogon, 1997).

So as to detect where a hydrate formation is going to happen, it is necessary to be aware of the composition of gas, the water salt content, and the vapor composition in the gas phases prior to and after the hydrate formation, the equilibrium pressure and the temperature conditions of hydrate formation, and the appropriate pressure and temperature changes. How intense hydrate accumulation is going to be depends on the state of the water, the subcooling degree, the flow turbulence, the gas-water free interface formation rate, and the severity of hydrate formers diffusion (Makogon, 1997).

1.4.3. Phase Behavior of Hydrocarbon Systems and Hydrates

It is possible to predict potential problems observing the way a petroleum fluid behaves. Temperature, pressure, as well as, the composition of the system is the critical properties. While in the reservoir, the fluid portions are in equilibrium. Nevertheless, when production activity starts, there is a change in balance, which may lead to the separation of the fluids out of the fluid phase. In Figure 1.15, we can see a generalized phase diagram of a petroleum fluid, in addition to the temperature and pressure path a fluid follows, as it is traveling from the reservoir inside the production system. The phase boundaries of asphaltenes, waxes, and hydrate solids illustrated in the Figure 1.15 are equilibrium phase boundaries, which show where saturation of a fluid will begin with the respective solid phase. Once the fluid gets into the solid-phase boundary, it is possible for the respective solid to deposit. However, the boundary does not show whether the solid will in fact deposit or, if it does, how much it will deposit. In many production scenarios, the phase boundaries are crossed over, but the solids do not accumulate and cause flow assurance problems (Frenier et al., 2010).

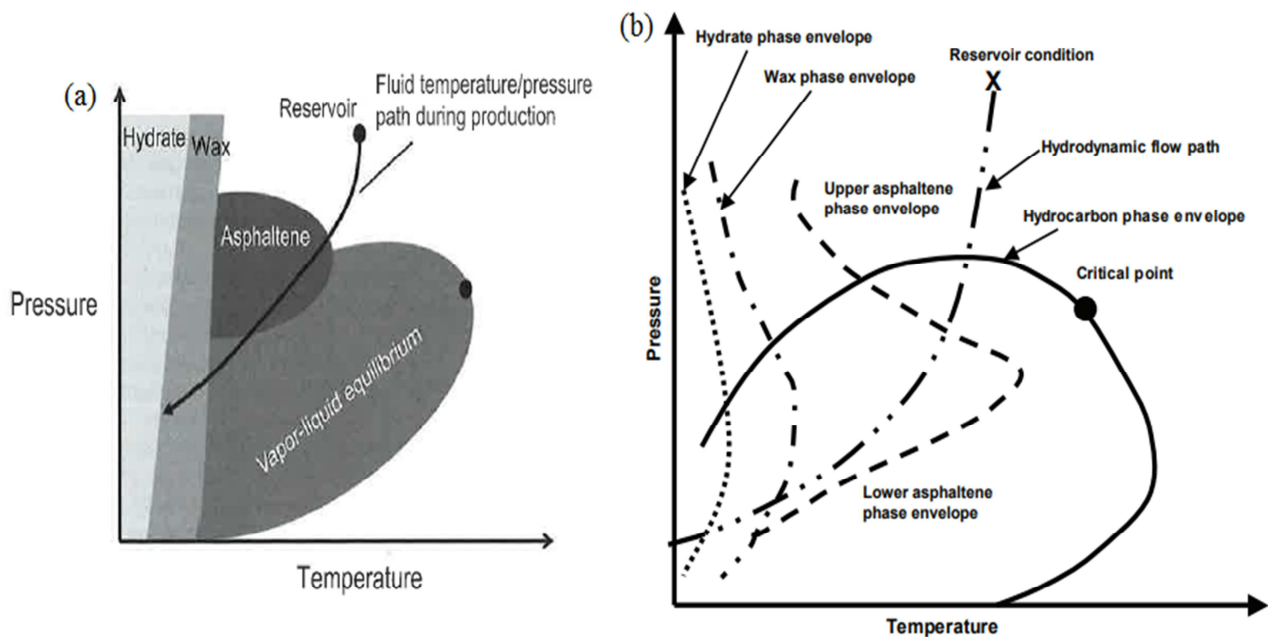


Figure 1.15: (a) *Precipitation regimes for hydrates, waxes, and asphaltenes (Frenier et al., 2010), and (b) Thermodynamic conditions of the flow assurance elements (Ahmed, 2007)*

A phase diagram is a starting point and provides key information for any study of flow assurance. Because the crossing of the phase boundary is an essential but not adequate condition for deposition of solids, it is effective in discriminating between solids that will not deposit and those that could possibly deposit and should be examined further (Frenier et al., 2010). On many occasions, the fluid temperature and pressure path may not transverse any fluid-solid phase boundaries when production starts. Nevertheless, as the pressure in the reservoir is depleted, or due to changes in the production system, the fluid path may shift and may cross one or more fluid-solid phase boundaries. As a result, even though at the beginning we may have a reservoir with no organic accumulations in the production systems, this may become a reality later on (Frenier et al., 2010).

In order for hydrates to form in surface gas-processing facilities, temperature and pressure have to be much lower than those occurring in production and reservoir processes. Simple pressure-temperature phase diagrams for water-hydrocarbon systems usually give the conditions for initial hydrate formation (Ahmed, 2007). Figure 1.16 gives a schematic example of the phase diagram for water and light hydrocarbon mixture, as well as the precarious areas of hydrate issues (Tohidi, 2018). It is obvious from Figure 1.16 that the issue of hydrates accumulations primarily arises in the drilling processes, as well as in the initial stages of downstream processing, primarily in the natural gas treatment plants. As can be seen in Figure 1.16.b, in order to avoid the problem of hydrate deposits, a safety margin has to be created by using several prevention methods, such as those mentioned in chapter 1.4.5.

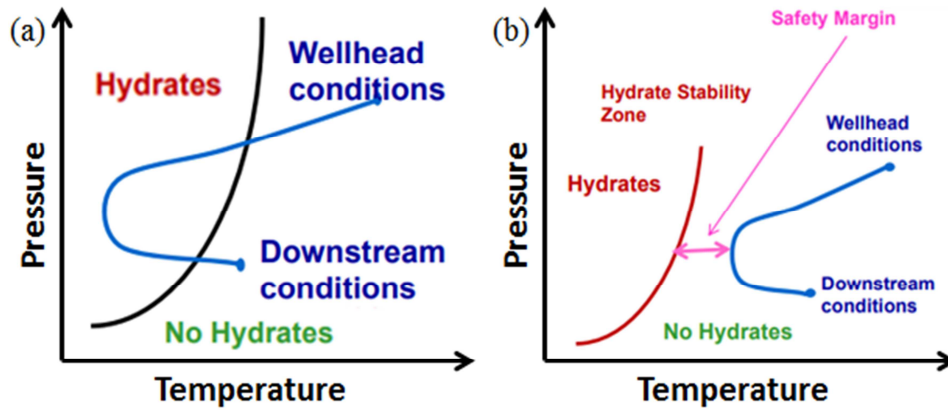


Figure 1.16: Precipitation regimes for hydrates formation (Tohidi, 2018)

The phase behavior of systems involving hydrates can be very complex; up to seven phases must be considered, even without considering the possibility of scale formation. The behavior is particularly complex if there is significant mutual solubility between phases, for example, when inhibitors or carbon dioxide are present (KBC, 2015). In Figure 1.17.a, the principal features of the phase diagram are displayed, when a hydrate is formed with a pure hydrocarbon, while Figure 1.17.b presents the regions of hydrate formation, from methane to butane paraffins (where: H is used to denote hydrates, I for ice, V for vapor, and L_w and LH_C for aqueous and hydrocarbon liquid phases, respectively). In this diagram, curve 1 represents the vapor pressure of the hydrocarbon. Curve 2,2',2'' delimits the hydrocarbon formation region. A lower quadruple point ($Q_1=LQP$) and upper quadruple point ($Q_2=HQP$) have been defined. The quadruple point represents the condition at which four phases are in equilibrium. Each quadruple point, unique for each hydrate former, lies at the intersection of four three-phase lines, providing a quantitative classification for hydrate components of natural gas. The slope change at LQP coincides with the water-ice phase change. At point LQP, the gaseous hydrocarbon, liquid water, ice and hydrate phases coexist. The slope change at HQP correlates to the phase change of the hydrocarbon. At point HQP, the liquid hydrocarbon, vapor hydrocarbon, liquid water and hydrate phases coexist (Rojey et al., 1997).

Several of the lighter natural-gas components, like methane and nitrogen, do not have an upper quadruple point, so in this case an upper temperature limit for hydrate formation does not exist. This is why hydrate formation is still possible at high temperatures (up to 50°C) on the surface facilities of high-pressure wells. Line 2' separates the area where water and gas blend to form hydrates. The vertical line from point HQP separates the area of water and hydrocarbon liquid from the area of hydrate and water. It is beneficial to divide hydrate formation into the following two categories (Ahmed, 2007):

- 1) Formation of hydrates because of the decrease in temperature with no sudden pressure drop, such as in the flow string or surface line.
- 2) Formation of hydrates where rapid expansion happens, such as in orifices, back-pressure regulators, or chokes.

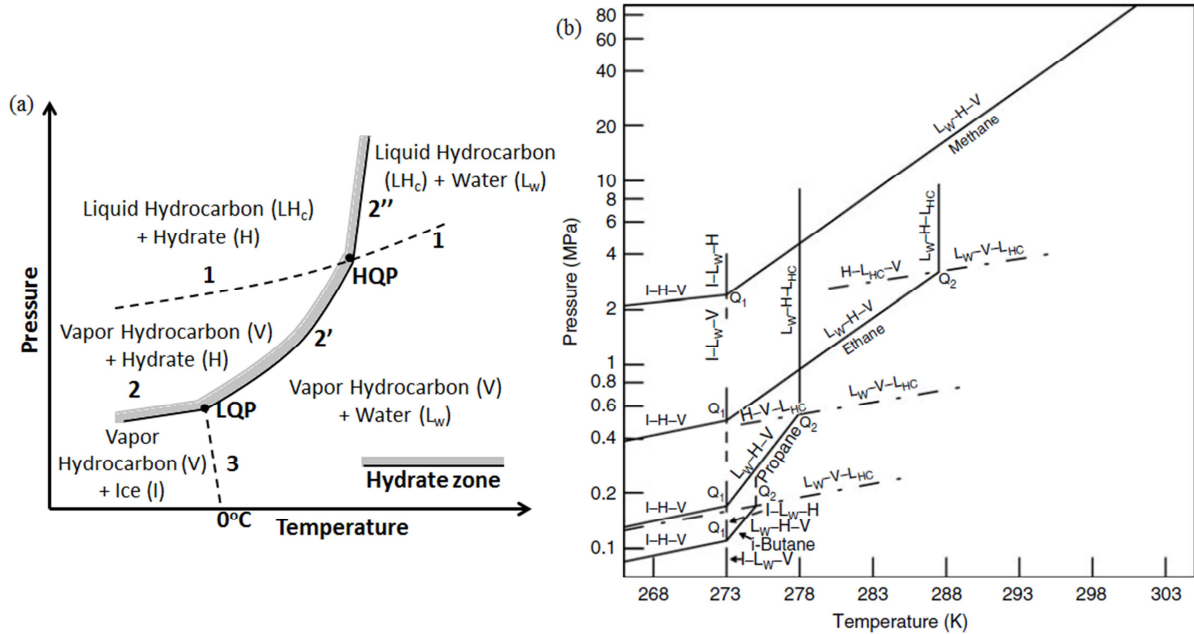


Figure 1.17: (a) A typical phase diagram for a pure hydrocarbon - larger than methane (Modification by Giavarini & Hester, 2011), and (b) The hydrate formation regions for C₁ to C₄ paraffins (Sloan & Koh, 2008)

1.4.4. Thermodynamic Equilibrium and Kinetics during Hydrates Formation

This chapter presents some of the basic principles of thermodynamic equilibrium and kinetics of hydrate formation in order to better understand the phenomenon. There is no detailed description of the models as the present project does not aim to represent such a model, however a lot of commercial software is based on these principles.

The modeling of the thermodynamic conditions of hydrate formation requires the knowledge of the chemical potential of water in the hydrate phase. The statistical model of van der Waals and Platteeuw is based on the calculation of the probability of occupation of a cavity by a gas molecule. Interactions between the gas molecules and the water molecules are assumed to involve van der Waals forces exclusively. The chemical potential of water in the hydrate phase is written in the form (1.2).

$$\mu_{\text{H}_2\text{O}} = \mu_{\text{H}_2\text{O}}^0 + R T \sum_i v_i \ln \left(1 - \sum_k y_{ki} \right) \quad (1.2)$$

$\mu_{\text{H}_2\text{O}}^0$: chemical potential of water forming a hypothetical gas-free hydrate phase. The difference between this chemical potential and that of the water in liquid form or in the form of ice at the reference temperature is determined by adjustment from experimental data.

v_i : number of cavities of type i per molecule of water. For each type of structure, only two sorts of cavity exist. Structure I: $v_1=1/23$ and $v_2=3/23$, and Structure II: $v_1=2/17$ and $v_2=1/17$.

y_{ki} : probability of occupation of type- i cavities by a type- k molecule, expressed by the equation (1.3) below.

$$y_{ki} = \frac{C_{ki} f_k}{1 + \sum_j C_{ji} f_j} \quad (1.3)$$

f_k : is the fugacity of component k in the gas phase

C_{ki} : is the Langmuir constant for component k occupying a type- i cavity

The conditions of hydrate formation are defined by designating that the chemical potentials of the water in each of the existent phases (liquid-hydrocarbon phase, solid-hydrate phase, vapor phase) are equal. The Langmuir constant C_{ki} can be related to the expression of the interaction energy potential of a molecule occupying the center of a cavity. Munck et al. (1988) suggested calculating the Langmuir constant C_{ki} not from an expression of the interaction potential but using an empirical equation (1.4) including the temperature.

$$C_{ki} = \left(\frac{A_{ki}}{T} \right) \exp \left(\frac{B_{ki}}{T} \right) \quad (1.4)$$

A_{ki} & B_{ki} : parameters that are adjusted by using a large number of experimental points

This approach is really suitable for a data-fitting procedure and, on condition there is a wide experimental data base available, it can apply to a variety of conditions. However, because of the empirical character of the method, it is precarious to make assumptions beyond the range covered by this data (Rojey et al., 1997).

According to Rojey et al. (1997), hydrate crystal formation happened through a nucleation step, followed by the development of the hydrate crystals from the nuclei. Several nucleation processes must be taken into account. Homogeneous nucleation occurs in a fluid phase when a solid-fluid surface is absent. Heterogeneous nucleation is a result of the presence of solid surfaces apart from the crystals themselves: pipe walls, solid particles in suspension. Secondary nucleation is connected to the existence of the crystals themselves.

In the gas phase, the likelihood of a nucleation nucleus being formed is low. Nucleation develops in preference in the region of the water/hydrocarbon interface (gaseous or probably

liquid). A nucleation seed is developed in the first step. If this nucleation seed has not developed to a significant size, it is unstable. Seeds that have developed to this crucial size represent nuclei, from which the hydrate crystals can evolve by growth. The time needed for the formation of such nuclei is referred to as the latency period or incubation time.

The critical radius (r_c) of a nucleation step nucleus can be calculated by using the following equation (1.5) for $r = r_c$.

$$\sigma dA_p = (-\Delta g) dV_c \quad (1.5)$$

dA_p : represents the elementary variation of the surface of the particle

σ : the free interfacial energy per unit surface area

dV_c : an elementary variation of the volume of the particle

Δg : the difference between the free energies per unit volume in the solid and liquid phases

The particle radius r_c can be calculated from equation (1.6) by assuming a spherical particle, if the composition of the hydrate phase is known, as well as the fugacities of each of the components respectively in the solid and liquid phases. The energy (E) required to form a stable nucleus is given by the equation (1.7).

$$r_c = -\frac{2\sigma}{\Delta g} \quad (1.6)$$

$$E = \frac{4}{3} \pi r_c^2 \sigma \quad (1.7)$$

The nuclei formation rate can be given for homogeneous nucleation by equation (1.8), where N stands for the number of nuclei formed per unit time and unit volume.

$$N = k \exp\left(-\frac{E}{R T}\right) \quad (1.8)$$

Equations (1.5) to (1.8) only yield approximate results and do not illustrate the intricacy of nucleation at the molecular scale. If solid surfaces and impurities are present, the formation of nuclei by heterogeneous nucleation is enhanced. Immediately after crystal formation, it is necessary to explain secondary nucleation. The speed at which stable seeds are formed by secondary nucleation happens in accordance with the surface area of the crystals formed earlier.

As mentioned before, after the nucleation stage the growth stage comes. This growth commonly happens in the aqueous phase. It necessitates the dissemination of the hydrocarbon molecules in the aqueous phase, and accelerates near the interface. For the determination of

the growth step, many experimental studies have been conducted, and for the creation of a model of the kinetics of hydrate formation many semi-empirical correlations were used.

The following kinetic equation for hydrate formation from pure methane was suggested by Vysniauskas & Bishnoi (1983) treating it as a chemical reaction.

$$r = A \alpha_s \exp\left(-\frac{\Delta E_a}{R T}\right) \exp\left(-\frac{\alpha}{\Delta T^b}\right) P^\gamma \quad (1.9)$$

r: the consumption of methane

A: the kinetic constant

α_s : the water-gas interfacial area

ΔE_a : the activation energy

γ : the overall order of the reaction with respect to pressure (P)

α & b: parameters related to the nucleation kinetics

In order to analyze the hydrate growth kinetics, more up-to-date models take into consideration a gas diffusion step in the liquid phase, succeeded by a step of gas molecules incorporation in the crystal lattice.

1.4.5. Prevention Methods

A number of factors may avert solid deposition once the equilibrium phase boundary is crossed and the solid-phase region is penetrated. The mixture can become supersaturated with the solid and the possibility of a separate solid phase diminishes; the deposition kinetics may not be powerful enough to cause deposition, or the conditions of flow may be such that the processes of shear removal are quicker than the deposition processes (Frenier et al., 2010).

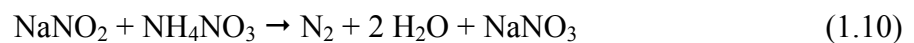
To operate outside the thermodynamic conditions of hydrate formation can be managed either by increasing the temperature at a given pressure (by keeping the gas at a greater temperature), or by decreasing the pressure at a given temperature. If this is not possible, then formation of hydrates can only be averted by lowering the water content of the gas by drying or by the use of inhibitors. Inhibitors behave as an "antifreeze". They are mainly obtained from solvents miscible in the aqueous phase, which, by changing water fugacity, reduce the temperature for hydrate formation. As mentioned before, the two typical strategies to reduce the formation of hydrates are thermal insulation and injecting chemical inhibitors (Rojey et al., 1997). Lastly, one mechanical way to cleanse the tubes from deposits is to use the "pig". The term "pig" is the most common term for any apparatus which is put into a pipeline and which moves independently through it, spurred by product flow (Cordell & Vanzant, 2003).

1.4.5.1. Heating

Insulation is a key factor to maintaining the temperature at levels higher than those conducive to hydrate formation. However, if the product has to be carried over longer distances, this method becomes insufficient or even overly costly. Insulation of the pipes is usually coupled with complementary electric heating. Heating is supplied by electric-heating strips, or by inducing superficial electric currents in the line that needs heating. Arctic zone facilities mainly use this type of prevention system (Rojey et al., 1997).

Temporary heating is another measure taken against hydrate plugging. This process, however, necessitates several safety measures. First of all, heating must be gradual, in order to prevent excessive stress in the pipe. It is also essential to start melting the ends of the plug, before advancing towards the center. Dissociation of the hydrates at the center could lead to detrimental overpressure, which in turn can lead to the fracturation of the line. When the plug melts, the water created should be discharged so as the formation of a new plug can be stopped (Rojey et al., 1997). When hydrate issues arise at pressure control valves or other equipment, heating it locally can offer a satisfactory solution (Nayyar, 2000).

An exothermic chemical reaction could be one way of providing the necessary heat reaction between sodium nitrite (NaNO_2) and ammonium nitrate (NH_4NO_3) is one of the most appropriate, as shown in expression (1.10):



Apart from the necessary heat, the sodium nitrate also behaves as an inhibitor in solution. One drawback of this process is nitrogen formation, which enhances the risk of overpressure (Rojey et al., 1997).

1.4.5.2. Pressure reduction

If we decrease the pressure at a stable temperature, we can operate outside the region of hydrate formation. However, when gas expands, it results in a decrease in temperature which negates the desired effect. Hence, isentropic or even isenthalpic expansion is conducive to hydrate formation. Depressurization can only inhibit hydrate plug if it is conducted almost isothermally. This means that there is no line insulation, and that the process of flash is slow enough. Depressurization is generally only conducted on a part of the pipe that can be subjected to insulation. It should be conducted on both sides of the plug at the same time, so as to diminish the risk of plug projection (Rojey et al., 1997).

1.4.5.3. Inhibitors

Prevention of hydrate formation can be achieved by dehydration of the gas or liquid so that a condensed water (liquid or solid) phase does not form. On some occasions, however, dehydration may not be realistic or financially viable. On these occasions, an efficient method of stopping the formation of hydrates can be chemical inhibition. Chemical inhibition employs thermodynamic inhibitors or low dosage hydrate inhibitors (LDHIs) which are injected. Thermodynamic inhibitors are the most common inhibitors (one of the glycols or methanol). They can be used to alter the hydrate line (to the left in the curve shown in Figure 1.17.a), and as a result decrease the temperature of hydrate formation and boost the hydrate-free operating envelope. LDHIs are either kinetic hydrate inhibitors (KHIs) or antiagglomerants (AAs), which do not totally eliminate hydrate formation but do reduce its consequences. KHIs reduce the hydrate formation rate, which impedes its progress for certain duration. AAs allow hydrate crystal formation but limit it to sub-millimeter size. They contribute to hydrate nucleation and agglomeration prevention so as to avert formation of blockage (Gas Processors Suppliers Association, 2004).

Hydrate inhibition lowers the temperature of hydrate formation or raises the pressure of hydrate formation in a certain mixture of gas and is generally linked to batch treatments for start-up or shut-down processes, either planned or unplanned. Steady injection also happens when there is a likelihood of cooling because of chokes and the unavoidable cooling of pipelines due to the low temperatures in the environment of the seabed (Bai & Bai, 2010).

- Salts

Electrolytes are very efficient inhibitors. Salts in solution attract the dipoles which are formed by water molecules. These molecules tend to mix with the ions in solution, and not form a lattice around the gas molecules in solution. Correspondingly, the hydrate lattice formation by the water molecules necessitates a decreased temperature at a certain pressure. The same rationale applies to the decrease of gas solubility in water. The salts that consist the most efficient inhibitors correspond to the following cations (1.11):



The vast majority of chlorides, especially NaCl, KCl, MgCl₂, CaCl₂, and AlCl₃ can be employed as inhibitors. Calcium chloride is usually chosen because of its efficiency and low cost. Sulfates, especially Na₂SO₄, MgSO₄, and Al(SO₄)₃ are also used. The use of phosphates and of sodium phosphate Na₃PO₄ especially, is also appropriate.

When water is present, it is advisable to consider dissolved salts for risks of formation of hydrates. Nevertheless, due to the corrosion and deposits risk, salts are rarely used as inhibitors (Rojey et al., 1997).

- Alcohols

The use of alcohols, in particular glycols and methanol (CH_3OH), as inhibitors is widely implemented. Ethylene glycol (EG: $\text{C}_2\text{H}_6\text{O}_2$) is one the most efficient hydrate inhibitors due to its low cost, low viscosity, and low solubility in liquid hydrocarbons. Because it has a low molecular weight, it is more efficient, at a certain mass concentration than diethylene glycol (DEG: $\text{C}_4\text{H}_{10}\text{O}_3$) or triethylene glycol (TEG: $\text{C}_6\text{H}_{14}\text{O}_4$). However, diethylene glycol use could be appropriate in order to reduce solvent losses in the gas. If gas dehydration takes place after pipe transport, diethylene glycol can be employed as a sole solvent all along the transport and dehydration steps (Rojey et al., 1997).

The use of glycols is advantageous because they can easily be recovered in the liquid phase, regenerated through distillation and recycled, but it also bears the disadvantage of glycols relative viscosity. Because methanol is effective, cheap and readily available, it is often used, either for a short time for the destruction of a plug, or permanently for the prevention of hydrate formation. Methanol is preferred due to its non-viscosity and non-corrosivity. Nevertheless, because of its high vapor pressure, losses in the gas phase occur. In addition, methanol regeneration by distillation is a costly process. Thus, methanol is consumed all the time, without being recovered (Rojey et al., 1997). Methanol is one of the hydrate inhibitors most commonly used, especially in subsea wells and in arctic areas where the quick drop in temperature of the produced fluid flow (gas and water) can enhance the formation of hydrates. Methanol is infused into the christmas-tree and in some cases downhole, just over the subsurface safety valve while the fluids are still hot (Bai & Bai, 2010).

Inhibitor efficiency is typically measured by subcooling (difference between the hydrate formation temperature with inhibitor subtracted from the formation temperature without inhibitor). Figure 1.18 illustrates the subcooling for different thermodynamic hydrate inhibitors as a result of aqueous accumulation on methane hydrate stability. As can be seen from Figure 1.18, the accumulation of inhibitor enhances the subcooling achieved. The hydrate is fixed to the left of each curve (Giavarini & Hester, 2011).

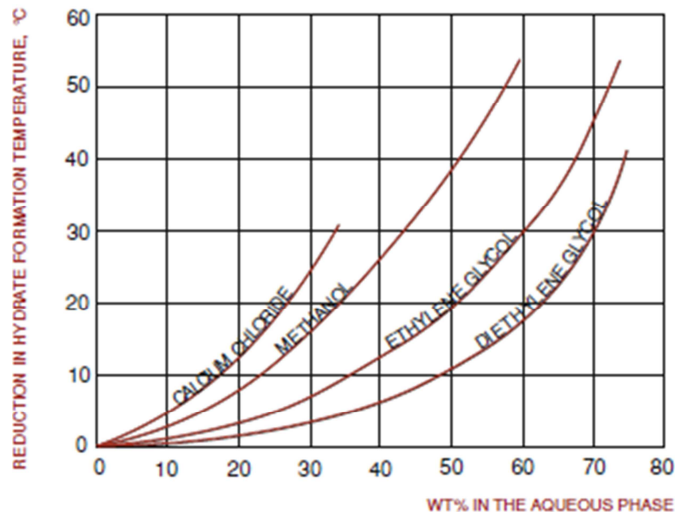


Figure 1.18: Lowering of the hydrate formation temperature by different inhibitors (Giavarini & Hester, 2011)

- Ammonia and Monoethanolamine

Ammonia is a very efficient inhibitor, but it exhibits corrosivity, toxicity; in addition, when water is present, carbonates obtained with carbon dioxide, can cause deposition of solid. Its vapor pressure is also intense and its recovery is particularly hard.

The use of monoethanolamine as an inhibitor has also been suggested. For a certain mass accumulation, it is more efficient than diethylene glycol and becomes attractive if also used for gas sweetening (Rojey et al., 1997).

1.4.5.4. Pigging

Nowadays, pigging is widely applied in the pipeline industry, whether construction, operation, inspection or maintenance takes place. According to the type of application and the conditions existent in the pipeline, various kinds of pigs are selected to diminish pigging operation costs. Even though pigs were initially used for clearing away deposits, which could block or decelerate flow in a pipeline, today pigs are employed for many different purposes and throughout the life of the pipeline. When pipelines are constructed, pigs are utilized for debris removal, gauging, cleaning, flooding and dewatering. When fluid production operations take place, pigging is used in order to remove deposits, such as wax in oil pipelines, to remove liquids in gas pipelines, and meter proving. Pigging is also used in order to inspect the pipeline and measure wall thickness or detect spanning and burial. Furthermore, pigs can be used to coat the inside surface of a pipeline with inhibitor and to provide resistance to pressure when other maintenance operations take place. A wide range of cleaning pigs are at our disposal, pigs that are based on the concept of inducing a flow bypass

through the pig body over the brushes or scrapers and out to the front. On occasions, chemical cleaning is employed in order to remove specific kinds of pipe deposits; this is a procedure that necessitates the use of pigs in combination with detergent-based cleaning fluids which are environmentally friendly (Guo & Ghalambor, 2005). Figure 1.19 shows numerous kinds of pigs employed in pipeline pigging operations.

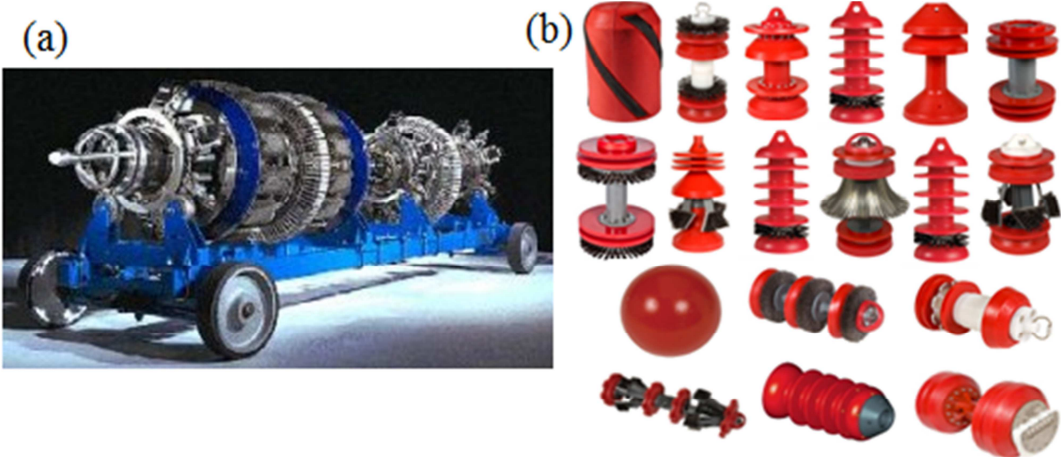


Figure 1.19: (a) Pipeline inspection tool (Natural Gas, 2013), and (b) Various types of pigs used in pipeline pigging operations (T.D. Williamson, 2020)

Pigs, a launcher and a receiver constitute the components of a pigging system. Pumps and a compressor may also be included in order to transport the product fluids. Even though individual pipelines have their own set of characteristics that influence how and why pigging is used, there are essentially three reasons for pigging a pipeline: 1) to group or separate products that are diverse, 2) to remove unwanted materials, and 3) to inspect the pipeline from the inside. Accordingly, the pigs employed to perform these tasks are divided into three categories. For cleaning, separating or dewatering processes, utility pigs are used. In-line inspection pigs are used to collect information on the state of the line, in addition to the degree and area of any problem. Gel pigs are employed together with regular pigs so as to perfect dewatering, cleaning, and drying work (Guo & Ghalambor, 2005).

Intelligent pigging is nowadays available. Robotic devices, referred to as smart pigs, are thrust down the pipelines to assess the pipe interior for safety and inspection reasons. Smart pigs are able to test the thickness and roundness of a pipe, monitor for corrosion signs, identify minor leaks, and inspect for any other fault in the interior of a pipeline which may either inhibit gas flow or consist a potential threat to the pipeline operation. Apart from smart pig inspection, there is a wide variety of alternative safety measures that can be taken to diminish accident risk (Natural Gas, 2013).

2. MATHEMATICAL MODELING

2.1. Hydrate Formation

Mathematical modeling is the development of mathematical descriptions of a phenomenon, system or process using mathematical concepts and symbols. As described by Carroll (2009), the first step when designing processes involving hydrates is to predict the conditions of pressure and temperature at which hydrates will form. There are two categories of calculation of hydrates formation. One is described as "hand calculation methods" and the other as "computer methods". The first one has graphical calculation methods and they can be performed with pencil and paper. The second category is based on the use of computer programs, including the rigorous thermodynamic models found in the literature.

The present study attempts to transfer the "hand calculation methods" to the computer through the MATLAB programming language so that they can be applied more quickly. "Computer methods" are not studied in the present project, although a number of ready software packages are available based on these calculations, such as Multiflash (KBC) and CSMGem (CSM: Colorado School of Mines). According to Carroll (2009), "hand calculation methods" are useful for rapid estimation of hydrate formation conditions. The drawback to these methods is that they are not very precise, but they remain widely used.

In contrast, "computer methods" are more explicit, because the physical properties of hydrates are taken into account when they are designed. For example, attention is given to the type of hydrate, the guest molecule in the hydrate, and the level of saturation (hydrates are non-stoichiometric; a stable hydrate can form without a guest molecule occupying all of the cages and the degree of saturation is a function of temperature and pressure) (Carroll, 2009). Generally "computer methods" contain fluid phase models based on equation of state models. They also have hydrate models consisting of lattice parameters for the empty hydrate and the interaction of gas molecules with water in the hydrate based on different hydrate structure. Finally, they have descriptors for different equilibrium phases, usually six (gas, hydrocarbon liquid, aqueous liquid, hydrate I, hydrate II, and ice) as shown in the phase envelop (Figure 1.17) (Schlumberger, 2010).

Below, three of the "hand calculation methods" are presented, as well as the attempt to represent them in the MATLAB programming language. The gas gravity method, the Joule-Thomson method mainly for the study of hydrate limits to gas expansion through a valve, and the distribution coefficient (K-factor method). Carroll (2009) describes other graphical methods which will not be considered in the present project.

2.1.1. The Gas Gravity Method

According to Sloan & Koh (2008), the simplest method of determining the temperature and pressure of a three-phase (L_w -H-V) gas conditions is available through the gas gravity charts developed by Katz (1945). The gas gravity chart is simply a graph of pressure and temperature with the specific gravity of the gas as a third parameter. The specific gravity of the gas (gas gravity - dimensional), which is also called the relative density, is defined as the molecular mass of the gas divided by the molecular mass of air, according to the following equation (2.1).

$$\gamma = \frac{M_w \text{ of gas}}{M_w \text{ of air}} = \frac{M_w \text{ of gas}}{28.9647} \frac{\text{gr/mol}_{\text{gas}}}{\text{gr/mol}_{\text{air}}} \quad (2.1)$$

Figure 2.1 illustrates a graphical method for approximating hydrate formation conditions and estimating the permissible expansion condition of natural gases without the formation of hydrates. Figure 2.1 shows the hydrate-forming conditions, as described by a group of "hydrate formation lines" representing natural gases with various specific gravities. Hydrates form whenever the coordinate of the point representing the pressure and temperature is located to the left of the hydrate formation line for the gas in question. This graphical correlation can be used to approximate the hydrate-forming temperature as the temperature decreases along flow string and flow lines (Ahmed, 2007).

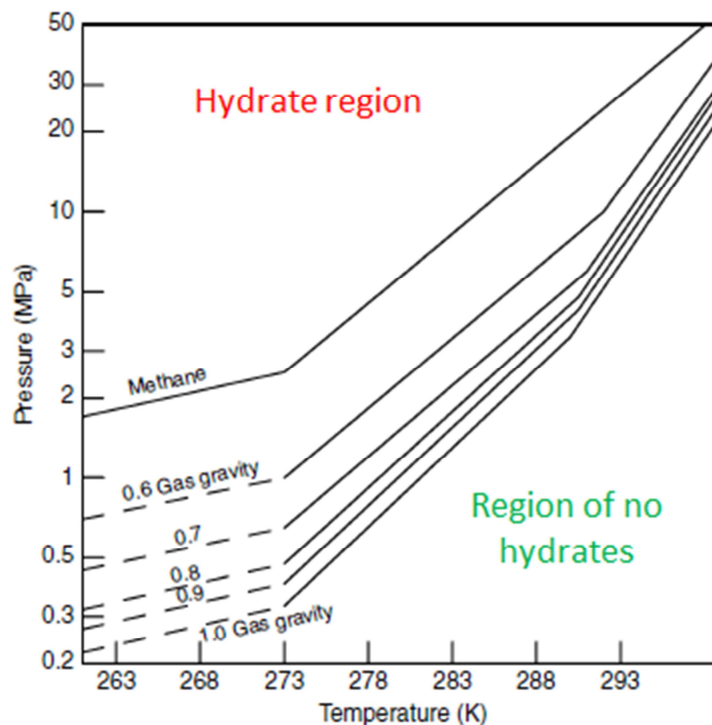


Figure 2.1: Gas gravity chart for prediction of three-phase (L_w -H-V) pressure and temperature (Sloan & Koh, 2008)

It should be pointed out that the original chart of Figure 2.1 was generated for gas containing only hydrocarbons, and should therefore be used with caution for those gases rich in noncombustibles (such as CO₂, H₂S, N₂). In addition, the gas gravity method to predict the formation of hydrates was generated from a restricted amount of data and constitutes a first estimate prediction method for hydrate formation (Sloan & Koh, 2008).

In this project, an attempt was made to represent Figure 2.1 on the computer to predict hydrate formation conditions through an algorithm (Chapter 6.1 - Appendix) for any specific gravity of the gas between the values $\gamma=1.5$ and $\gamma=0.55$. When pressure values are specified, we can calculate the hydrate formation temperature and vice versa; when we know the temperature, the hydrate formation pressure can be calculated.

For the representation of Figure 2.1, the values of the diagram were first read by assigning the pixels of the screen to the values indicated on the diagram, taking into account the logarithmic scale of the y-axis of the coordinates, the pressure axis. The process could also have been done with some graph digitizer software. In both cases, however, there is subjectivity in reading values.

- P versus T (Pressure versus Temperature) for gas gravity curves $0.6 \leq \gamma \leq 1.0$

As shown in Figure 2.2, five turning points (A_1 , A_2 , A_3 , TA_3 , and A_4) of the five curves (specifically for gas gravity $\gamma=0.6$, $\gamma=0.7$, $\gamma=0.8$, $\gamma=0.9$, and $\gamma=1.0$) of Figure 2.1 were identified, in order to design the change of the logarithm of the pressure as a function of the specific gravity for points A_1 , A_2 , A_3 , and A_4 , as well as the change of the temperature according to the specific gravity for the point TA_3 . The variations are described by linear and polynomial equations as shown in relationships from (2.2) to (2.6), as well as in Figures 2.3, 2.4, 2.5, 2.6, and 2.7.

$$A_1 = 2.0716\gamma^2 - 4.5714\gamma + 1.8435 \quad (2.2)$$

$$A_2 = 1.899\gamma^2 - 4.2227\gamma + 1.8428 \quad (2.3)$$

$$A_3 = -14.907\gamma^3 + 37.883\gamma^2 - 32.567\gamma + 10.123 \quad (2.4)$$

$$TA_3 = 3.7793\gamma + 288.26 \quad (2.5)$$

$$A_4 = -8.5599\gamma^3 + 21.234\gamma^2 - 17.817\gamma + 6.4905 \quad (2.6)$$

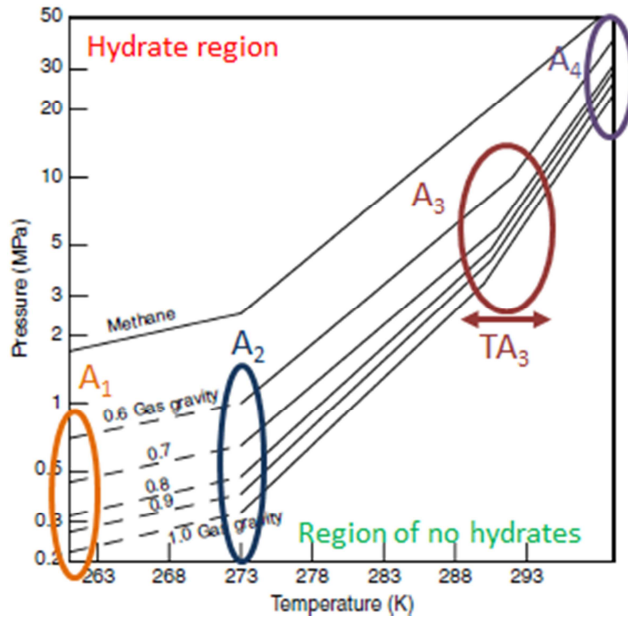


Figure 2.2: Gas gravity chart - Definition of turning points

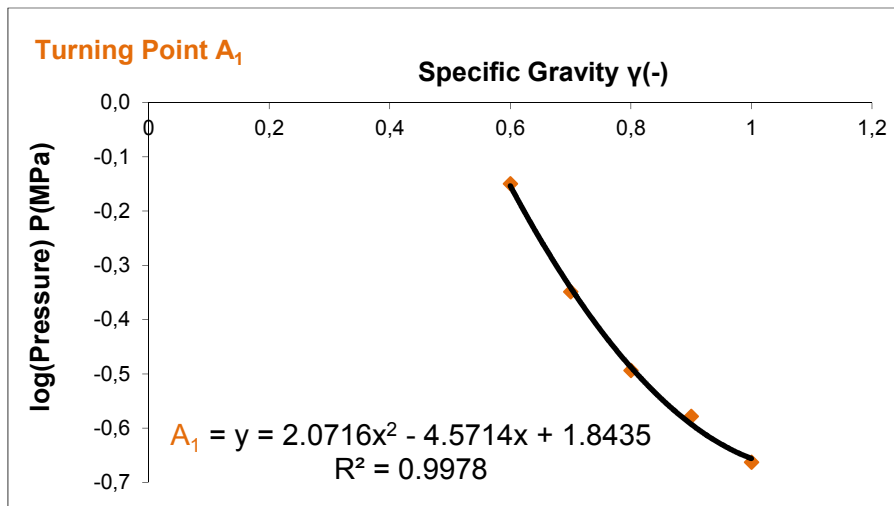


Figure 2.3: Logarithm of pressure versus specific gravity for turning point A1

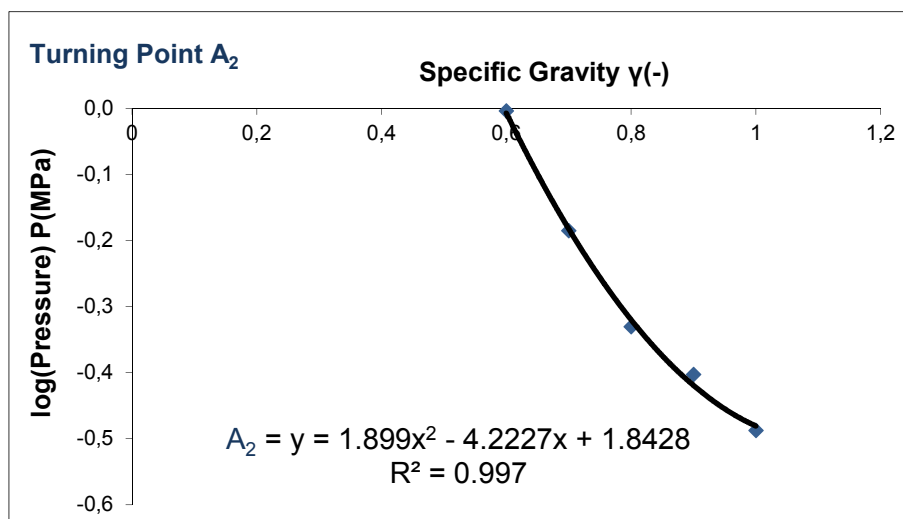


Figure 2.4: Logarithm of pressure versus specific gravity for turning point A2

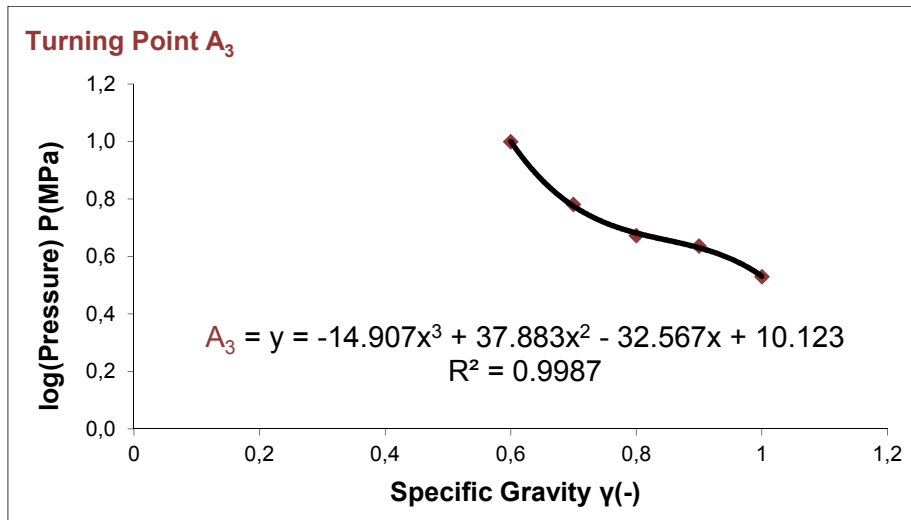


Figure 2.5: Logarithm of pressure versus specific gravity for turning point A₃

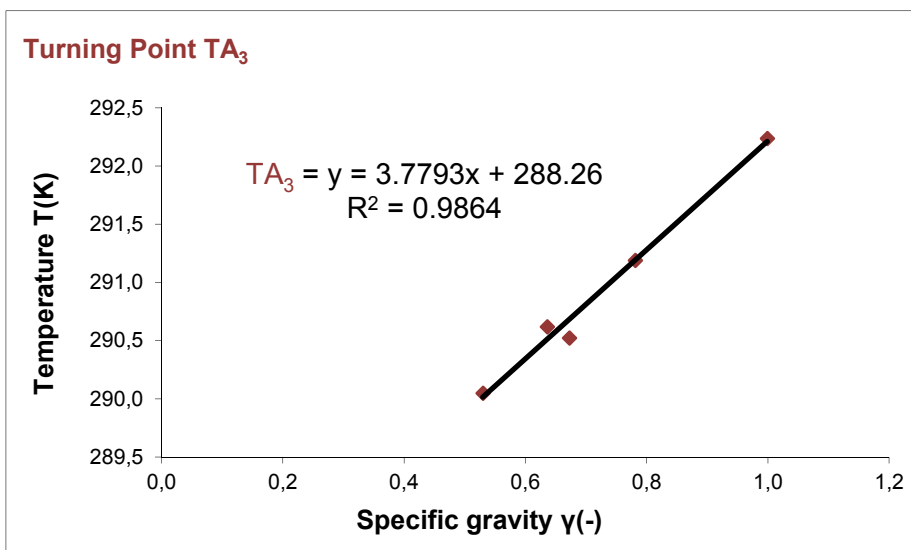


Figure 2.6: Temperature versus specific gravity for turning point TA₃

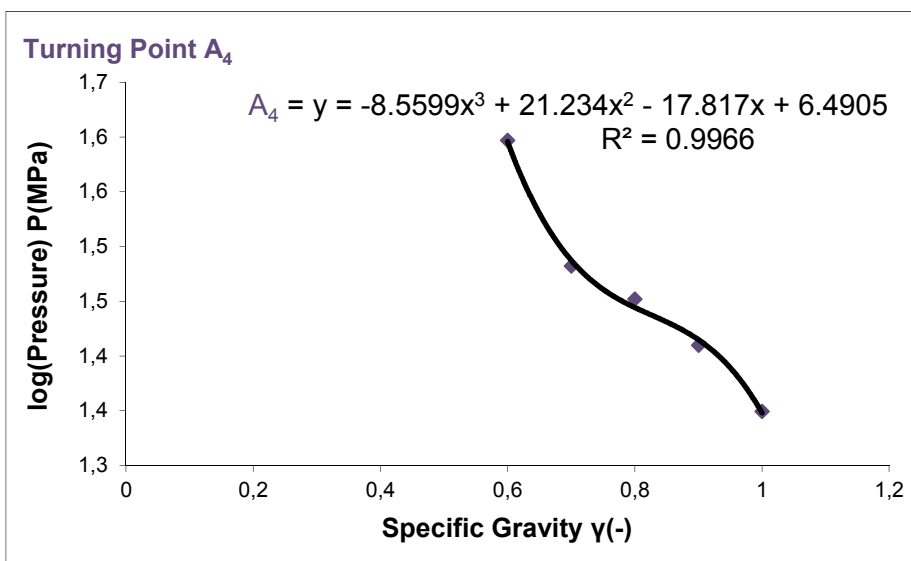


Figure 2.7: Logarithm of pressure versus specific gravity for turning point A₄

Relationships (2.7) to (2.9) give the hydrate formation pressure for specific gravity between the values $\gamma=0.6$ and $\gamma=1.0$ for a temperature range from $T=261\text{K}$ to $T=299\text{K}$ (x-axis limits of Figure 2.1), by using linear interpolation.

$$\text{For } 261 \text{ K} \leq T < 273 \text{ K} \text{ then } \log(P) = A_1 + \frac{(A_2 - A_1)(T - 261)}{(273 - 261)} \text{ where } P(\text{MPa}) \quad (2.7)$$

$$\text{For } 273 \text{ K} \leq T < T_{A_3} \text{ K} \text{ then } \log(P) = A_2 + \frac{(A_3 - A_2)(T - 273)}{(T_{A_3} - 273)} \text{ where } P(\text{MPa}) \quad (2.8)$$

$$\text{For } T_{A_3} \text{ K} \leq T < 299 \text{ K} \text{ then } \log(P) = A_3 + \frac{(A_4 - A_3)(T - T_{A_3})}{(299 - T_{A_3})} \text{ where } P(\text{MPa}) \quad (2.9)$$

- T versus P (Temperature versus Pressure) for gas gravity curves $0.6 \leq \gamma \leq 1.0$

The "Bisection Method" was used to prepare the inverse diagram of Figure 2.1, namely the temperature as a function of pressure. The bisection method is a root-finding method that applies to any continuous function given two values with opposite signs, as in our case. The method is also called the "interval halving method", the "binary search method", or the "dichotomy method", and is based on Bolzano's theorem for continuous functions.

More precisely, for $T_a=261\text{K}$ and $T_b=299\text{K}$ (x-axis limits of Figure 2.1) the average temperature was calculated ($T_{\text{avg}}=(T_a+ T_b)/2$) and based on this temperature and the specific gravity value we are interested in, which lies between the ranges $\gamma=0.6$ and $\gamma=1.0$, the hydrate formation pressure was calculated, based on the above equations (2.7), (2.8), and (2.9). When the difference between the calculated pressure and the initial pressure assumed (operating pressure of the stream) is less than an error of 0.001MPa , the iteration procedure stops. If the difference is bigger than the error, then a new temperature range is assumed, with one of the two new temperature limits being the average temperature value.

- P versus T and T versus P for methane gas gravity curve ($\gamma = 0.55$)

For the completion of Figure 2.1, the methane curve is missing, where the specific gravity of pure methane is $\gamma_{\text{methane}}=0.55$ ($\gamma_{\text{methane}}=M_{w,\text{methane}}/M_{w,\text{air}}=16.043/28.9647$) based on equation (2.1). The methane curve differs from the other five curves of Figure 2.1, for specific gravity from $\gamma=0.6$ to $\gamma=1.0$, therefore the points of methane curve were not included in the above procedure, as shown in Figure 2.2.

The procedure performed for adding the methane curve is similar to the procedure described above. Points A_1 , A_2 , A_3 and T_{A_3} were initially read for methane curve. The

hydrate formation pressure was then calculated for a specific gravity value of $\gamma_{\text{methane}}=0.55$ using equation (2.7) for a temperature range of $T=261\text{K}$ to $T=273\text{K}$ and equation (2.8) for a temperature range of $T=273\text{K}$ to $T=291\text{K}$. The reverse procedure for reading the hydrate formation temperature knowing the operating pressure, for $\gamma_{\text{methane}}=0.55$, was performed again via the bisection method.

- P versus T and T versus P for gas gravity curves $0.55 \leq \gamma < 0.6$

To predict the hydrate formation pressure for specific gravity values between $\gamma_{\text{methane}}=0.55$ and $\gamma=0.6$, a linear interpolation was performed taking into account the logarithmic scale of the pressure values. Specifically, for temperature range $T=261\text{K}$ and $T=299\text{K}$ (x-axis limits of Figure 2.1) and specific gravity range between $\gamma_{\text{methane}}=0.55$ and $\gamma=0.6$, the hydrate formation pressure was assumed to be given by the equation (2.10). Conversely, to calculate the hydrate formation temperature for a range of specific gravity values between $\gamma_{\text{methane}}=0.55$ and $\gamma=0.6$ at any operating pressure, equation (2.11) was used. The pressure is in MPa, and the temperature in Kelvin degrees in equations (2.10) and (2.11) below.

$$\text{For } 0.55 \leq \gamma < 0.6 \text{ then } \log(P) = \log(P_{\text{methane}}) + \frac{[\log(P_{\gamma=0.6}) - \log(P_{\text{methane}})] (\gamma - 0.55)}{(0.6 - 0.55)} \quad (2.10)$$

$$\text{For } 0.55 \leq \gamma \leq 0.6 \text{ then } T = T_{\text{methane}} + \frac{(T_{\gamma=0.6} - T_{\text{methane}}) (\gamma - 0.55)}{(0.6 - 0.55)} \quad (2.11)$$

- P versus T - Graphical representation of the Figure 2.1

Figure 2.8 depicts the virtual representation of Figure 2.1 of the literature. From Figure 2.8, it is possible to read the hydrate formation pressure or temperature conditions, having as its initial values the specific gravity of the gas which lies between the values $\gamma_{\text{methane}}=0.55$ and $\gamma=1.0$, and the operating temperature or pressure of the stream, respectively.

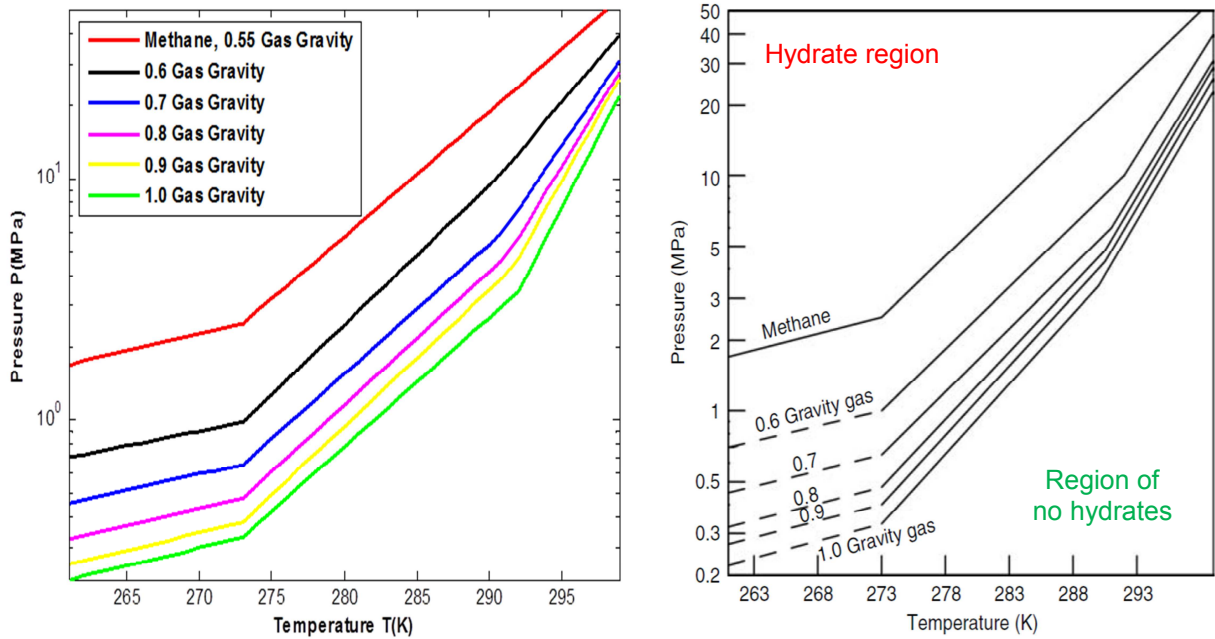


Figure 2.8: Representation of Figure 2.1 - Hydrate locus using the gas gravity method

- P versus T and T versus P for gas gravity curves for $\gamma < 0.55$ and $\gamma > 1.0$

For specific gravity smaller than $\gamma_{\text{methane}}=0.55$, it is apparent that hydrate formation problem still exist, as shown in the respective graph area. We can no longer calculate hydrate formation pressure or temperature, as the pure methane curve is the lightest curve in the phase envelop chart, as illustrated in Figure 1.17.b.

For specific gravity greater than $\gamma=1.0$, according to the Gas Processors Suppliers Association (2004), Figure 2.9 gives the hydrate pressure-temperature equilibrium curves for pure methane, ethane, propane, and for a nominal 70% ethane and 30% propane mix. Figure 2.9 gives the conditions for hydrate formation for light gases.

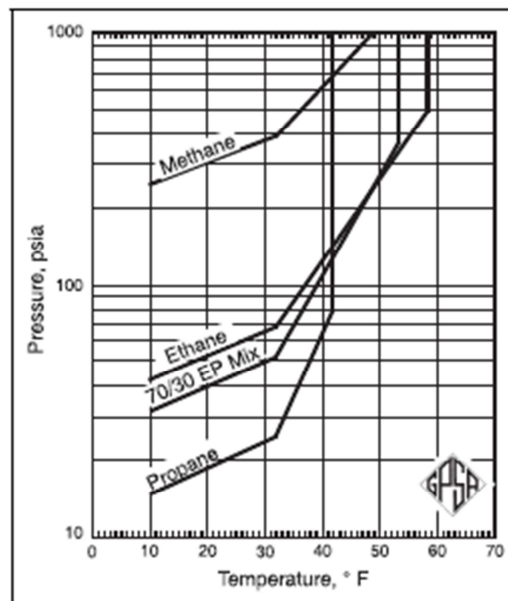


Figure 2.9: Conditions for hydrate formation for light gases (GPSA, 2004)

For the representation of Figure 2.9, the same procedure as described for the representation of Figure 2.1 was followed. The diagram values were initially read by finding the intersection points A_1 , A_2 , A_3 , and TA_3 of the ethane curve with $\gamma_{\text{ethane}}=1.04\approx 1.0$ ($\gamma_{\text{ethane}}=M_{w,\text{ethane}}/M_{w,\text{air}}=30.070/28.9647$) and propane curve with specific gravity $\gamma_{\text{propane}}=1.5$ ($\gamma_{\text{propane}}=M_{w,\text{propane}}/M_{w,\text{air}}=44.097/28.9647$). A correlation of ethane mol fraction (F_{ethane}) with specific gravity, as indicated by the equation (2.12), was used to read the pressure versus temperature diagram values between $\gamma_{\text{ethane}}=1.0$ and $\gamma_{\text{propane}}=1.5$.

$$\begin{aligned}\gamma &= \frac{M_{w \text{ of gas}}}{M_{w \text{ of air}}} = \frac{F_{\text{ethane}} M_{w, \text{ethane}} + (1 - F_{\text{ethane}}) M_{w, \text{propane}}}{M_{w \text{ of air}}} = \frac{[F_{\text{ethane}} 30.070 + (1 - F_{\text{ethane}}) 44.097] \text{ gr/mol}}{28.9647 \text{ gr/mol}} \\ &\Rightarrow \gamma = 1.038 F_{\text{ethane}} + 1.522 (1 - F_{\text{ethane}}) \\ &\Rightarrow \gamma = 1.522 - 0.484 F_{\text{ethane}} \\ &\Rightarrow F_{\text{ethane}} = 3.145 - 2.066 \gamma\end{aligned}\quad (2.12)$$

For the temperature range from $T=10^\circ\text{F}$ to $T=32^\circ\text{F}$, equation (2.13) was used based on linear interpolation, while for the temperature range from $T=32^\circ\text{F}$ to the turning point TA_3 , equation (2.14) was used, based on the slope of the straight lines of pure ethane (SL_{ethane}) and propane (SL_{propane}).

$$\text{For } 10^\circ\text{F} \leq T < 32^\circ\text{F} \text{ then } \log(P) = A_1 + \frac{(A_2 - A_1)(T - 10)}{(32 - 10)} \text{ where } P(\text{psia}) \quad (2.13)$$

$$\begin{aligned}\text{For } 32^\circ\text{F} \leq T < TA_3^\circ\text{F} \text{ then } \log(P) &= A_2 + [SL_{\text{ethane}} F_{\text{ethane}} + SL_{\text{propane}} (1 - F_{\text{ethane}})](T - 32) \\ &\text{where } P(\text{psia}) \quad (2.14)\end{aligned}$$

In order to read the reverse diagram, the temperature values as a function of pressure were again used in the bisection method. It is worth noting that the units of measurement in Figure 2.9 are in field units, while in Figure 2.1 in SI units, therefore units must be converted as well. Figure 2.10 depicts the virtual representation of Figure 2.9 of the literature.

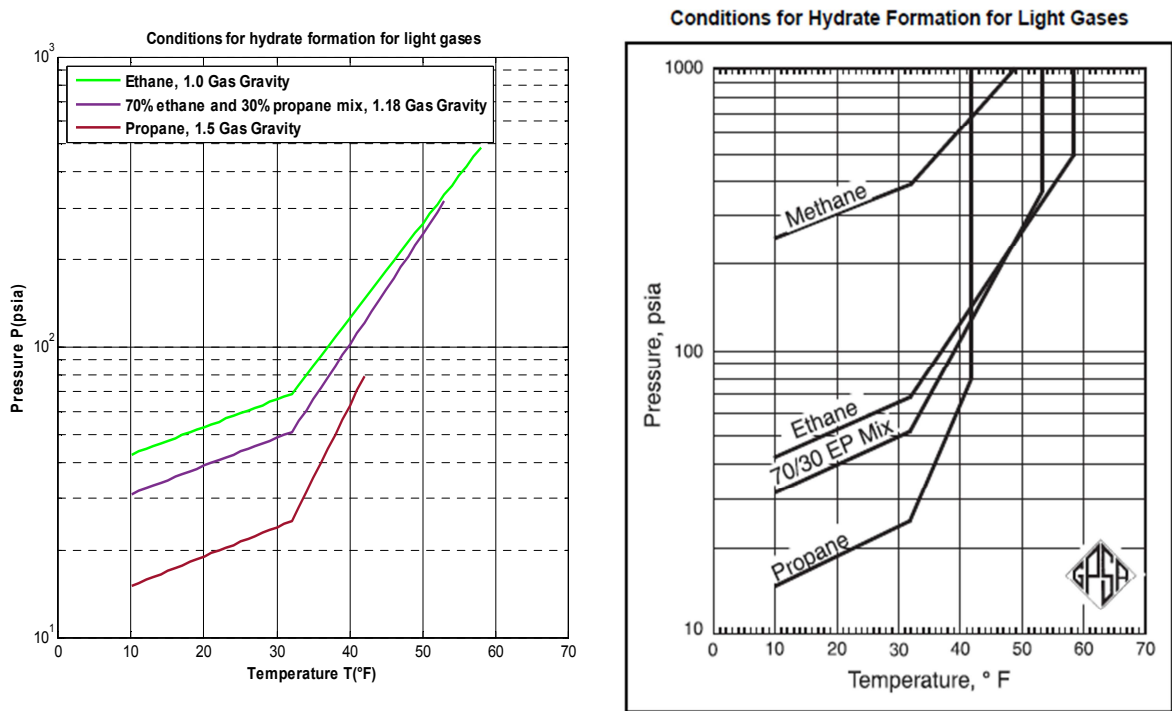


Figure 2.10: Representation of Figure 2.9 - Hydrate locus using the gas gravity method for light gases

It is worth noting that in Figure 2.10 there is good accuracy for approaching temperature values, but for pressure there is a deviation. The error is about 30psia of pressure reading in the diagram, where relevant, so the logic for the intermediate slope between the pure ethane and propane components does not accurately yield the data in Figure 2.9.

For specific gravity greater than $\gamma_{\text{propane}}=1.5$, it becomes apparent that the hydrate formation problem is not present as it is shown in the respective graph area. It is observed from phase envelope of Figure 1.17.b that a similar procedure could be performed for n-butane and i-butane components; however, for heavier components than pentane (C_{5+}) it is not probable.

2.1.2. Joule-Thomson Charts - Hydrate Limits to Gas Expansion through a Valve

According to Ahmed & McKinney (2005), the graphical correlation presented in Figure 2.1 (the gas gravity method) was developed for pure water-gas systems; however, when dissolved solids are present in the water, temperature reduction takes place so natural gases form hydrates. On water-wet gas rapid expansion, through a valve, orifice, or other restrictions, hydrates may form due to rapid gas cooling caused by Joule-Thomson expansion, as described in equation (2.15).

$$\frac{\partial T}{\partial P} = \frac{R T^2}{P C_p} \left(\frac{\partial Z}{\partial T} \right)_p \quad (2.15)$$

T & P: Temperature & Pressure

Z & C_p: Gas compressibility factor & Specific heat at constant pressure

This decrease in temperature because of the rapid pressure decrease ($\partial T/\partial P$) could lead to condensation of water vapor from the gas and make the mixture conducive to the formation of hydrates. Figures 2.11, 2.12, and 2.13 (for gas gravities of $\gamma=0.6$, $\gamma=0.7$, $\gamma=0.8$, $\gamma=0.9$, and $\gamma=1.0$) can be used to calculate the maximum pressure reduction without inducing the hydrates formation. These Figures are provided for hydrate limits to isenthalpic ($\Delta H=0$) Joule-Thomson expansions, such as that which happens when a gas containing free water droplets flows through a valve. The chart is entered at the intersection of the initial pressure and initial temperature isotherm; and the lowest pressure to which the gas can be expanded without forming hydrate lies directly from the x-axis below the intersection.

Furthermore, according to Gas Processors Suppliers Association (2004), the Figure 2.11.a would predict permissible expansion only to a pressure around 700psia. The Katz correlation is not recommended above 1000-1500psia, depending on composition. Prediction of hydrate formation conditions at higher pressures demands the use of other methods, such as K-factor method (presented in the next chapter 2.1.3), which, in general, are valid to 4000psia. Experimental studies have also yielded correlations for hydrate formation at pressures up to 14500psia. Therefore, Joule-Thomson charts should only be used for first approximation of hydrate formation conditions, like the gas gravity charts due to their method of derivation.

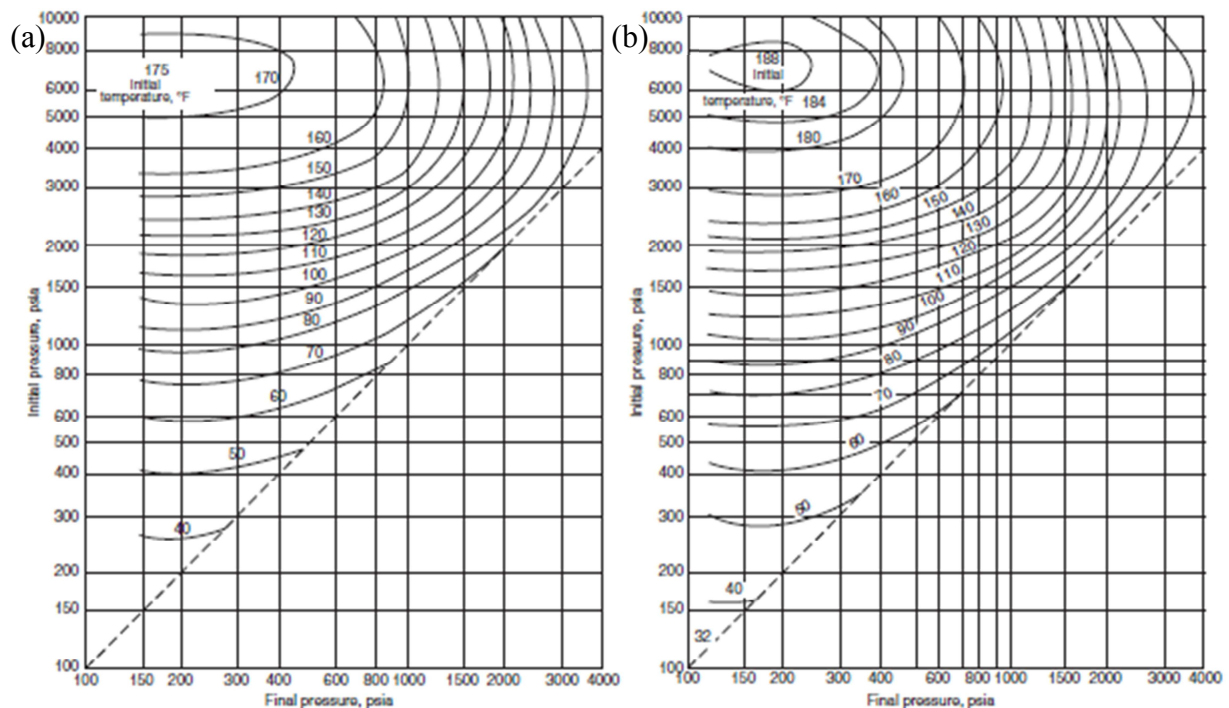


Figure 2.11: Permissible expansion of (a) a 0.6, and (b) a 0.7 gravity natural gas without hydrate formation (Ahmed & McKinney, 2005)

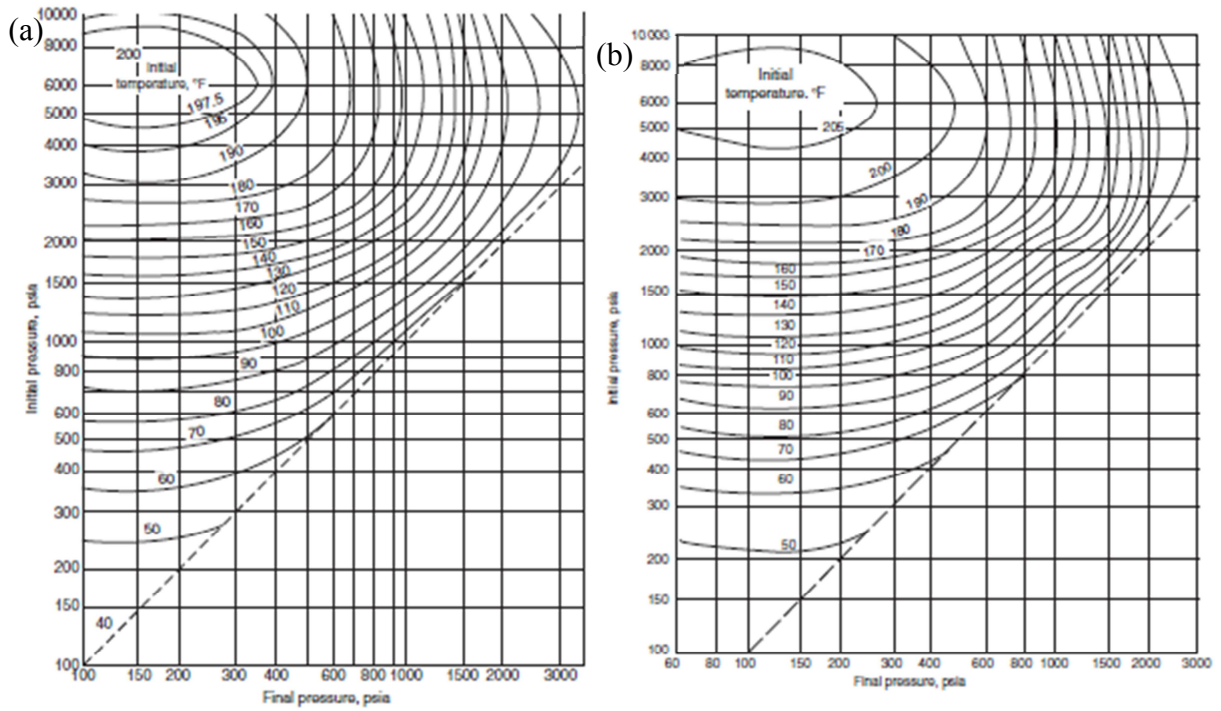


Figure 2.12: Permissible expansion of (a) a 0.8, and (b) a 0.9 gravity natural gas without hydrate formation (Ahmed & McKinney, 2005)

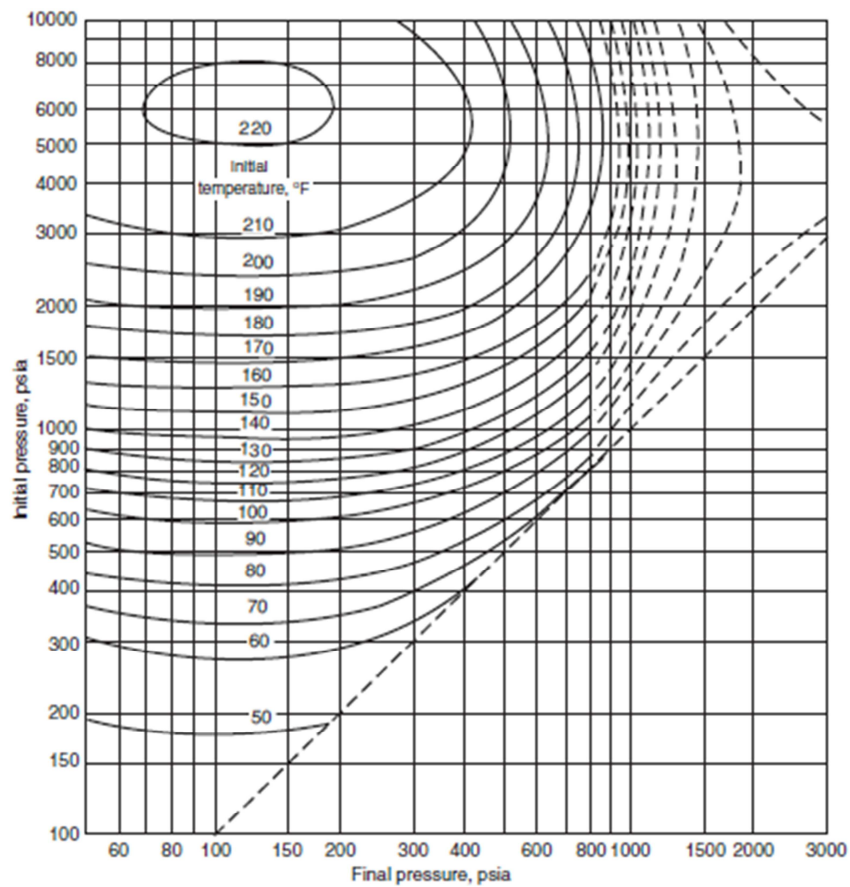


Figure 2.13: Permissible expansion of a 1.0 gravity natural gas without hydrate formation (Ahmed & McKinney, 2005)

Based on Ahmed & McKinney (2005), the mathematical modeling of Figures 2.11, 2.12, and 2.13 is presented; this modeling was performed according to the study by Ostergaard et al. (1998), who introduced a new correlation to foresee the hydrate-free zone of reservoir fluids that vary in composition from black oil to lean natural-gas systems. The components of the hydrocarbon system were divided into two groups. The first includes components such as methane, ethane, propane, and butanes and is called hydrate-forming hydrocarbons. The second contains pentanes and heavier components and is called non-hydrate-forming hydrocarbons. Based on the above two categories, the following correlating parameters were determined, as indicated by the relationships (2.16) through (2.19).

$$f_h = y_{C_1} + y_{C_2} + y_{C_3} + y_{i-C_4} + y_{n-C_4} \quad (2.16)$$

$$f_{nh} = y_{C_{5+}} \quad (2.17)$$

$$F_m = \frac{f_{nh}}{f_h} \quad (2.18)$$

$$\gamma_h = \frac{M_{w \text{ of h}}}{M_{w \text{ of air}}} = \frac{\sum_{i=C_1}^{n-C_4} y_i M_{w i}}{28.9647 \text{ gr/mol}_{\text{air}}} \quad (2.19)$$

h: hydrate-forming components C_1 through C_4

nh: non-hydrate-forming components, C_5 and heavier

F_m : molar ratio between the non-hydrate-forming and hydrate-forming components

γ_h : specific gravity of hydrate-forming components

The hydrate dissociation pressure (P_h in psia) of fluids containing only hydrocarbons is given by the equation (2.20), where temperature is in Rankine degrees, while the parameters (α_i) of the equation (2.20) are given in Table 2.1. The equation (2.20) can also be arranged and solved for the temperature, as describes equation (2.21). According to Ahmed & McKinney (2005), equation (2.20) was developed using data on black oil, volatile oil, gas condensate, and natural gas systems in the range of 32°F (0°C) to 68°F (20°C), which covers the practical range of hydrate formation for reservoir fluids transportation.

$$P_h = 0.1450377 \exp \left\{ \left[\frac{\alpha_1}{(\gamma_h + \alpha_2)^3} + \alpha_3 F_m + \alpha_4 F_m^2 + \alpha_5 \right] T + \left[\frac{\alpha_6}{(\gamma_h + \alpha_7)^3} + \alpha_8 F_m + \alpha_9 F_m^2 + \alpha_{10} \right] \right\} \quad (2.20)$$

$$T = \frac{\ln(6.89476 P_h) - \left[\frac{\alpha_6}{(\gamma_h + \alpha_7)^3} + \alpha_8 F_m + \alpha_9 F_m^2 + \alpha_{10} \right]}{\left[\frac{\alpha_1}{(\gamma_h + \alpha_2)^3} + \alpha_3 F_m + \alpha_4 F_m^2 + \alpha_5 \right]} \quad (2.21)$$

Table 2.1: The values of constants in equation (2.20) (Ahmed & McKinney, 2005)

a_i	Value	a_i	Value
a₁	2.5074400E-03	a₆	3.6625000E-04
a₂	0.4685200	a₇	-0.4850540
a₃	1.2146440E-02	a₈	-5.4437600
a₄	-4.6761110E-04	a₉	3.8900000E-03
a₅	0.0720122	a₁₀	-29.9351000

In addition, the nitrogen and carbon dioxide components were noted not to adhere to equation (2.20) describing the general behavior for hydrocarbons. Therefore, in order to estimate the pressure of the above components (y_{N_2} : mole fraction of nitrogen and y_{CO_2} : mole fraction of carbon dioxide) in the hydrocarbon system, correction factors were developed for each of the two non-hydrocarbon fractions, as described in equations (2.22) through (2.27).

$$E_{CO_2} = 1.0 + \left[(b_1 F_m + b_2) \frac{y_{CO_2}}{1 - y_{N_2}} \right] \quad (2.22)$$

$$E_{N_2} = 1.0 + \left[(b_3 F_m + b_4) \frac{y_{N_2}}{1 - y_{CO_2}} \right] \quad (2.23)$$

$$b_1 = -2.0943 \times 10^{-4} T^3 + 3.809 \times 10^{-3} T^2 - 2.42 \times 10^{-2} T + 0.423 \quad (2.24)$$

$$b_2 = 2.3498 \times 10^{-4} T^2 - 2.086 \times 10^{-3} T^2 + 1.63 \times 10^{-2} T + 0.650 \quad (2.25)$$

$$b_3 = 1.1374 \times 10^{-4} T^3 + 2.61 \times 10^{-4} T^2 + 1.26 \times 10^{-2} T + 1.123 \quad (2.26)$$

$$b_4 = 4.335 \times 10^{-5} T^3 - 7.7 \times 10^{-5} T^2 + 4.0 \times 10^{-3} T + 1.048 \quad (2.27)$$

where

$$T: \text{Temperature in Celsius degrees } (^{\circ}C), \quad T (^{\circ}C) = \frac{T (^{\circ}R)}{1.8} - 273.15$$

Therefore, the total hydrate dissociation pressure (P_{corr} in psia) is given by the equation (2.28).

$$P_{corr} = P_h E_{CO_2} E_{N_2} \quad (2.28)$$

2.1.3. The Distribution Coefficient Method (The K-factor Method)

According to Sloan & Koh (2008), the distribution coefficient method or " K_{vs} -value" or "K-factor method" was devised and originated in the early 1940s from Carson & Katz (1942); however, the most detailed methane, ethane, and propane charts are from the latter reference. The distribution coefficient charts for each of the components, commonly found in natural gas for performing hydrate calculations, are illustrated in Figures 2.14, 2.15, 2.16, and 2.17 in SI system units.

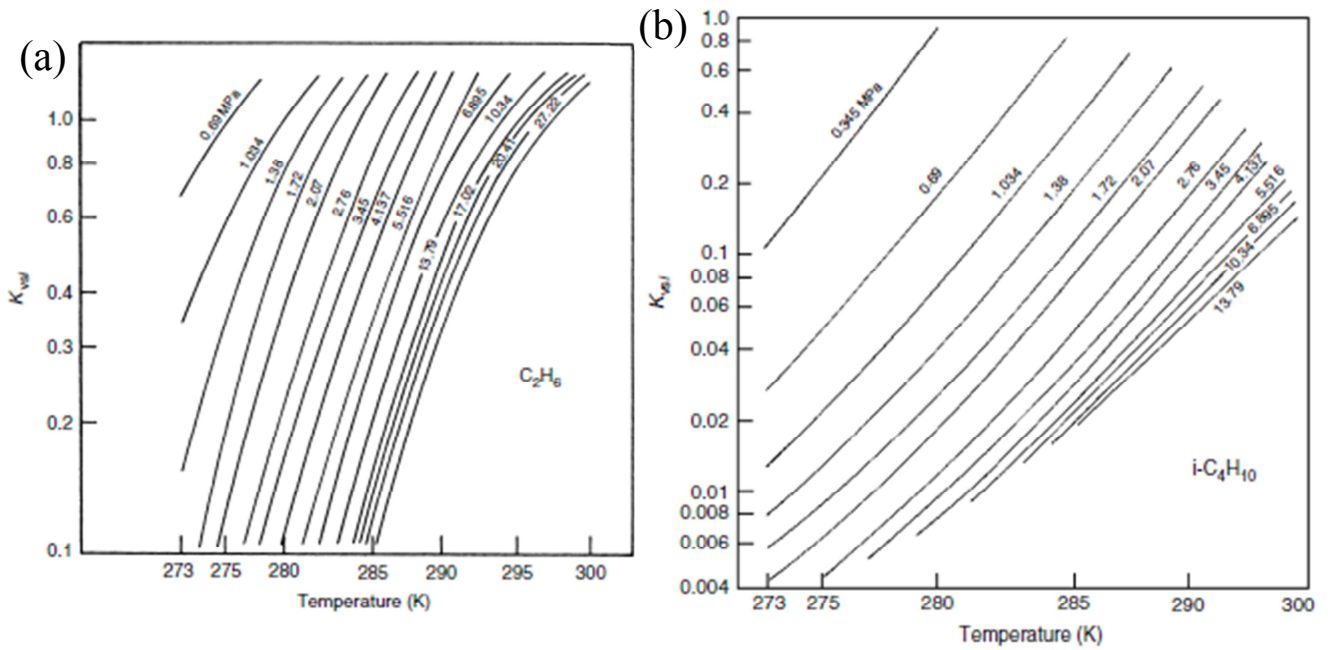


Figure 2.14: Vapor-solid equilibrium constants for (a) ethane, and (b) isobutane (Sloan & Koh, 2008)

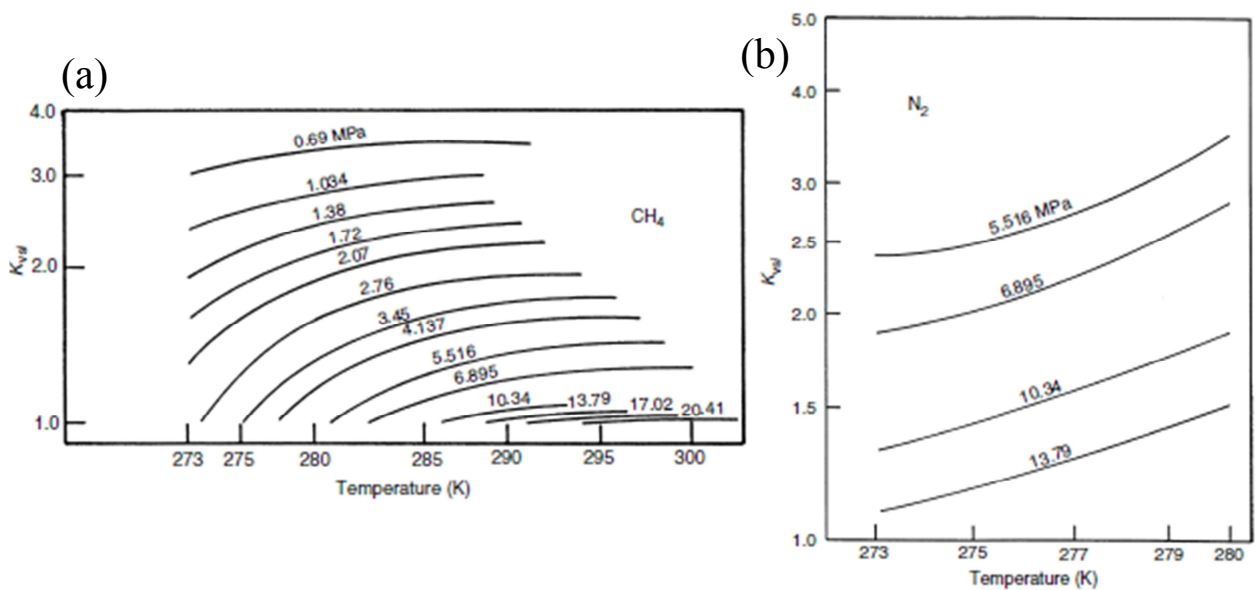


Figure 2.15: Vapor-solid equilibrium constants for (a) methane, and (b) nitrogen (Sloan & Koh, 2008)

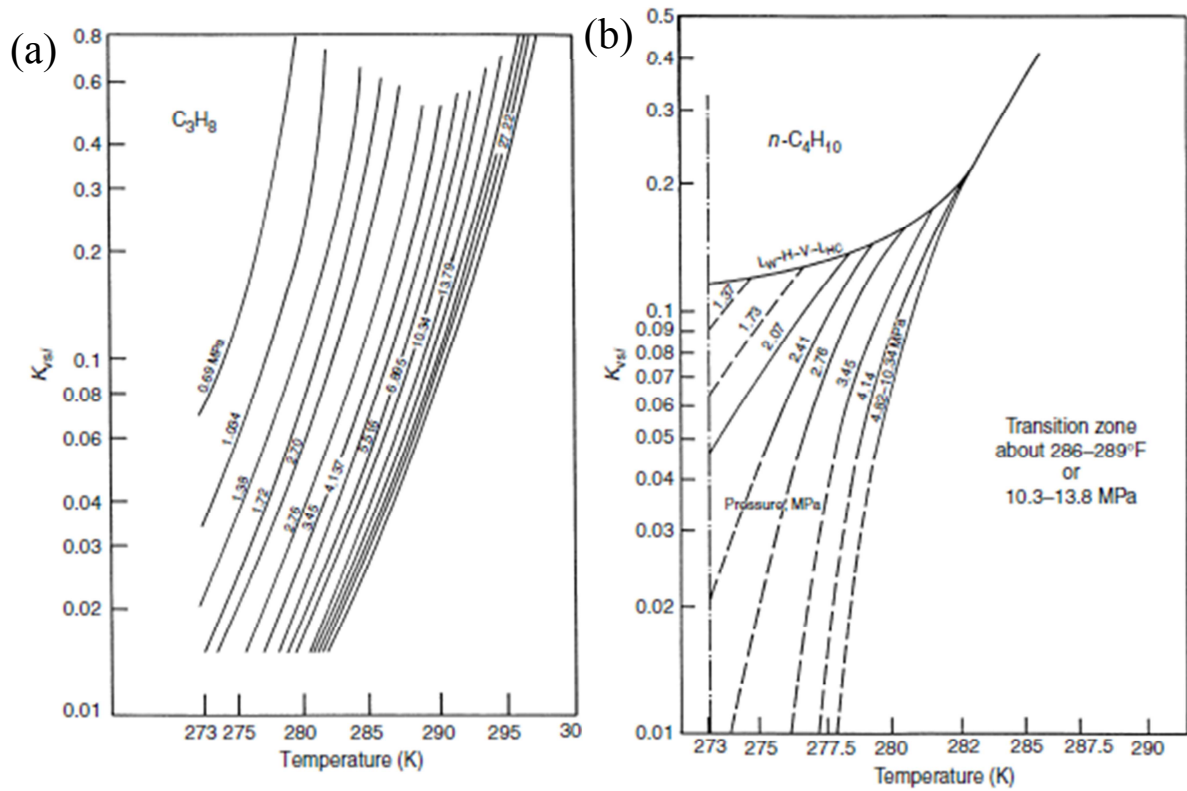


Figure 2.16: Vapor-solid equilibrium constants for (a) propane, and (b) n-butane (Sloan & Koh, 2008)

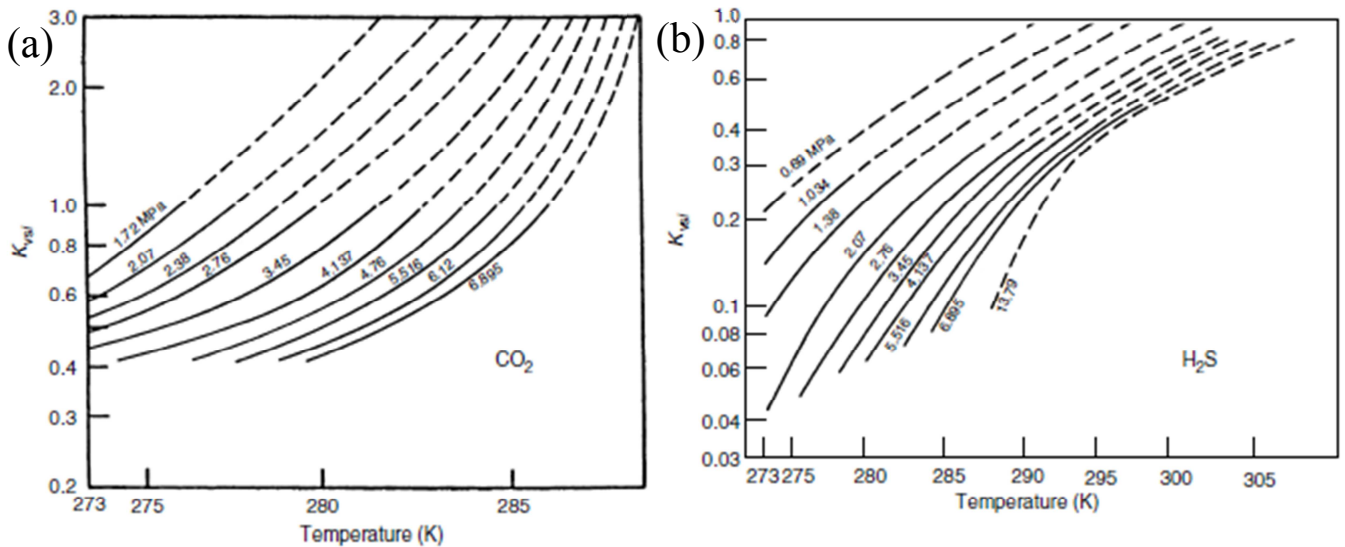


Figure 2.17: Vapor-solid equilibrium constants for (a) carbon dioxide, and (b) hydrogen sulfide (Sloan & Koh, 2008)

Carson and Katz (1942) adopted the concept of the equilibrium ratios (K values), for estimating the three-phase (L_w-H-V) hydrate-forming conditions. They suggested that hydrates are the equivalent of solid solutions and not mixed crystals, and therefore argued that hydrate-forming conditions could be estimated from empirically determined vapor-solid equilibrium ratios as defined by equation (2.29):

$$K_{v-si} = \frac{y_i}{x_{si}} \quad (2.29)$$

K_{v-si} : equilibrium ratio of component i between vapor and solid

y_i : mole fraction of component i in the water-free vapor (gas) phase

x_{si} : mole fraction of component i in the solid phase on a water-free basis

Equation (2.29) refers only to mixtures and is not recommended for pure components. In particular, normal butane cannot form a hydrate by itself but can be conducive to hydrate formation in a mixture. For calculation purposes, all molecules too large to form hydrates have a K_{v-si} of infinity. These include all normal paraffin hydrocarbon molecules larger than normal butane. Nitrogen is assumed to be a non-hydrate former and is also assigned a K_{v-si} of infinity (Gas Processors Suppliers Association, 2004).

The above Figures (2.14 through 2.17) have been converted to correlations in temperature and pressure using the equation (2.30) based on Sloan & Koh (2008), where pressure is in psia units and temperature in Fahrenheit degrees. Table 2.2 provides the values of coefficients A through S for each component in Sloan's equation (2.30).

$$\begin{aligned} \ln(K_{v-si}) = & A + B T + C P + D T^{-1} + E P^{-1} + F P T + G T^2 + H P^2 + \\ & + I P T^{-1} + J \ln(P T^{-1}) + K P^{-2} + L T P^{-1} + M T^2 P^{-1} + \\ & + N P T^{-2} + O T P^{-3} + Q T^3 + R P^3 T^{-2} + S T^4 \end{aligned} \quad (2.30)$$

Table 2.2: The values of coefficients A through S in equation (2.30) (Sloan & Koh, 2008)

Component	CH ₄	C ₂ H ₆	C ₃ H ₈	<i>i</i> -C ₄ H ₁₀	<i>n</i> -C ₄ H ₁₀	N ₂	CO ₂	H ₂ S
A	1.63636	6.41934	-7.8499	-2.17137	-37.211	1.78857	9.0242	-4.7071
B	0.0	0.0	0.0	0.0	0.86564	0.0	0.0	0.06192
C	0.0	0.0	0.0	0.0	0.0	-0.001356	0.0	0.0
D	31.6621	-290.283	47.056	0.0	732.20	-6.187	-207.033	82.627
E	-49.3534	2629.10	0.0	0.0	0.0	0.0	0.0	0.0
F	-5.31E-06	0.0	-1.17E-06	0.0	0.0	0.0	4.66E-05	-7.39E-06
G	0.0	0.0	7.145E-04	1.251E-03	0.0	0.0	-6.992E-03	0.0
H	0.0	-9.0E-08	0.0	1.0E-08	9.37E-06	2.5E-07	-2.89E-06	0.0
I	0.128525	0.129759	0.0	0.166097	-1.07657	0.0	-6.223E-03	0.240869
J	-0.78338	-1.19703	0.12348	-2.75945	0.0	0.0	0.0	-0.64405
K	0.0	-84600	16690	0.0	0.0	0.0	0.0	0.0
L	0.0	-71.0352	0.0	0.0	-66.221	0.0	0.0	0.0
M	0.0	0.596404	0.23319	0.0	0.0	0.0	0.27098	0.0
N	-5.3569	-4.7437	0.0	0.0	0.0	0.0	0.0	-12.704
O	0.0	78200	-44800	-884	917000	587000	0.0	0.0
Q	-2.3E-07	0.0	5.5E-06	0.0	0.0	0.0	8.82E-05	-1.3E-06
R	-2.0E-08	0.0	0.0	-5.4E-07	4.98E-06	1.0E-08	2.55E-06	0.0
S	0.0	0.0	0.0	-1.0E-08	-1.26E-06	1.1E-07	0.0	0.0

According to Sloan & Koh (2008), the above charts (Figures 2.14 through 2.17) determine in which phase a component will concentrate. More precisely, components such as methane and nitrogen have K_{v-si} values always greater than unity, so they concentrate in the vapor rather than the hydrate; components such as propane or isobutane with K_{v-si} values normally less than unity are concentrated in the hydrate phase.

The condition for initial hydrate formation from free water and gas is calculated from an equation analogous to the dew point in vapor-liquid equilibrium, as described by equation (2.31). The calculation is iterative and convergence is achieved when the objective function (2.31) is satisfied.

$$\sum_{i=1}^{i=n} X_{si} = \sum_{i=1}^{i=n} \frac{Y_i}{K_{v-si}} = 1 \quad (2.31)$$

In this project, an attempt was made to represent the above method based on the three equations (2.29), (2.30), and (2.31). Two types of calculations were performed (Chapter 6.2 - Appendix). The first process having as data the gas composition and operating temperature gives the hydrate formation pressure. The second one having as data the gas composition and operating pressure gives the hydrate formation temperature.

The iterative method, which was used for mathematical modeling of the above problem, is based on "Newton-Raphson". This method (presumably the most popular) is based on the development of a non-linear function in Taylor series and is a root-finding method. The Taylor expansion is used to calculate the approximate value of a function, with the desired precision in the area of the point of interest.

More precisely, in the first case a hypothesis of hydrate formation pressure was made. If the original assumption is correct, and the equation (2.31) is satisfied with a tolerance of 10^{-5} , the process stops. If the initial hypothesis of hydrate formation pressure does not satisfy the equation (2.31), an iterative process is initiated, with a maximum repetition rate of 100 iterations.

A pressure difference $dP=10^{-4}$ psia is added to the assumed initial pressure. Under the new pressure, the sum of mole fractions for all components in liquid phase of Table 2.2 is calculated. This needs to be equal to unity according to the equation (2.31). The new pressure satisfying the constraint (2.31) is given by the equation (2.32) as shown below.

$$\sum_{i=1}^{i=n} X_{si, \text{ for } P=P^{\text{assumption}}+\Delta P} = \sum_{i=1}^{i=n} X_{si, \text{ for } P^{\text{assumption}}} + \frac{d\left(\sum_{i=1}^{i=n} X_{si}\right)}{dP} \Delta P$$

$$\begin{aligned}
(2.31) \quad & \Rightarrow 1 - \sum_{i=1}^{i=n} x_{si, \text{ for } P^{\text{assumption}}} = \frac{d\left(\sum_{i=1}^{i=n} x_{si}\right)}{dP} \Delta P \\
& \Rightarrow \Delta P = \frac{1 - \sum_{i=1}^{i=n} x_{si, \text{ for } P^{\text{assumption}}}}{d\left(\sum_{i=1}^{i=n} x_{si}\right)/dP} \\
& \Rightarrow P = P^{\text{assumption}} + \frac{1 - \sum_{i=1}^{i=n} x_{si, \text{ for } P^{\text{assumption}}}}{d\left(\sum_{i=1}^{i=n} x_{si}\right)/dP} \quad (2.32)
\end{aligned}$$

$$\text{where } \frac{d\left(\sum_{i=1}^{i=n} x_{si}\right)}{dP} = \frac{\sum_{i=1}^{i=n} x_{si, \text{ for } P=P^{\text{assumption}}+\Delta P} - \sum_{i=1}^{i=n} x_{si, \text{ for } P^{\text{assumption}}}}{dP}$$

In the second case, a similar technique is followed to determine the three-phase temperature at a given operating pressure and composition of the gas. In this case, the difference is that the sum of mole fractions is calculated for all the components of Table 2.2 for each temperature. This again needs to be equal to unity according to the equation (2.31). In this iteration procedure, a maximum number of repetitions of 100 was set, a tolerance equal to 10^{-7} for the sum of the equation (2.31), and a temperature difference $dT=10^{-4}$ °F. Its corresponding equation (2.32) for temperature change is the equation (2.33).

$$T = T^{\text{assumption}} + \frac{1 - \sum_{i=1}^{i=n} x_{si, \text{ for } T^{\text{assumption}}}}{d\left(\sum_{i=1}^{i=n} x_{si}\right)/dT} \quad (2.33)$$

$$\text{where } \frac{d\left(\sum_{i=1}^{i=n} x_{si}\right)}{dT} = \frac{\sum_{i=1}^{i=n} x_{si, \text{ for } T=T^{\text{assumption}}+\Delta T} - \sum_{i=1}^{i=n} x_{si, \text{ for } T^{\text{assumption}}}}{dT}$$

In both cases, the initial estimate of the pressure or temperature should be within the range of the final solution. As mentioned above, the Newton-Raphson method is based on the use of

Taylor expansion of non-linear equations in the region around an initial estimate of the solution, cutting off higher order terms and maintaining only the linear terms, and sequential improvement of the initial estimate.

Therefore, for this system, we do not know in advance how many solutions there are and some solutions may not have a physical meaning, such as negative pressure or absolute temperature in response. Therefore, a constraint is introduced; if pressure or absolute temperature is negative, then the method stops and a better initial estimate is asked for.

The distribution coefficient method (K-factor method) was conceived before the determination of the hydrate crystal structures. It should be thermodynamically impossible for one set of K_{v-si} charts to serve both hydrate structures (sI and sII), due to different energies of formation. That is, the K_{v-si} at a given temperature for methane in a mixture of sI formers cannot be the same as that for methane in a mixture of sII formers because the crystal structures differ dramatically. Different crystal structures lead to different x_{si} values that are the denominator of $K_{v-si}=y_i/x_{si}$. This imprecision may be reduced because, in addition to the major component methane, most natural gases contain small amounts of components such as ethane, propane, and isobutane, which cause sII hydrate structure to predominate in production/transportation/processing applications (Sloan & Koh, 2008). Furthermore, according to Gas Processors Suppliers Association (2004), caution should be shown when some higher molecular weight isoparaffins and certain cycloalkanes are present as they can form structure H hydrates.

According to Ahmed & McKinney (2005), the vapor-solid equilibrium ratio cannot be used to perform flash calculations (Joule-Thomson charts are more appropriate) and determine hydrate-phase splits or equilibrium phase compositions, since K_{v-si} is based on the mole fraction of a "guest" component in the solid-phase hydrate mixture on a water-free basis.

Even with such restrictions, the K-factor method was the first predictive method, and it was used as the basis for the calculations in the gravity method, so it is logical that the K-factor method should be more accurate.

2.2. Injection of Inhibitors

The hydrate dissociation curve may be shifted toward lower temperatures by adding a hydrate inhibitor. Methanol, ethanol, glycols, sodium chloride, and calcium chloride are common thermodynamic inhibitors. Hammerschmidt (1939) proposed an empirical formula for the lowering of the hydrate formation temperature by injection of inhibitors.

The minimum amount of hydrate inhibitor required can be calculated by equation (2.34).

$$W_h = \frac{100 M_{w_{inh}} \Delta T_h}{M_{w_{inh}} \Delta T_h + K_H} \quad (2.34)$$

W_h : concentration of pure inhibitor (weight percent) in the aqueous phase (liquid water phase)

$M_{w_{inh}}$: molecular weight of the inhibitor

ΔT_h : temperature shift, depression of hydrate formation temperature (°F)

K_H : empirical factor (Hammerschmidt constant), which is defined in Table 2.3

Table 2.3: *The constants of equation (2.34) for various inhibitors (Bai & Bai, 2010)*

Inhibitor	K_H (-)	Inhibitor	K_H (-)
Methanol & Ethanol	2335	Diethylene glycol (DEG)	4000
Ethylene glycol (MEG)	2700	Triethylene glycol (TEG)	5400

As pointed out by Bai & Bai (2010), the Hammerschmidt equation (2.34) was generated based on more than 100 natural gas hydrate measurements with inhibitor concentrations of 5wt% to 25wt% in water. The accuracy (of hydrate formation temperature) of the equation is 5% average error compared to 75 data points. Hydrate inhibition abilities are lower for substances with a higher molecular weight of alcohol, for example, methanol's ability is higher than that of ethanol and glycols. With the same weight percent, methanol has a higher temperature shift than that of glycols, but ethylene glycol has a lower volatility than methanol and ethylene glycol may be recovered and recycled more easily than methanol on platforms in upstream processes.

Guo & Ghalambor (2005) describe that if glycol is used as an inhibitor at an operating temperature below 20°F, the freezing point of the glycol must be taken into account. It is common practice to keep glycol concentrations (W_h) between 60wt% and 80wt% to avoid "mushy" glycol in the system. If the calculated W_h value from equation (2.34) is less than 60 percent, the quantity of inhibitor required should be calculated by a material balance, for which the equations are described by Guo & Ghalambor (2005).

All recent calculation methods used thermodynamic models derived from equations of state models to calculate hydrate formation equilibrium in the presence of inhibitors. In the field, there is always some over-planning of the process with a view to ensuring that the problem of hydrate deposition is eliminated.

3. SIMULATION RESULTS

The results of the "hand calculation methods" computer implementation, namely of the gas gravity method and the K-factor method modeled in the previous chapter, are compared for their accuracy with commercial software, such as Multiflash (KBC) and CSMGem (CSM: Colorado School of Mines). This software contains fluid phase models based on equation of state models. Equations of state (EoS) describe the pressure, volume and temperature (PVT) behavior of pure components and mixtures. The phase state and most thermodynamic properties (e.g. density, enthalpy, entropy) are derived from the equation of state. Separate models are used for transport properties, such as viscosity, conductivity, and surface tension.

With the Multiflash, KBC's advanced thermodynamics software, recommended hydrate model and nucleation model, the hydrate dissociation and formation boundaries can be predicted and between these two boundaries is the area of potential hydrate formation. The thermodynamic models representing hydrate formation are CPA (salt components are not supported), CPA with electrolytes (salt components are supported) and RKSA. The recommended hydrate model is the CPA-Infochem (Cubic Plus Association) EoS for the fluid phases plus the van der Waals and Platteuw model for the hydrate phases. The CPA model extends the capabilities of standard cubic EoS to polar and hydrogen-bonding components. The Multiflash CPA model is based on the RKSA-Infochem (advanced Redlich-Kwong-Soave) EoS, which is a model with excess Gibbs energy mixing rules and preferred at higher pressure. The CPA has the advantage for non-polar substances, because it reduces the RKSA equations of state, so that all the characterization methods and parameters for standard oil and gas mixtures can be used. Extra terms in the equation describe polar and associating compounds, such as water and methanol. The model also represents the inhibition effects and partitioning between phases of the common hydrate inhibitors methanol, ethanol, MEG, DEG, TEG, and salts. Also, CPA shows improvements over standard cubic EoS for other systems such as acid gases and water (KBC, 2015).

As for CSMGem software, the first statistical thermodynamic model for hydrates involved many assumptions, including assuming that the volume is constant. Newer models relaxed the constant volume assumption, coupled with the most up-to-date models for the aqueous, vapor, liquid hydrocarbon, ice, and solid salt phases. CSMGem can calculate multi-phase equilibrium at any given temperature and pressure using an algorithm based on Gibbs energy minimization (Sloan & Koh, 2008).

3.1. Assessment of the "Hand Calculation Methods" with Artificial Hydrocarbon Feeds

Mixtures of light hydrocarbons with or without inorganic constituents (such as carbon dioxide, hydrogen sulfide, and nitrogen) were used to compare the results between the representation of the "hand calculation methods" with MATLAB programming language and the "computer methods", with the commercial available software.

First, for a mixture of 75% methane and 25% ethane and vice versa, then for a mixture of 67.5% methane, 22.5% ethane, and 10% hydrogen sulfide, and finally for a mixture with 22.5% methane, 67.5% ethane, and 10% hydrogen sulfide, the hydrate formation pressure for different operating temperatures was determined, based on the above methods. The results for different molar components of the mixtures are presented in Tables 3.1 to 3.4 below, as well as in Figures 3.1 and 3.2.

The gas gravity method requires both the specific gravity of the mixture and the operating temperature as data. The K-factor method, like the commercial software, requires the mol fraction of the components of the mixture and the operating temperature. It is worth noting that both software (Multiflash and CSMGem) to produce results require the existence of water for the formation of hydrates, so a value of 0.001 moles of water was recommended. For 0.1, or 0.01, or 0.001 moles of water in the mixture the same results of the hydrate generation conditions are obtained based on the thermodynamic models of commercially available software. However, by further minimizing the water content, the hydrate formation is affected. It should be pointed out that the CPA and CPA with electrolytes models of the KBC Multiflash software yield similar results, so only the CPA model results are presented in the Tables and Figures below.

Table 3.1: Results for a mixture of 75% methane and 25% ethane ($\gamma=0.675$)

Temperature Operation			Hydrate Formation Pressure P_{hydrate} (MPa)				
T (°F)	T (°C)	T(K)	Gas Gravity Method	K-factor Method	Multiflash CPA	Multiflash RKSA	CSMGem
10.00	-12.22	260.93	-	0.074	0.553	0.553	0.610
10.13	-12.15	261.00	0.503	0.074	0.554	0.554	0.612
20.00	-6.67	266.48	0.593	0.091	0.690	0.690	0.764
30.00	-1.11	272.04	0.700	0.869	0.854	0.853	0.949
32.00	0.00	273.15	0.734	0.976	0.898	0.897	0.999
40.00	4.44	272.59	0.712	1.558	1.514	1.513	1.673
50.00	10.00	283.15	2.534	2.998	2.881	2.881	3.171
60.00	15.56	288.71	5.046	6.164	5.654	5.657	6.257
70.00	21.11	294.26	12.784	17.539	12.784	12.802	14.392
78.53	25.85	299.00	32.073	35.980	28.519	28.589	31.232
80.00	26.67	299.82	-	36.490	32.369	32.454	35.221
90.00	32.22	305.37	-	29.339	67.365	67.613	70.748
100.00	37.78	310.93	-	14.639	115.596	116.073	120.990

Table 3.2: Results for a mixture of 25% methane and 75% ethane ($\gamma=0.917$)

Temperature Operation			Hydrate Formation Pressure P_{hydrate} (MPa)				
T (°F)	T (°C)	T (K)	Gas Gravity Method	K-factor Method	Multiflash CPA	Multiflash RKSA	CSMGem
10.00	-12.22	260.93	-	0.084	0.323	0.323	0.313
10.13	-12.15	261.00	0.247	0.086	0.324	0.324	0.314
20.00	-6.67	266.48	0.297	0.242	0.411	0.411	0.401
30.00	-1.11	272.04	0.358	0.551	0.564	0.557	0.587
32.00	0.00	273.15	0.376	0.617	0.615	0.607	0.640
40.00	4.44	272.59	0.364	0.978	0.909	0.909	0.901
50.00	10.00	283.15	1.373	1.972	1.744	1.744	1.733
60.00	15.56	288.71	2.819	4.309	3.559	3.562	8.193
70.00	21.11	294.26	7.832	12.682	12.033	12.067	-
78.53	25.85	299.00	25.535	35.866	31.459	31.555	-
80.00	26.67	299.82	-	37.433	35.559	35.669	-
90.00	32.22	305.37	-	43.017	68.115	68.342	118.860
100.00	37.78	310.93	-	43.826	107.875	108.246	200.740

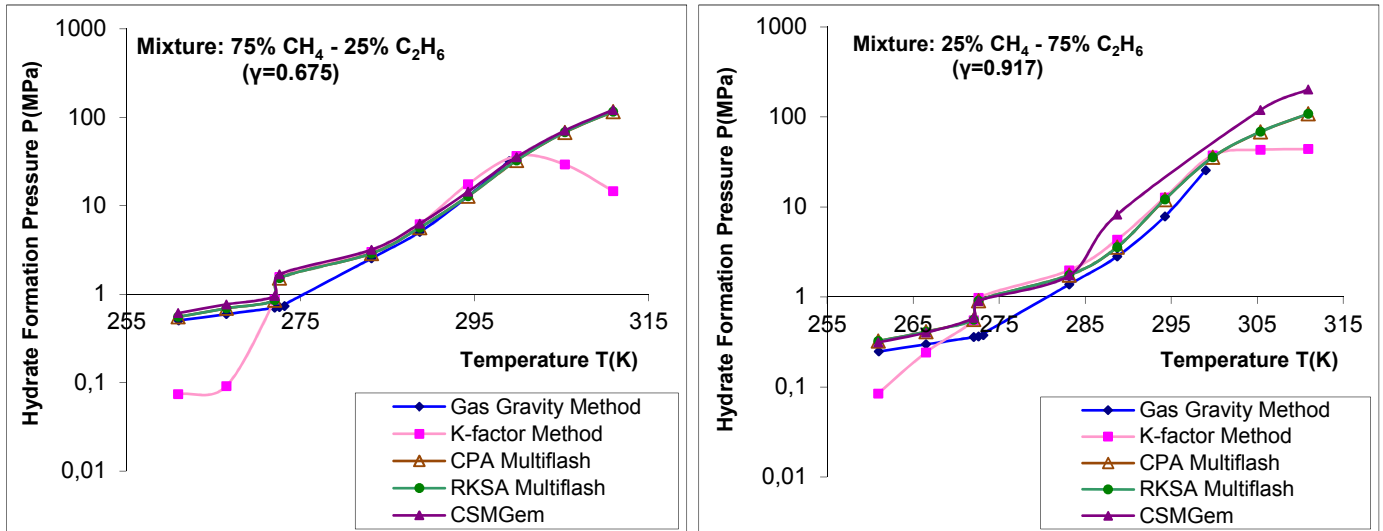


Figure 3.1: Results for methane - ethane mixtures

Table 3.3: Results for a mixture of 67.5% methane, 22.5% methane, and 10% hydrogen sulfide ($\gamma=0.725$)

Temperature Operation			Hydrate Formation Pressure P_{hydrate} (MPa)				
T (°F)	T (°C)	T (K)	Gas Gravity Method	K-factor Method	Multiflash CPA	Multiflash RKSA	CSMGem
10.00	-12.22	260.93	-	0.072	0.226	0.226	0.224
10.13	-12.15	261.00	0.415	0.072	0.227	0.227	0.225
20.00	-6.67	266.48	0.492	0.088	0.350	0.343	0.357
30.00	-1.11	272.04	0.584	0.917	0.548	0.536	0.561
32.00	0.00	273.15	0.613	1.033	0.598	0.585	0.613
40.00	4.44	272.59	1.060	1.670	0.846	0.823	0.869
50.00	10.00	283.15	2.103	3.303	1.291	1.246	1.333
60.00	15.56	288.71	4.173	7.293	2.288	2.296	-
70.00	21.11	294.26	10.975	31.327	4.609	4.624	5.552
78.53	25.85	299.00	29.665	40.523	11.152	11.202	8.974
80.00	26.67	299.82	-	41.023	14.379	14.440	21.202
90.00	32.22	305.37	-	38.176	48.730	48.815	48.793
100.00	37.78	310.93	-	20.035	99.110	99.341	99.203

Table 3.4: Results for a mixture of 22.5% methane, 67.5% ethane, and 10% hydrogen sulfide ($\gamma=0.943$)

Temperature Operation			Hydrate Formation Pressure P_{hydrate} (MPa)				
T (°F)	T (°C)	T (K)	Gas Gravity Method	K-factor Method	Multiflash CPA	Multiflash RKSA	CSMGem
10.00	-12.22	260.93	-	0.085	0.209	0.207	0.211
10.13	-12.15	261.00	0.237	0.086	0.210	0.208	0.212
20.00	-6.67	266.48	0.285	0.244	0.333	0.329	0.336
30.00	-1.11	272.04	0.343	0.593	0.521	0.514	0.526
32.00	0.00	273.15	0.361	0.667	0.569	0.561	0.575
40.00	4.44	272.59	0.639	1.063	0.803	0.791	0.836
50.00	10.00	283.15	1.305	2.132	1.219	1.199	1.237
60.00	15.56	288.71	2.663	4.764	1.829	1.795	-
70.00	21.11	294.26	7.395	18.094	3.471	3.482	-
78.53	25.85	299.00	24.737	38.536	13.745	13.831	-
80.00	26.67	299.82	-	39.881	17.643	17.729	-
90.00	32.22	305.37	-	44.912	49.487	49.624	48.984
100.00	37.78	310.93	-	45.778	90.206	90.427	107.100

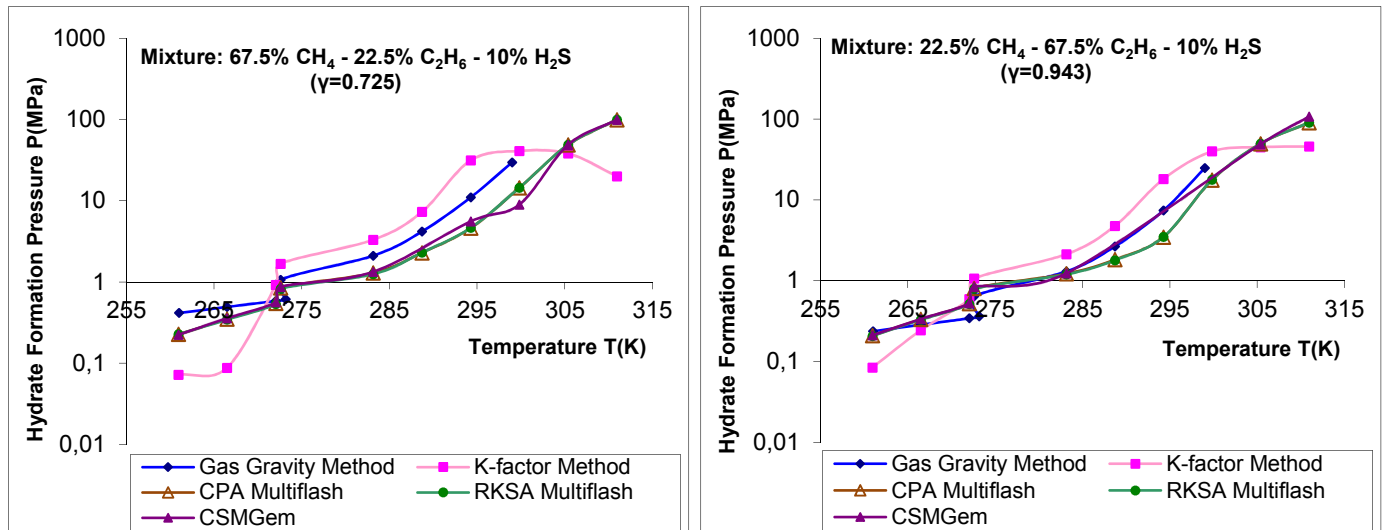


Figure 3.2: Results for methane - ethane - hydrogen sulfide mixtures

From the above aggregate results, it is observed that the expected trends were achieved, that is, with increasing temperature, the pressure increases, as indicated by phase envelopes. In addition, it is observed that for high temperature values there is a greater divergence between the methods of calculating the hydrate formation conditions. This is reasonable, as the diagrams are derived from experimental measurements and apply up to a certain range of pressures and temperatures. As for the pressure limits applied to each method, according to the Gas Processors Suppliers Association (2004), the gas gravity method is not recommended above 6.89-10.34MPa, the K-factor method in general is valid up to 27.28MPa and experimental studies have also yielded correlations for hydrate formation at pressures up to 99.97MPa. In addition, although the error is not negligible, it is unrealistic to consider hydrate

formation at elevated temperatures or extremely high pressures because usually low-temperature environments prevail.

Furthermore, in the range between 30°F (272.04K) and 70°F (294.26K), reasonable estimates and greater convergence of methods are observed for all the mixtures tested. Better estimates are obtained for mixtures with higher methane content, whereas for mixtures that tend to have specific gravity in the unity there is an underestimation of the hydrate formation tendency and errors are greater.

In the mixtures with the addition of inorganic hydrogen sulphide, sensitivity to high temperatures is once again observed. There is also a decrease in the hydrate formation pressure for the same operating temperatures in mixtures with hydrogen sulphide as compared to mixtures without addition. This is mainly observed in mixtures containing higher amounts of ethane, as the hydrate formation pressure decreases further. The gas gravity method does not yield very different results in the case of inorganic components compared to mixtures without them. According to Sloan & Koh (2008), the original diagrams were created for gas containing only hydrocarbons, and so should be used with caution for those gases with substantial amounts of noncombustible (carbon dioxide, hydrogen sulfide, and nitrogen).

Based on all of the above, it is verified that the "hand calculation methods" charts perform very well for the first approximation of hydrate formation conditions.

3.2. Assessment of Motor Oil Streams

In the present project, two refinery streams from MOTOR OIL (Hellas) S.A. Corinth Refineries were examined to determine the hydrate deposition conditions in transport pipelines within the refinery. Fuel Gas and LPG (Liquefied Petroleum Gas) streams were screened to assess the risk of formation of solid hydrate crystals within the streams.

3.2.1. Fuel Gas

Fuel Gas is one of the typical products obtained from atmospheric and vacuum distillation of crude oil. Generally, the products of the above mentioned distillations, from the lightest to the heaviest hydrocarbon constituents, are Fuel Gas, Wet Gas, Light Straight Run Gasoline, Heavy Straight Run Gasoline or Naphtha, Gas Oil, and Residual Oil. The Fuel Gas stream contains primarily methane and ethane, sometimes propane, and is often referred to as "dry gas" (Peyton, 1998). Due to the high levels of light hydrocarbons contained in the stream, the possibility of hydrate formation is considered high.

Initially, the company provided data on the composition of Fuel Gas stream from daily measurements carried out throughout the year 2019, based on laboratory analysis by the method of gas chromatography. An average of the composition measurements over the year is given in Figure 3.3. Furthermore, the average molecular weight of Fuel Gas was given as $M_w=20.031\text{gr/mol}$, whereby the specific gravity, calculated based on equation (2.1), is equal to $\gamma=0.692$. The operating conditions of the stream are $T=120^\circ\text{C}$ and $P=19.5\text{kg/cm}^2$.

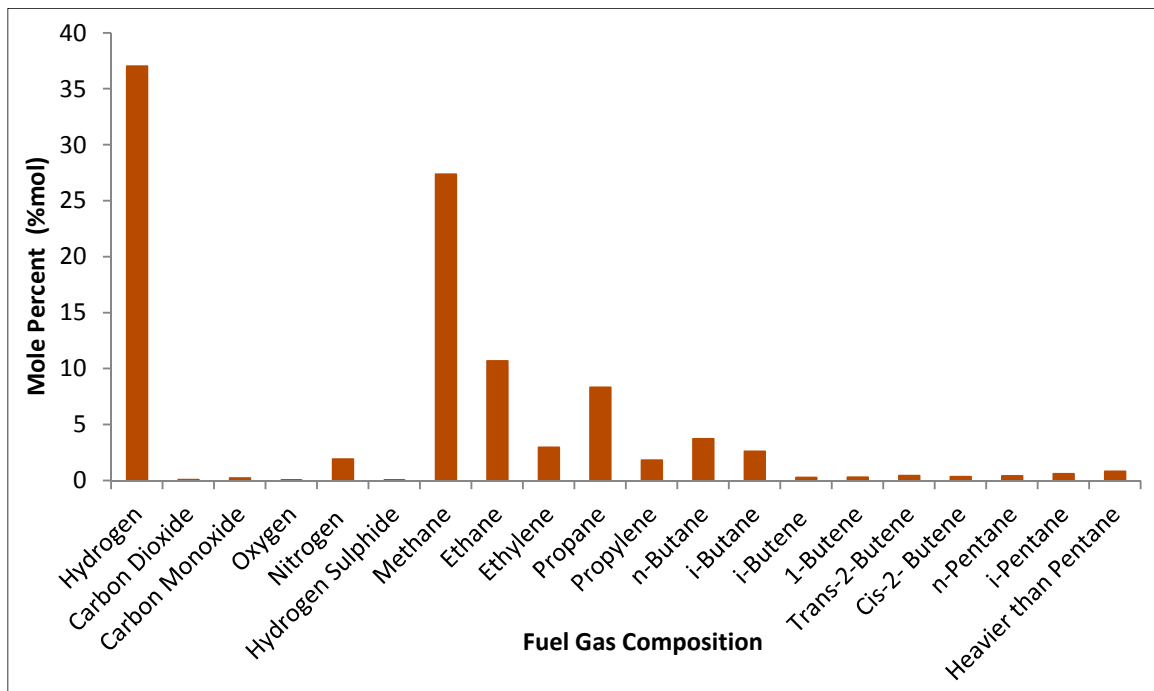


Figure 3.3: Average of mol rate of Fuel Gas composition

Based on the above Fuel Gas composition, the hydrate formation temperature or pressure was calculated for various pressure or temperature operating values, as listed in Tables 3.5 and 3.6, as well as in Figure 3.4. The diagram of the gas gravity method is given in Figure 3.5 for the operating pressure of $P=19.5\text{kg/cm}^2$ of the Fuel Gas stream.

Table 3.5: Fuel Gas hydrate formation temperature results

Pressure Operation			Hydrate Formation Temperature T_{hydrate} (K)				
P (kg/cm ²)	P (MPa)	P (psia)	Gas Gravity Method	K-factor Method	Multiflash CPA	Multiflash RKSA	CSMGem
19.5	1.912	277.360	281.78	-	239.02	240.23	283.59
7.03	0.689	100.000	273.47	279.07	230.63	230.93	274.88
9.14	0.896	130.000	275.84	280.90	232.85	233.33	278.38
11.25	1.103	160.000	277.03	282.69	234.59	235.23	279.80
11.95	1.172	170.000	277.03	283.64	235.09	235.78	280.22
12.16	1.193	173.000	277.03	284.22	235.23	235.94	280.34
15.00	1.471	213.350	279.41	-	236.95	237.86	281.78
21.00	2.059	298.690	281.78	-	239.59	240.90	284.10

Table 3.6: Fuel Gas hydrate formation pressure results

Temperature Operation			Hydrate Formation Pressure $P_{hydrate}$ (MPa)				
T (°F)	T (°C)	T (K)	Gas Gravity Method	K-factor Method	Multiflash CPA	Multiflash RKSA	CSMGem
14.00	-10.00	263.15	0.502	-	364.937	73.293	0.271
23.00	-5.00	268.15	0.584	-	499.884	141.816	0.408
32.00	0.00	273.15	0.690	-	646.958	231.322	1.244
41.00	5.00	278.15	1.278	0.569	805.770	345.229	0.880
50.00	10.00	283.15	2.368	1.142	975.146	481.607	1.795
59.00	15.00	288.15	4.387	1.072	-	638.752	3.742
68.00	20.00	293.15	9.673	0.893	-	815.279	8.625
248.00	120.00	393.15	-	-	-	-	-

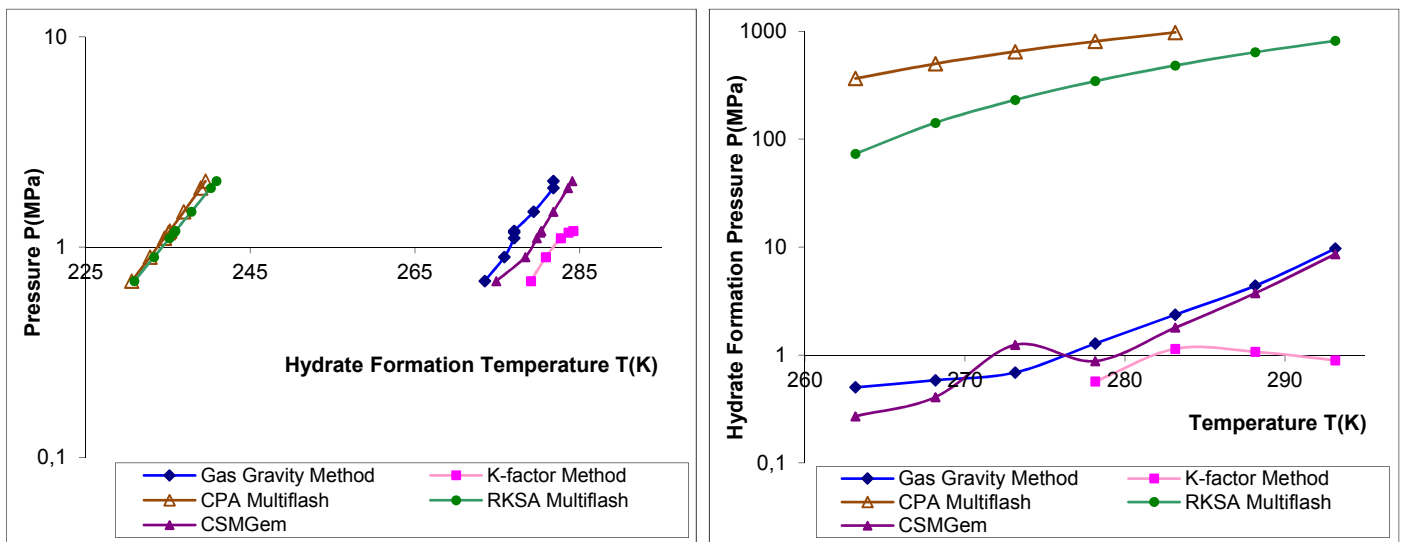


Figure 3.4: Fuel Gas hydrate formation conditions

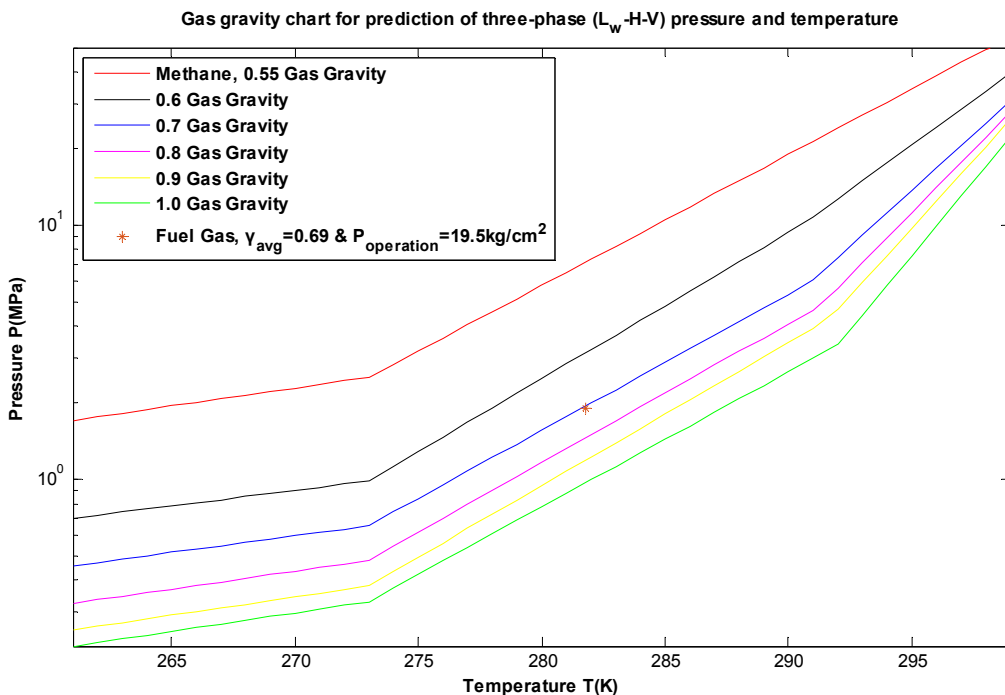


Figure 3.5: Gas gravity method for operating pressure Fuel Gas $P=19.5\text{kg/cm}^2$

From the above results, for Fuel Gas operating pressure $P=19.5\text{kg/cm}^2$, all methods agree that there is no risk of hydrate formation. The operating temperature of the stream is $T_{\text{operation}}=393.15\text{K}$, much higher than the average formation temperature resulting from the five different calculation methods $T_{\text{avg.hydrate}}=261.15\text{K}$, as presented in Table 3.5. At this hydrate formation temperature, three phases coexist: gas or vapor hydrocarbon, liquid hydrocarbon, and sII hydrate, while the solution stability is stable.

Regarding the results of the hydrate formation pressure for different operating temperatures, as presented in Table 3.6, there is a very large variation in the predicted values, especially at high temperatures, even among the thermodynamic models. At operating temperature of Fuel Gas stream $T_{\text{operation}}=393.15\text{K}$, none of the models show results for hydrate formation pressure, as there is no problem of hydrate deposition at such a high temperature and the methods work for smaller temperature ranges. The operating temperature of this particular Fuel Gas stream is high, as the stream flow through the furnaces and boilers of the refinery for combustion and power generation, thus undergoing a warm-up process. So one possible problem in the Fuel Gas stream is corrosion of the pipes due to hydrogen sulfide liquefaction, which despite its low stream content is corrosive. The composition of the stream in hydrogen is high, compared to the other constituents, as hydrogen unit streams sometimes reach this flow, although the Fuel Gas stream is intended for combustion.

The above results show that the graphical methods (gas gravity method and K-factor) are sufficiently satisfactory for the initial estimation of the hydrate formation temperature when the operating pressure is constant compared to the thermodynamic models of commercial software. One of the reasons this happens is that the components of the Fuel Gas stream have a low content of inorganic components, so the gas gravity method converges with the other methods. It should be pointed out that the graphical methods use some light hydrocarbons to predict hydrate formation, such as methane, ethane, propane, butane, and isobutane, in contrast to commercial software, where all the components are used, so a difference in results is expected. However, the discrepancies are negligible when simulated with or without the heavier hydrocarbons in the thermodynamic models of Multiflash and CSMGem software, as the heavier components have a low content of the mixture, and do not play a major role in the formation of hydrates. It is also noted that for the commercial software to give results the presence of water in the stream is required, where 0.001mol is indicated.

In some cases, there is no convergence of the iterative calculation methods based on the initial guess provided. More precisely, the K-factor method does not work at some turning points or extremalities and fails to satisfy the constraint (2.31) which requires the sum of mole

fractions for all components in liquid phase to be equal to unity. The pathological behavior of the equation in some pressure-temperature regions may be due to the fact that the Newton-Raphson method uses derivatives to find the solution. In the case of division by zero, the method does not work as the derivatives do not give reasonable results. In addition, in some pressure-temperature regions the thermodynamic models do not respond to a solution either. Therefore, the use of graphical methods, as the gas gravity method, is one-way for an initial estimation of the hydrate formation conditions, in some pressure-temperature locus.

3.2.2. Liquefied Petroleum Gas (LPG)

Generally, Liquefied Petroleum Gas (LPG) is any light hydrocarbon fuel that must be compressed and liquefied to keep it from boiling away. LPG is primarily propane with low concentrations of ethane and butane (mixtures of C₃s and C₄s). As mentioned in the section 3.2.1, one of the light typical products obtained from atmospheric and vacuum distillation of crude oil is Wet Gas. The Wet Gas stream contains primarily propane and butane, and can also include methane and ethane. Propane and butane are used in LPG and butane can also be used as gasoline blendstock (Peyton, 1998). Due to the high levels of light hydrocarbons contained in the stream, it was considered a potential problem for hydrates formation.

Initially, the company provided data on the composition of LPG stream from distillate or tops by atmospheric distillation, for two different distillate feeds, namely "Arabian Light" and "Arabian Medium". In particular, according to the process flow diagram of crude distillation, the top by atmospheric distillation is subjected to separation through two horizontal separators in series. The LPG stream (Stream 85 in the process flow diagram provided for data collection - not presented in this project) arising after this separation is subject to hydrate deposition study, as it contains high levels of light hydrocarbons, as well as hydrogen sulfide. The LPG composition (Stream 85) for two different atmospheric feeds is shown in Figure 3.6, according to the results of the quality control and mass balances in the distillation column.

It is noted that heavier components than pentane are given by the Normal Boiling Point (NBP), which is the temperature at which the vapor pressure of a liquid is equal to one atmosphere. The heaviest components, which occupy a very small percentage of the LPG stream, were assumed to be hexane, heptane, and octane in smaller composition; with the last one (octane) being present only in Arabian Medium distillation feed. This assumption is not entirely accurate as there are many intermediate components with a normal boiling point that correspond to the given ranges. However, it is a reasonable assumption that it does not affect

the final result, since the heavier components are in low percentage on the stream and do not play a major role in the formation of hydrate. This is also verified by commercial software, where simulations are run for the same operating conditions of the stream, taking into account all the components of the stream in one case, and only the light components in the other. The final results are similar in both cases, as shown in the Tables 3.11 and 3.12.

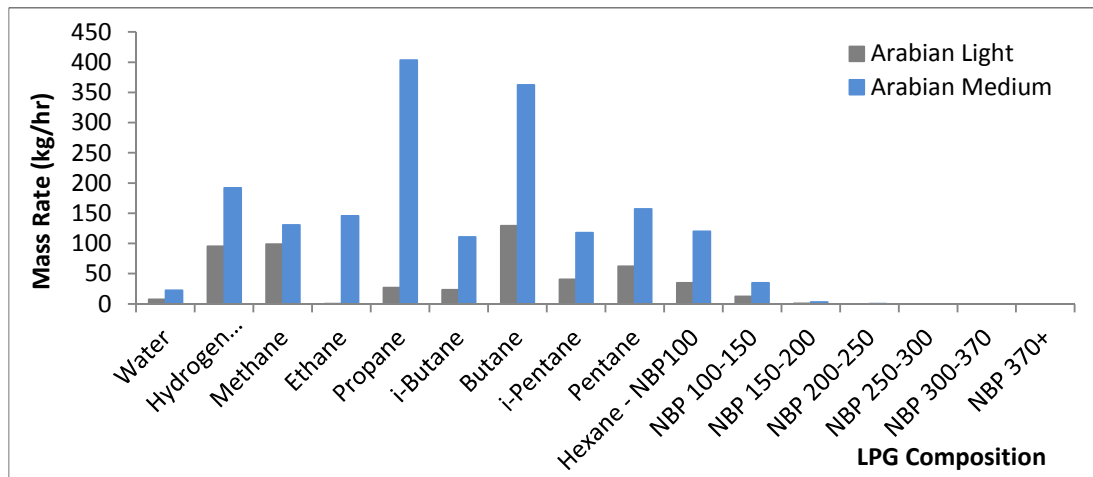


Figure 3.6: LPG composition of mass rate for Arabian Light and Arabian Medium distillation feeds

Furthermore, the molecular weight and operating conditions of the two LPG streams were given. Specifically, for the Arabian Light atmospheric distillation feed the LPG molecular weight is $M_w=36.59\text{gr/mol}$, whereby the specific gravity was calculated based on equation (2.1) equal to $\gamma=1.263$; while for the Arabian Medium atmospheric distillation feed the specific gravity of the LPG is $\gamma=1.457$ based on the given molecular weight that is $M_w=42.20\text{gr/mol}$. The operating conditions of the LPG stream, regardless of the atmospheric distillation feed, are $T=35^\circ\text{C}$ and $P=2.96\text{kg/cm}^2$.

Based on the above LPG composition and operating pressure, the hydrate formation temperature was calculated, and accordingly, based on the operating temperature of the stream, the hydrate formation pressure was calculated.

The aggregated results of the hydrate formation conditions for different operating temperatures or pressures are presented in Tables 3.7 and 3.8 for Arabian Light atmospheric distillation feed while Tables 3.9 and 3.10 show the results for Arabian Medium atmospheric distillation feed. The graphical visualization of the results is presented in Figures 3.7 and 3.8. The gas gravity charts are given in Figures 3.9 and 3.10 for the operating pressure of $P=2.96\text{kg/cm}^2$ for the two different atmospheric distillation feeds. The operating temperature of the LPG stream is $T=35^\circ\text{C}=308.15\text{K}=95^\circ\text{F}$, marginally outside the limits of the gas gravity diagram, therefore the hydrate formation pressure was not calculated at this operating temperature by the gas gravity method.

Table 3.7: LPG hydrate formation temperature results for Arabian Light distillation feed

Pressure Operation			Hydrate Formation Temperature $T_{hydrate}$ (K)				
P (kg/cm ²)	P (MPa)	P (psia)	Gas Gravity Method	K-factor Method	Multiflash CPA	Multiflash RKSA	CSMGem
2.96	0.290	42.101	272.58	261.91	278.27	278.25	281.28
0.50	0.049	7.112	261.28	-	250.58	250.58	257.68
1.00	0.098	14.223	261.28	-	263.42	263.42	270.12
2.50	0.245	35.558	268.34	262.49	276.81	276.80	279.78
3.00	0.294	42.670	272.93	261.87	278.38	278.36	281.40
3.50	0.343	49.782	273.99	261.53	279.71	279.68	282.76
4.00	0.392	56.893	274.70	261.42	280.84	280.82	283.93

Table 3.8: LPG hydrate formation pressure results for Arabian Light distillation feed

Temperature Operation			Hydrate Formation Pressure $P_{hydrate}$ (MPa)				
T (°F)	T (°C)	T(K)	Gas Gravity Method	K-factor Method	Multiflash CPA	Multiflash RKSA	CSMGem
23.00	-5.00	268.15	0.243	2.377	0.125	0.125	0.088
32.00	0.00	273.15	0.297	3.023	0.160	0.160	0.012
41.00	5.00	278.15	0.690	18.635	0.286	0.287	0.204
50.00	10.00	283.15	1.605	22.341	0.517	0.519	0.359
59.00	15.00	288.15	-	26.268	0.982	0.986	0.646
68.00	20.00	293.15	-	30.410	2.196	2.208	1.255
95.00	35.00	308.15	-	43.851	77.079	77.050	59.526

Table 3.9: LPG hydrate formation temperature results for Arabian Medium distillation feed

Pressure Operation			Hydrate Formation Temperature $T_{hydrate}$ (K)				
P (kg/cm ²)	P (MPa)	P (psia)	Gas Gravity Method	K-factor Method	Multiflash CPA	Multiflash RKSA	CSMGem
2.96	0.290	42.101	274.88	264.02	280.25	280.24	282.93
0.50	0.049	7.112	261.23	-	255.16	255.16	260.93
1.00	0.098	14.223	261.23	-	268.39	268.39	273.39
2.50	0.245	35.558	274.28	318.73	278.79	278.78	281.38
3.00	0.294	42.670	274.88	263.98	280.36	280.35	283.05
3.50	0.343	49.782	276.06	263.59	281.71	281.70	284.47
4.00	0.392	56.893	276.66	263.42	282.88	282.87	285.70

Table 3.10: LPG hydrate formation pressure results for Arabian Medium distillation feed

Temperature Operation			Hydrate Formation Pressure $P_{hydrate}$ (MPa)				
T (°F)	T (°C)	T(K)	Gas Gravity Method	K-factor Method	Multiflash CPA	Multiflash RKSA	CSMGem
23.00	-5.00	268.15	0.161	1.312	0.097	0.097	0.073
32.00	0.00	273.15	0.198	2.441	0.124	0.124	0.396
41.00	5.00	278.15	0.532	14.116	0.228	0.228	0.171
50.00	10.00	283.15	-	21.265	0.405	0.405	0.297
59.00	15.00	288.15	-	25.615	0.726	0.727	0.512
68.00	20.00	293.15	-	29.901	1.456	1.460	0.911
95.00	35.00	308.15	-	43.462	73.913	73.938	50.163

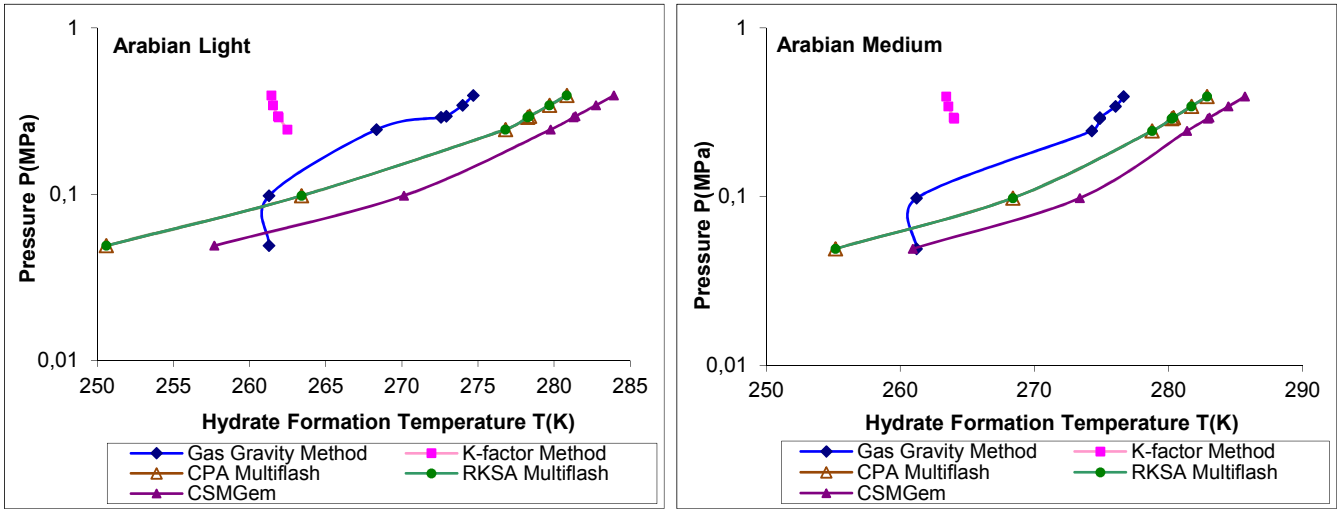


Figure 3.7: LPG hydrate formation temperature results for Arabian Light and Medium distillation feeds

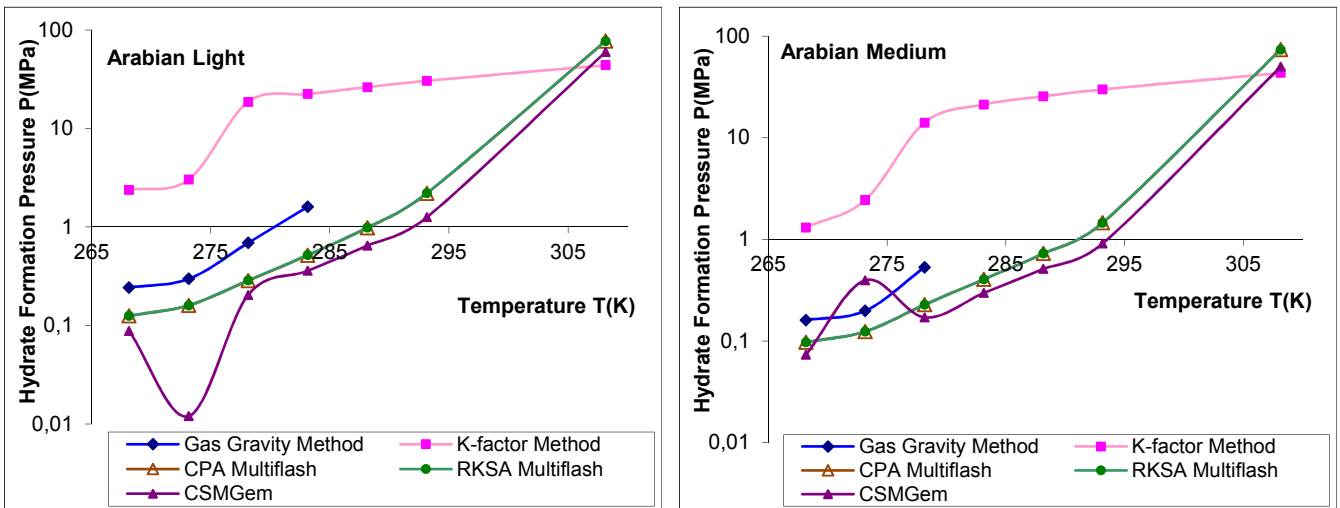


Figure 3.8: LPG hydrate formation pressure results for Arabian Light and Medium distillation feeds

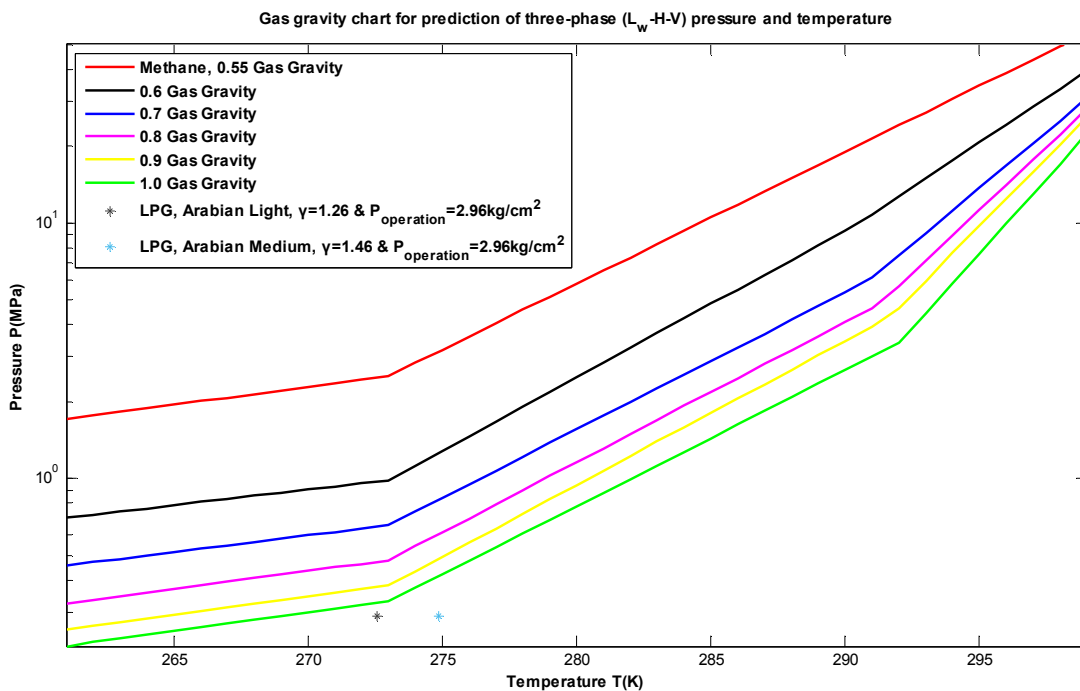


Figure 3.9: Gas gravity method for operating pressure LPG $P=2.96\text{kg}/\text{cm}^2$

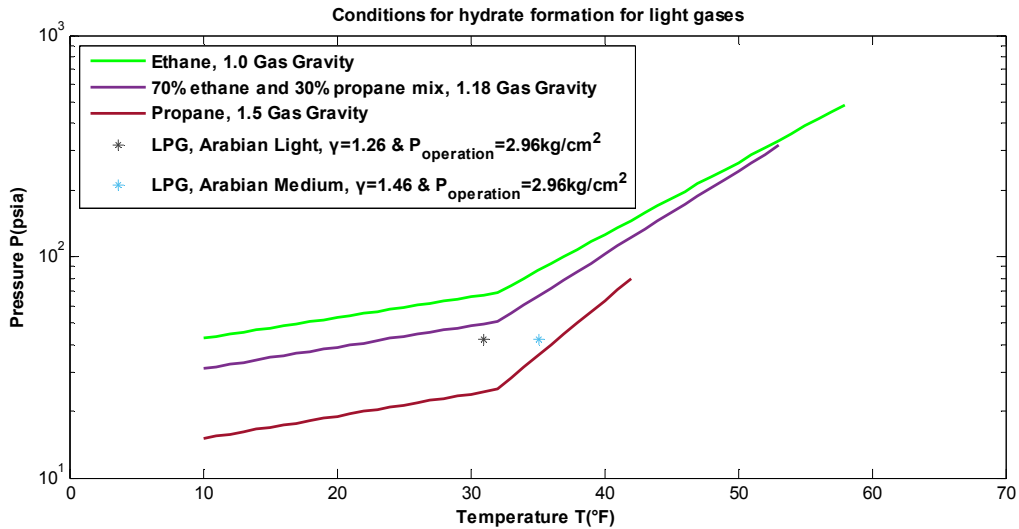


Figure 3.10: Gas gravity chart for light gases for operating pressure LPG $P=2.96\text{kg/cm}^2$

Tables 3.11 and 3.12 show the results of the hydrate formation temperature for various pressures based on the commercially available software. Case A represents the simulation with all components of the LPG stream. Case B represents the simulation only with the components of the LPG stream, which most strongly influence the hydrate formation, namely methane, ethane, propane, butane, isobutane, and hydrogen sulfide.

Table 3.11: LPG hydrate formation results of commercial software with (Case A) and without (Case B) the heavier components for Arabian Light distillation feed

Pressure Operation P (MPa)	Hydrate Formation Temperature T_{hydrate} (K)					
	Multiflash CPA		Multiflash RKSA		CSMGem	
	Case A	Case B	Case A	Case B	Case A	Case B
0.290	278.27	278.98	278.25	278.96	281.28	282.02
0.049	250.58	252.27	250.58	252.27	257.68	259.68
0.098	263.42	265.30	263.42	265.30	270.14	272.31
0.245	276.81	277.54	276.80	277.52	279.78	280.54
0.294	278.38	279.09	278.36	279.08	281.40	282.14
0.343	279.71	280.42	279.68	280.40	282.76	283.49
0.392	280.84	281.58	280.82	281.56	283.93	284.67

Table 3.12: LPG hydrate formation results of commercial software with (Case A) and without (Case B) the heavier components for Arabian Medium distillation feed

Pressure Operation P (MPa)	Hydrate Formation Temperature T_{hydrate} (K)					
	Multiflash CPA		Multiflash RKSA		CSMGem	
	Case A	Case B	Case A	Case B	Case A	Case B
0.290	280.25	280.55	280.24	280.54	282.93	283.24
0.049	255.17	256.95	255.16	256.95	260.93	262.98
0.098	268.39	270.34	268.39	270.34	273.39	274.27
0.245	278.79	279.18	278.78	279.17	281.38	281.81
0.294	280.36	280.66	280.35	280.65	283.05	283.36
0.343	281.71	281.92	281.70	281.91	284.47	284.68
0.392	282.88	283.03	282.87	283.02	285.70	285.83

The assumption made for the heaviest components of the LPG, that is hexane, heptane and traces of octane (only in the case of Arabian Medium distillation feed), is acceptable, since from the results of Tables 3.11 and 3.12 the relative error between the two cases (Case A and Case B) ranges from 0.04% to 0.80%.

From the above results, for LPG operating pressure $P=2.96\text{kg/cm}^2$, all methods agree that there is no risk of hydrate formation for the two different distillation feeds. The operating temperature of the stream is $T_{\text{operation}}=308.15\text{K}$, much higher than the average formation temperature resulting from the five different calculation methods, where $T_{\text{avg,hydrate}}=274.46\text{K}$ for Arabian Light distillation feed and $T_{\text{avg,hydrate}}=276.46\text{K}$ for Arabian Medium distillation feed, as presented in Tables 3.7 and 3.9. At this hydrate formation temperature, for both distillation feeds, four phases coexist: gas or vapor hydrocarbon, liquid hydrocarbon, sII hydrate, and water, while the solution stability is stable. At operating temperature of LPG stream $T_{\text{operation}}=308.15\text{K}$, all methods (except for the gas gravity method which is not applicable as the operating temperature is outside of the diagram limits) yield higher hydrate formation pressures than stream operating pressure which is $P_{\text{operation}}=0.29\text{MPa}$ for both distillate feeds. Therefore, once again, we come to the conclusion that there is no risk of hydrate formation in LPG stream.

Regarding the results of the hydrate formation pressure for different operating temperatures, as presented in Tables 3.8 and 3.10, there is a large variation in the predicted values, especially at high temperatures, between the representation of "hand calculation methods" and the commercial software. For the gas gravity method, this is due to the mathematical modeling used to predict hydrate formation conditions in light gases. As noted above, Figure 2.10, which constitutes the representation attempt of Figure 2.9, has good accuracy for approaching temperature values, but for pressure there is a deviation of about 30psia or 0.21MPa. Therefore, for the LPG stream, which contains high levels of ethane and propane, the calculation of the hydrate formation is based on the use of Figure 2.10 where there is a divergence in the calculation of the hydrate formation pressure for a constant operating temperature of the stream. In addition, the gas gravity method differs from other methods, as it does not include hydrogen sulfide in the stream in the prediction of hydrate formation. As for the K-factor method, it yields results only in some temperature-pressure regions where the Newton-Raphson method converges.

The above results show that the graphical methods (gas gravity method and K-factor) are sufficiently satisfactory for the initial estimation of hydrate formation conditions and the mathematical model represents the literature charts.

4. CONCLUSIONS

With the completion of the master thesis on the study of hydrate formation conditions in oil and gas pipelines, some conclusions might be offered regarding the use of "hand calculation methods" compared to computational thermodynamic models of commercial software. Based on the results of the study, the literature finding is confirmed that the "hand calculation methods" provide a first estimate of the hydrate formation conditions, particularly in the temperature range between 272.04K and 294.26K for mixtures with increased methane percent. They are popular computation methods even nowadays because they use less data than thermodynamic models. According to Carroll (2009), "in general, the less information required as input, the less accurate the calculation results".

Implementation of the "hand calculation methods" in a computer program, based on MATLAB in this project, allows data to be read with great speed and facility, as well as higher accuracy and objectivity. The overriding purpose of the above diploma thesis is the quick first estimation of hydrate formation conditions, which is the main added advantage of computer implementation of "hand calculation methods". Especially in the field, where fast initial estimations are required, the process is made easier by using a computer than reading diagrams, specifically logarithmic ones.

The computer program developed in this thesis adopts the same assumptions, which are the basis of the mathematical models in the original "hand calculation methods". The main approach used is that the components which most strongly influence hydrate formation are methane, ethane, propane, butane, isobutane, nitrogen, carbon dioxide, and hydrogen sulfide. The last three inorganic components are not included in the "gas gravity method", so the "K-factor" method should be more accurate. The above assumption is verified by commercial software, since the results do not differ appreciably when simulating only the above components, on one hand, and all components of the mixture, on the other.

The hydrate deposits in oil and gas pipelines are a common problem in the upstreaming, midstreaming, and downstreaming processes of the oil industry. In the present thesis, neither of the examined streams from MOTOR OIL (Hellas) Corinth Refineries S.A., namely Fuel Gas and LPG are found at risk of forming solid hydrate crystals in oil and gas pipelines within the refinery. The locations where the hydrate deposition problems occur are mainly in offshore drilling processes where the temperature is particularly low, in combination with high pressures. In addition, in the first stages of gas production processes the phenomenon is more pronounced compared to refinery processes. However, it is worth noting that the facilities of MOTOR OIL refinery are located in Greece, where the Mediterranean climate is

prevalent. The problem may be more acute in refineries in locations with lower temperatures prevailing.

It is worth noting that, thanks to the encouraging results of the simulations, some issues can be proposed for future research, in a more complex and realistic examination of the phenomena. More specifically, some future research proposals are:

- Using a different approach to modeling the "gas gravity" chart for light gases, since interpolating between the slopes of the straight lines for ethane and propane to approximate intermediate mixtures showed deviations of 30psia for the pressure. However, there is good accuracy in interpolating temperature values.
- To further explore and attempt to remedy the peculiar behavior of the K-factor method at extremely high or low temperatures. More specifically, it was observed that the temperature-pressure relation for hydrate formation had a non-monotonic character.
- The examination of thermodynamic and kinetic behavior during hydrate formation, as applied in the commercial software.

5. BIBLIOGRAPHY

Ahmed T. & McKinney P.D. (2005) *Advanced Reservoir Engineering*, Gulf Professional Publishing - Elsevier, U.S.A., U.K.

Ahmed T. (2007) *Equations of State and PVT Analysis - Applications for Improved Reservoir Modeling*, Gulf Publishing Company, U.S.A.

Bai Y. & Bai Q. (2010) *Subsea Structural Engineering Handbook*, 2nd ed., Gulf Professional Publishing - Elsevier, U.S.A., U.K.

Barker C., Barnicki S.D., Bartholomew C. et al. (2007) *Wiley Critical Content: Petroleum Technology*, Volume 1, John Wiley & Sons Inc. Publication (Wiley-Interscience & Wiley-VCH), U.S.A.

BP (2016) *BP Statistical Review of World Energy*, [online] Available at: <http://oilproduction.net/files/especial-BP/bp-statistical-review-of-world-energy-2016-full-report.pdf> [Accessed 26 January 2020]

BSI Standards Publication (2007) *Installation and equipment for liquefied natural gas - Design of onshore installations (BS EN 1473:2007)*, [online] Available at: <http://www.golng.eu/files/upload/10.1.1.470.7021.pdf> [Accessed 26 January 2020]

Carroll J. (2009) *Natural Gas Hydrates - A Guide for Engineers*, 2nd ed., Gulf Professional Publishing - Elsevier, U.S.A., U.K.

Carson D.B. & Katz D.L. (1942) "Natural Gas Hydrates", *Petroleum Transactions AIME*, **146**:150-158

Cholet H. (2000) *Well Production Practical Handbook*, Institut Français du Pétrole Publications - t Editions TECHNIP, France

Cordell J. & Vanzant H. (2003) *The Pipeline Pigging Handbook*, 3rd ed., Clarion Technical Publishers - Scientific Surveys, U.S.A.

Crabtree M., Eslinger D., Fletcher P., Miller M., Johnson A. & King G. (1999) "Fighting Scale - Removal and Prevention", *Oilfield Review*, **11**(3):30-45, [online] Available at: <https://pdfs.semanticscholar.org/5ddd/cdc5e89e335bacdf40bd1de0f7768c480ba8.pdf> [Accessed 26 January 2020]

DESFA - Hellenic Gas Transmission System Operator S.A. (2018) *National Natural Gas Transmission System*, [online] Available at: <https://www.desfa.gr/en/national-natural-gas-system/transmission> [Accessed 26 January 2020]

Frenier W.W. & Ziauddin M. (2008) *Formation, Removal, and Inhibition of Inorganic Scale in the Oilfield Environment*, Society of Petroleum Engineers, U.S.A.

Frenier W.W., Ziauddin M. & Venkatesan R. (2010) *Organic Deposits in Oil and Gas Production*, Society of Petroleum Engineers, U.S.A.

Gas Processors Suppliers Association - GPSA (2004) *Engineering Data Book*, 12th ed., FPS version, I & II volumes, 1-26 sections, Gas Processors Suppliers Association, U.S.A.

- Gerding M. (1986) *Fundamentals of Petroleum*, 3rd ed., Petroleum Extension Service - The University of Texas at Austin, U.S.A.
- Giavarini C. & Hester K. (2011) *Gas Hydrates - Immense Energy Potential and Environmental Challenges*, Green Energy and Technology, Springer-Verlag, U.K.
- Guo B. & Ghalambor A. (2005) *Natural Gas Engineering Handbook (CD-ROM Included)*, Gulf Publishing Company, U.S.A.
- Hammerschmidt E.G. (1939) "Preventing and removing gas hydrate formation in natural gas pipelines", *Oil & Gas Journal*, **37**(52):66,69,71-72
- Ilyaeva M.A. & Andrianova Ju.G. (2011) *Oil, Oil Products and Gas Transportation and Storage*, Publishing house «Reactive», Russia
- Information Technology Associates (2017) *Europe Pipelines map - Crude Oil (petroleum) pipelines - Natural Gas pipelines - Products pipelines*, [online] Available at: [«https://www.theodora.com/pipelines/europe_oil_gas_and_products_pipelines.html»](https://www.theodora.com/pipelines/europe_oil_gas_and_products_pipelines.html) [Accessed 26 January 2020]
- International Gas Union - IGU (2018) *World LNG Report*, [online] Available at: [«https://www.igu.org/sites/default/files/node-document-field_file/IGU_LNG_2018_0.pdf»](https://www.igu.org/sites/default/files/node-document-field_file/IGU_LNG_2018_0.pdf) [Accessed 26 January 2020]
- Kassinis S. (2015) *About Oil & Gas (Petrochemistry, Upstream, Midstream and Downstream)*, Kassinis International Consulting, Cyprus
- Katz D.L. (1945) "Prediction of Conditions for Hydrate Formation in Natural Gases", *Petroleum Transactions AIME*, **160**:140-149
- KBC Advanced Technologies Ltd. (2015) *Multiflash Help - Manual*, Multiflash Software for Schlumberger Flow Modeling, Version 6.1
- LLC «Express Logistics» (2020) *International transportation of goods by railway transport - Railway cargo delivery*, [online] Available at: [«https://exp-imp.ru/en/international-transportation/by-railroad-transport»](https://exp-imp.ru/en/international-transportation/by-railroad-transport) [Accessed 26 January 2020]
- Makogon Y.F. (1997) *Hydrates of Hydrocarbons*, PennWell Publishing Company, U.S.A.
- Mao W.L., Koh C.A. & Sloan E.D. (2007) "Clathrate hydrates under pressure", *Physics Today - American Institute of Physics*, **60**(10):42-47
- Mullins O.C., Rodgers R.P., Weinheber P., Klein G.C., Venkataramanan L., Andrews A.B. & Marshall A.G. (2006) "Oil Reservoir Characterization via Crude Oil Analysis by Downhole Fluid Analysis in Oil Wells with Visible-Near-Infrared Spectroscopy and by Laboratory Analysis with Electrospray Ionization Fourier Transform Ion Cyclotron Resonance Mass Spectrometry", *Energy & Fuels*, **20**(6):2448-2456
- Mullins O.C. (2008) *The Physics of Reservoir Fluids: Discovery through downhole fluid analysis*, Schlumberger
- Munck J., Skjold-Jorgensen S. & Rasmussen P. (1988) "Computations of the formation of gas hydrates", *Chemical Engineering Science*, **43**(10):2661-2672

Natural Gas (2013) *The Transportation of Natural Gas*, [online] Available at: <http://naturalgas.org/naturalgas/transport/> [Accessed 26 January 2020]

Nayyar M.L. (2000) *Piping Handbook*, 7th ed., McGraw-Hill Companies, U.S.A.

O'Connell D.J. (2018) "Cargo Truck Tanks: An Often-Unrecognized Confined Space Hazard", *American Society of Safety Engineers - Professional Safety*, **63**(06):46-51

OILFIELD WIKI (2016) *Naphtenates*, [online] Available at: <http://www.oilfieldwiki.com/wiki/Naphtenates> [Accessed 26 January 2020]

Ostergaard K.K., Danesh A., Tohidi B., Todd A.C. & Burgass R.W. (1998) "Effect of Reservoir Fluid Production on Gas Hydrate Phase Boundaries", *Society of Petroleum Engineers*, SPE-50689-MS, Presented at the SPE European Petroleum Conference, 20-22 October, The Hague, Netherlands

Peyton K.B. (1998) *Fuel Field Manual - Sources and Solutions to Performance Problems*, NALCO/EXXON ENERGY CHEMICALS L.P., McGraw-Hill, U.S.A.

Rojey A., Jaffret C., Cornot-Gandolphe S., Durand B., Jullian S. & Valais M. (1997) *Natural Gas - Production Processing Transport*, Institut Français du Pétrole Publications - t Editions TECHNIP, France

Schlumberger (2010) *PIPESIM Fundamentals - Workflow/Solutions Training*, Version 2010.1, Schlumberger Information Solutions, [online] Available at: https://www.academia.edu/30969260/PIPESIM_Fundamentals_Workflow_Solutions_Training_Schlumberger_Information_Solutions [Accessed 26 January 2020]

Sloan E.D. & Koh C.A. (2008) *Clathrate Hydrates of Natural Gases*, 3rd ed., CRC Press - Taylor and Francis Group, Chemical Industries, U.S.A.

T.D. Williamson (TDW Inc.) - Pipeline Performance (2020) *Pipeline pigs & scrapers*, [online] Available at: <http://www.tdwilliamson.com/solutions/pipeline-pigging/pipeline-pigs> [Accessed 26 January 2020]

Tohidi B. (2018) *New Techniques in Controlling Gas Hydrates*, [online] Available at: <http://www.hydrifact.com/pdfs/New%20Techniques%20in%20Corolling%20Gas%20Hydrates-January%202018.pdf> [Accessed 26 January 2020]

Tractebel Engineering S.A. (2015) *CNG for commercialization of small volumes of associated gas*, World Bank Group Energy & Extractions - Global Gas Flaring Reduction, [online] Available at: <http://documents.worldbank.org/curated/en/210571472125529218/pdf/104200-V2-WP-CNG-commercialization-PUBLIC-Main-report-REPLACEMENT.pdf> [Accessed 26 January 2020]

U.S. Department of Transportation (2019) *Agency Financial Report*, [online] Available at: <https://www.transportation.gov/sites/dot.gov/files/docs/mission/budget/357706/2019-agency-financial-report-current1211-508-final.pdf> [Accessed 26 January 2020]

Vysniauskas A. & Bishnoi P.R. (1983) "A kinetic study of methane hydrate formation", *Chemical Engineering Science*, **38**(7):1061-1072

6. APPENDIX

6.1. MATLAB Code - The Gas Gravity Method

In the gas gravity method the available charts (Figures 2.1 and 2.9) were interpolated and reproduced numerically, as described in the chapter 2.1.1. The following is the Matlab code having as input data the specific gravity of the gas and an operating condition pressure or temperature, in order to calculate the hydrate formation temperature or pressure respectively.

- **m-file**, with name: P_vs_T.m

```
clear all; clc;
%Required Input Data
sp_gr = 0.675; %Specific gravity (Units: -)
T = 273; %Temperature (Units: Kelvin)
[P] = fun_PvsT (T,sp_gr); %Hydrate Formation Pressure
```

- **m-file**, with name: T_vs_P.m

```
clear all; clc;
%Required Input Data
sp_gr = 0.675; %Specific gravity (Units: -)
P_des = 1000; %Pressure (Units: MPa)
[T] = fun_TvsP (P_des,sp_gr); %Hydrate Formation Temperature
```

- **function-file**, with name: fun_A1234.m

```
function [A1,A2,A3,A4,TA3] = fun_A1234(x)

A1 = 2.0716*x^2 - 4.5714*x + 1.8435; %log(P) vs sp_gr (turning point A1)
A2 = 1.899*x^2 - 4.2227*x + 1.8428; %log(P) vs sp_gr (turning point A2)
A3 = -14.907*x^3 + 37.883*x^2 - 32.567*x + 10.123; %log(P) vs sp_gr (turning point A3)
A4 = -8.5599*x^3 + 21.234*x^2 - 17.817*x + 6.4905; %log(P) vs sp_gr (turning point A4)
TA3 = 3.7793*x + 288.26; %T vs sp_gr (turning point TA3)

return
```

- **function-file**, with name: fun_P.m

```
function [P] = fun_P(T,sp_gr)

P = 0;

[A1,A2,A3,A4,TA3] = fun_A1234(sp_gr);

if T < 261;
    disp('The temperature is too low.')
end

if T >= 261 && T < 273;
    x = (A2-A1)*(T-261)/(273-261) + A1;
```

```

    P = 10.^(x);
end

if T >= 273 && T < TA3;
    x = (A3-A2)*(T-273)/(TA3-273) + A2;
    P = 10.^(x);
end

if T >= TA3 && T <= 299;
    x = (A4-A3)*(T-TA3)/(299-TA3) + A3;
    P = 10.^(x);
end

if T > 299;
    disp('The temperature is too high.')
end

return

```

- **function-file**, with name: fun_methane.m

```

function [P] = fun_methane(T)

P = 0;

A1 = 0.232;
A2 = 0.401;
A3 = 1.295;
TA3 = 290.33;

if T < 261;
    disp('The temperature is too low.')
end

if T >= 261 && T < 273;
    x = (A2-A1)*(T-261)/(273-261) + A1;
    P = 10.^(x);
end

if T >= 273 && T <= 299;
    x = (A3-A2)*(T-273)/(TA3-273) + A2;
    P = 10.^(x);
end

if T > 299;
    disp('The temperature is too high.')
end

return

```

▪ **function-file**, with name: fun_mixEP_P.m

```
function [P] = fun_mixEP_P(T,sp_gr)

P = 0;

if sp_gr <= 1
    disp('Use the fun_PvsT program.')
    return
end

if sp_gr > 1.5
    disp('No hydrate formation.')
    return
end

ef = 3.145 - 2.066*sp_gr; %ethane fraction
T = (T-273.15)*1.8 + 32; %Convert Kelvin to Fahrenheit

Ae1 = 1.63; %log(P)_ethane P(psia) (turning point A1)
Ae2 = 1.838; %log(P)_ethane P(psia) (turning point A2)
TAe3 = 58.2; %T_ethane T(°F) (turning point TA3)

Ap1 = 1.178; %log(P)_propane P(psia) (turning point A1)
Ap2 = 1.4; %log(P)_propane P(psia) (turning point A2)
TAp3 = 42; %T_propane T(°F) (turning point TA3)

%For ethane - propane mixtures
A1 = Ae1*ef + Ap1*(1-ef);
A2 = Ae2*ef + Ap2*(1-ef);
TA3 = TAe3*ef + TAp3*(1-ef);
SL = 0.0327*ef + 0.0499*(1-ef); %slope

if T < 10;
    disp('The temperature is too low.')
end

if T >= 10 && T < 32;
    x = (A2-A1)*(T-10)/(32-10) + A1;
    P = 10.^(x);
end

if T >= 32 && T <= TA3;
    x = SL*(T-32) + A2;
    P = 10.^(x);
end

if T > TA3;
    disp('No hydrate formation at any pressure.')
end

P = P*0.0068947; %Convert psia to MPa

return
```

▪ **function-file**, with name: fun_mixEP_T.m

```
function [T] = fun_mixEP_T (P_des,sp_gr)

T = 0;

ef = 3.145 - 2.066*sp_gr; %ethane fraction

Ae1 = 1.63; %log(P)_ethane P(psia) (turning point A1)
Ae2 = 1.838; %log(P)_ethane P(psia) (turning point A2)
TAe3 = 58.2; %T_ethane T(°F) (turning point TA3)

Ap1 = 1.178; %log(P)_propane P(psia) (turning point A1)
Ap2 = 1.4; %log(P)_propane P(psia) (turning point A2)
TAp3 = 42; %T_propane T(°F) (turning point TA3)

%For ethane - propane mixtures
A1 = Ae1*ef + Ap1*(1-ef);
A2 = Ae2*ef + Ap2*(1-ef);
TA3 = TAe3*ef + TAp3*(1-ef);
SL = 0.0327*ef + 0.0404*(1-ef); %slope

T1 = 10;
T2 = TA3;

for it = 1:100;
    Tm = (T1 + T2)/2;
    Tm_K = (Tm-32)/1.8 + 273.15;
    [P] = fun_mixEP_P(Tm_K,sp_gr);
    if abs(P-P_des) <= 0.001;
        T = Tm_K;
        return
    end

    if P > P_des;
        T2 = Tm;
    else
        T1 = Tm;
    end

    if (T2 - T1) < 1
        Tm_K = (Tm-32)/1.8 + 273.15;
        T = Tm_K;
        return
    end
end
Tm_K = (Tm-32)/1.8 + 273.15;
T = Tm_K;
disp('Check if the answer is reasonable.')

return
```

▪ **function-file**, with name: fun_PvsT.m

```
function [P] = fun_PvsT (T,sp_gr)

P = 0;

if sp_gr < 0.55;
    disp('The specific gravity is too low. Hydrate formation graph area.')
end

if sp_gr == 0.55;
    [P_methane] = fun_methane(T);
    disp(['The hydrate formation pressure for specific gravity 0.55',...
        ' and temperature ',num2str(T),' K, is ',num2str(P_methane),' MPa.'])
end

if sp_gr < 0.6 && sp_gr > 0.55;
    [P_06] = fun_P(T,0.6);
    [P_meth] = fun_methane(T);
    P_interpolation = 10.^(log10(P_meth) + ((log10(P_06) - log10(P_meth))/0.05)*(sp_gr - 0.55));
    disp(['The hydrate formation pressure for specific gravity ',num2str(sp_gr),...
        ' and temperature ',num2str(T),' K, is between the values: ',...
        num2str(P_06),' MPa and ',num2str(P_meth),' MPa.'])
    disp(['The hydrate formation pressure with interpolation of the above values results: ',...
        num2str(P_interpolation),' MPa.'])
end

if sp_gr <= 1 && sp_gr >= 0.6;
    [P] = fun_P(T,sp_gr);
    disp(['The hydrate formation pressure for specific gravity ',num2str(sp_gr),...
        ' and temperature ',num2str(T),' K, is ',num2str(P),' MPa.'])
end

if sp_gr > 1 && sp_gr <= 1.5;
    [P_mixEP] = fun_mixEP_P(T,sp_gr);
    disp(['The hydrate formation pressure for specific gravity ',num2str(sp_gr),...
        ' and temperature ',num2str(T),' K, is ',num2str(P_mixEP),' MPa.'])
    T_F = (T-273.15)*1.8 + 32; %Convert Kelvin to Fahrenheit
    P_MPa = P_mixEP/0.0068947; %Convert MPa to psia
    disp(['OR'])
    disp(['The hydrate formation pressure for specific gravity ',num2str(sp_gr),...
        ' and temperature ',num2str(T_F),' °F, is ',num2str(P_MPa),' psia.'])
end

if sp_gr > 1.5;
    disp('The specific gravity is too high. No hydrate formation.')
end

return
```

▪ **function-file**, with name: fun_TvsP.m

```
function [T] = fun_TvsP (P_des,sp_gr)

T = 0;

if sp_gr < 0.55;
    disp('The specific gravity is too low. Hydrate formation graph area.')
end

if sp_gr == 0.55 ;
    T1 = 261;
    T2 = 299;
    for it = 1:100
        Tm = (T1 + T2)/2;
        [P] = fun_methane(Tm);
        if abs(P-P_des) <= 0.001;
            T = Tm;
            disp(['The hydrate formation temperature for methane',...
                ' at pressure ',num2str(P_des),' MPa, is ',num2str(Tm),' K.'])
            return
        end

        if P > P_des;
            T2 = Tm;
        else
            T1 = Tm;
        end

        if (T2 - T1) < 1
            T = Tm;
            disp(['The hydrate formation temperature for methane',...
                ' at pressure ',num2str(P_des),' MPa, is ',num2str(Tm),' K.'])
            return
        end
    end
end

if sp_gr < 0.6 && sp_gr > 0.55;

    T1 = 261;
    T2 = 299;
    for it = 1:100
        Tm = (T1 + T2)/2;
        [P] = fun_P(Tm,0.6);
        if abs(P-P_des) <= 0.001;
            T = Tm;
            disp(['The hydrate formation temperature for specific gravity 0.6',...
                ' and pressure ',num2str(P_des),' MPa, is ',num2str(Tm),' K.'])
            return
        end
        if P > P_des;
            T2 = Tm;
        else
            T1 = Tm;
        end
    end
end
```

```

        if (T2 - T1) < 1
            T = Tm;
            disp(['The hydrate formation temperature for specific gravity 0.6',...
                ' and pressure ', num2str(P_des), ' MPa, is ', num2str(Tm), ' K.'])
            return
        end
    end
end
T_06 = Tm;

T1 = 261;
T2 = 299;
for it = 1:100
    Tm = (T1 + T2)/2;
    [P] = fun_methane(Tm);
    if abs(P-P_des) <= 0.001;
        T = Tm;
        disp(['The hydrate formation temperature for methane',...
            ' at pressure ', num2str(P_des), ' MPa, is ', num2str(Tm), ' K.'])
        return
    end

    if P > P_des;
        T2 = Tm;
    else
        T1 = Tm;
    end

    if (T2 - T1) < 1
        T = Tm;
        disp(['The hydrate formation temperature for methane',...
            ' at pressure ', num2str(P_des), ' MPa, is ', num2str(Tm), ' K.'])
        return
    end
end
T_methane = Tm;

T_interpolation = T_methane + ((T_06 - T_methane)/0.05)*(sp_gr - 0.55);
T = T_interpolation;
disp(['The hydrate formation temperature for specific gravity ', num2str(sp_gr),...
    ' and pressure ', num2str(P_des), ' MPa, is between the above values.'])
disp(['The hydrate formation temperature with interpolation of the above values results: ',...
    num2str(T_interpolation), ' K.'])
end

if sp_gr <= 1 && sp_gr >= 0.6;
    T1 = 261;
    T2 = 299;
    for it = 1:100
        Tm = (T1 + T2)/2;
        [P] = fun_P(Tm, sp_gr);
        if abs(P-P_des) <= 0.001;
            T = Tm;
            disp(['The hydrate formation temperature for specific gravity ', num2str(sp_gr),...
                ' and pressure ', num2str(P_des), ' MPa, is ', num2str(Tm), ' K.'])
            return
        end
    end
end

```

```

    if P > P_des;
        T2 = Tm;
    else
        T1 = Tm;
    end
    if (T2 - T1) < 1
        T = Tm;
        disp(['The hydrate formation temperature for specific gravity ', num2str(sp_gr), ...
            ' and pressure ', num2str(P_des), ' MPa, is ', num2str(Tm), ' K.'])
        return
    end
end
end

if sp_gr > 1 && sp_gr <= 1.5;
    [T] = fun_mixEP_T (P_des, sp_gr);
    disp(['The hydrate formation temperature for specific gravity ', num2str(sp_gr), ...
        ' and pressure ', num2str(P_des), ' MPa, is ', num2str(T), ' K.'])
end

if sp_gr > 1.5;
    disp('The specific gravity is too high. No hydrate formation.')
end

return

```

- **function-file**, with name: fun_mixEP_graph.m

```

function [P] = fun_mixEP_graph(T, ef)

P = 0;

Ae1 = 1.63; %log(P)_ethane P(psia) (turning point A1)
Ae2 = 1.838; %log(P)_ethane P(psia) (turning point A2)
TAe3 = 58.2; %T_ethane T(°F) (turning point TA3)

Ap1 = 1.178; %log(P)_propane P(psia) (turning point A1)
Ap2 = 1.4; %log(P)_propane P(psia) (turning point A2)
TAp3 = 42; %T_propane T(°F) (turning point TA3)

%For ethane - propane mixtures
A1 = Ae1*ef + Ap1*(1-ef);
A2 = Ae2*ef + Ap2*(1-ef);
TA3 = TAe3*ef + TAp3*(1-ef);
SL = 0.0327*ef + 0.0499*(1-ef); %slope

if T >= 10 && T < 32;
    x = (A2-A1)*(T-10)/(32-10) + A1;
    P = 10.^(x);
end

if T >= 32 && T <= TA3;
    x = SL*(T-32) + A2;
    P = 10.^(x);
end

```

```

if T > TA3;
    P = 0;
end

return

```

▪ **m-file**, with name: GGM_graph.m

```

%The Gas Gravity Method - graphic representation
%First approximation of hydrate formation conditions

%BIBLIOGRAPHY
%Sloan E.D. & Koh C.A. (2008) Clathrate Hydrates of Natural Gases, 3rd ed.,
%CRC Press - Taylor and Francis Group, Boca Raton

clear all; clc;

Table = zeros(39,7);

for i = 1:39
    T = i + 260;
    Table(i,1) = T;
    for j = 1:5
        sp_gr = 0.1*j + 0.5;
        [P] = fun_P(T,sp_gr);
        Table(i,j+1) = P;
    end
    Table(i,7) = fun_methane(T);
end
Table

figure(1)
a = Table(:,1);
b = Table(:,2);
c = Table(:,3);
d = Table(:,4);
e = Table(:,5);
f = Table(:,6);
g = Table(:,7);
semilogy(a,g,'r',a,b,'k',a,c,'b',a,d,'m',a,e,'y',a,f,'g','linewidth',1.5)

ylim([0 50])
xlim([261 299])

title('Gas gravity chart for prediction of three-phase (L_w-H-V) pressure and temperature',...
    'FontName','Arial','FontWeight','bold','FontSize',10)
xlabel('Temperature T(K)', 'Fontname', 'arial','FontWeight','bold','FontSize',10)
ylabel('Pressure P(MPa)', 'Fontname', 'arial','FontWeight','bold','FontSize',10)
legend({'Methane, 0.55 Gas Gravity','0.6 Gas Gravity','0.7 Gas Gravity',...
    '0.8 Gas Gravity','0.9 Gas Gravity','1.0 Gas Gravity'}, 'Fontname','arial',...
    'FontWeight','bold','FontSize',10, 'Location','northwest')

```

- **m-file**, with name: `GGM_graph_mixEP.m`

```

%The Gas Gravity Method - graphic representation
%Conditions for Hydrate Formation for Light Gases

%BIBLIOGRAPHY
%Gas Processors Suppliers Association - GPSA (2004) Engineering Data Book,
%12th ed., FPS version, I & II volumes, 1-26 sections,
%Gas Processors Suppliers Association, Oklahoma

clear all; clc;

Table = zeros(71,4);

for i = 1:71
    T = i-1;
    Table(i,1) = T;
    Table(i,2) = fun_mixEP_graph(T,1); %Ethane curve
    Table(i,3) = fun_mixEP_graph(T,0.7); % 70% ethane and 30% propane mix curve
    Table(i,4) = fun_mixEP_graph(T,0); %Propane curve
end
Table

figure(1)
a = Table(:,1);
b = Table(:,2);
c = Table(:,3);
d = Table(:,4);

semilogy(a,b,'g','linewidth',1.5)
hold on
semilogy(a,c,'Color',[0.4940 0.1840 0.5560],'linewidth',1.5)
semilogy(a,d,'Color',[0.6350, 0.0780, 0.1840],'linewidth',1.5)
hold off

grid on
set(gca, 'gridlinestyle','-')

xlim([0 70])
ylim([10 1000])

title('Conditions for hydrate formation for light gases',...
      'FontName','Arial','FontWeight','bold','FontSize',10)
xlabel('Temperature T(°F)', 'Fontname', 'arial','FontWeight','bold','FontSize',10)
ylabel('Pressure P(psia)','Fontname', 'arial','FontWeight','bold','FontSize',10)
legend({'Ethane, 1.0 Gas Gravity','70% ethane and 30% propane mix, 1.18 Gas Gravity',...
      'Propane, 1.5 Gas Gravity'},...
      'Fontname', 'arial','FontWeight','bold','FontSize',10,'Location','northwest')

```

6.2. MATLAB Code - The Distribution Coefficient Method (The K-factor Method)

As described in the chapter 2.1.3, the iterative method used in order to solve the non-linear Sloan's equation (2.30) is based on the Newton-Raphson method. It is a root-finding method based on the expansion of a non-linear function in Taylor series and truncating to keep only linear terms. Two calculation types were utilized. In the first, gas composition and operating temperature are taken into account to give the hydrate formation pressure and in the second, the gas composition and operating pressure are taken into account to give the hydrate formation temperature.

- **function-file**, with name: fun_K.m

```
function [sum_x] = fun_K(y,T,P)

%BIBLIOGRAPHY
%Sloan E.D. & Koh C.A. (2008) Clathrate Hydrates of Natural Gases, 3rd ed.,
%CRC Press - Taylor and Francis Group, Boca Raton

%Table B (18,8): It gives the parameters of the equation for each component
%Each column is a component (8 in total) and each line is a parameter (18 in total)
%Components: CH4, C2H6, C3H8, i-C4H10, n-C4H10, N2, CO2, H2S

B = [1.63636 0 0 31.6621 -49.3534 -5.31e-06 0 0 0.128525 -0.78338 0 0 0 -5.3569 0 -2.3e-07 -2.0e-08 0;...
6.41934 0 0 -290.283 2629.1 0 0 -9.0e-08 0.129759 -1.19703 -84600 -71.0352 0.596404 -4.7437 78200 0 0 0;...
-7.8499 0 0 47.056 0 -1.17e-06 0.0007145 0 0 0.12348 16690 0 0.23319 0 -44800 5.5e-06 0 0;...
-2.17137 0 0 0 0 0.001251 1.0e-08 0.166097 -2.75945 0 0 0 -884 0 -5.4e-07 -1.0e-08;...
-37.211 0.86564 0 732.2 0 0 0 9.37e-06 -1.07657 0 0 -66.221 0 0 917000 0 4.98e-06 -1.26e-06;...
1.78857 0 -0.001356 -6.187 0 0 0 2.5e-07 0 0 0 0 587000 0 1.0e-08 1.1e-07;...
9.0242 0 0 -207.033 0 4.66e-05 -0.006992 -2.89e-06 -0.006223 0 0 0 0.27098 0 0 8.82e-05 2.55e-06 0;...
-4.7071 0.06192 0 82.627 0 -7.39e-06 0 0 0.240869 -0.64405 0 0 0 -12.704 0 -1.30e-06 0 0].';

%Table A(8,18): Each column is a parameter and each line is a component
A = transpose(B);

%temperature T(°F) and pressure P(psia)
for i = 1:7
K_i(i) = exp(A(i,1)+ (A(i,2)*T) + (A(i,3)*P) + (A(i,4)/T) + (A(i,5)/P) +...
(A(i,6)*P*T) + (A(i,7)*T^2) + (A(i,8)*P^2) + (A(i,9)*(P/T)) +...
(A(i,10)*(log(P/T))) + (A(i,11)/(P^2)) + (A(i,12)*(T/P)) +...
(A(i,13)*(T^2/P)) + (A(i,14)*(P/T^2)) + (A(i,15)*(T/P^3)) +...
(A(i,16)*T^3) + (A(i,17)*(P^3/T^2)) + (A(i,18)*T^4));
K_i_all(i,:) = K_i(i);

x(i) = y(i,1)/K_i_all(i,1);
x_all(i,1) = x(i);
end

K_i_all;
x_all;
sum_x = sum(x_all);

return
```

▪ **function-file**, with name: fun_P.m

```
function [P] = fun_P(y,T,P)

dP = 0.0001;
itmax = 100;
tol = 0.00001;

for k = 1:itmax;
[sum_x] = fun_K(y,T,P);
    if abs(sum_x - 1) <= tol;
        disp(['Method has converged after ', num2str(k), ' iterations.'])
        disp(['The hydrate formation pressure is ', num2str(P), ' psia.'])
        P_MPa = P*0.006894757; %Conversion psia to MPa
        P_kg_cm_2 = P*0.070306958; %Conversion psia to kg/cm^2
        disp(['OR'])
        disp(['The hydrate formation pressure is ',...
            num2str(P_MPa), ' MPa OR ', num2str(P_kg_cm_2), ' kg/cm^2.'])
        return
    else
        P = P + dP;
        [sum_x1] = fun_K(y,T,P);
        dx_dP = (sum_x1 - sum_x)/dP;
        P = P - dP + (1 - sum_x)/dx_dP;
        if P < 0
            disp('Method did not converge. Try another pressure.')
            return
        end
    end
end
disp('Method did not converge. Try another pressure.')

return
```

▪ **function-file**, with name: fun_T.m

```
function [T] = fun_T(y,T,P)

dT = 0.0001;
itmax = 100;
tol = 0.0000001;

for k = 1:itmax;
[sum_x] = fun_K(y,T,P);
    if abs(sum_x - 1) <= tol;
        disp(['Method has converged after ', num2str(k), ' iterations.'])
        disp(['The hydrate formation temperature is ', num2str(T), ' °F.'])
        disp(['OR'])
        T_K = (T-32)/1.8 +273.15; %Conversion °F to K
        T_C = (T-32)/1.8; %Conversion °F to °C
        disp(['The hydrate formation temperature is ',...
            num2str(T_K), ' K OR ', num2str(T_C), ' °C.'])
        return
    else
        T = T + dT;
```

```

        [sum_x1] = fun_K(y,T,P);
        dx_dT = (sum_x1 - sum_x)/dT;
        T = T - dT + (1 - sum_x)/dx_dT;
        if T < 0
            disp('Method did not converge. Try another temperature.')
            return
        end
    end
end
disp('Method did not converge. Try another temperature.')

return

```

- **m-file**, with name: K_Factor_Method_Phydrate.m

```

clear all; clc;

%BIBLIOGRAPHY
%Sloan E.D. & Koh C.A. (2008) Clathrate Hydrates of Natural Gases, 3rd ed.,
%CRC Press - Taylor and Francis Group, Boca Raton

%Import Data:
%Components y-table(1,8): [CH4, C2H6, C3H8, i-C4H10, n-C4H10, N2, CO2, H2S]
y = [0.784 0.060 0.036 0.005 0.019 0.094 0.002 0].';

%Import Data:
%Temperature Operation
T = 50.94; %°F
%Assumptions:
P_assum = 306.0; %psia

%Hydrate Formation Pressure
[P] = fun_P(y,T,P_assum);

```

- **m-file**, with name: K_Factor_Method_Thydrate.m

```

clear all; clc;

%BIBLIOGRAPHY
%Sloan E.D. & Koh C.A. (2008) Clathrate Hydrates of Natural Gases, 3rd ed.,
%CRC Press - Taylor and Francis Group, Boca Raton

%Import Data:
%Components y-table(1,8): [CH4, C2H6, C3H8, i-C4H10, n-C4H10, N2, CO2, H2S]
y = [0.784 0.060 0.036 0.005 0.019 0.094 0.002 0].';

%Import Data:
%Pressure Operation
P = 306; %psia
%Assumptions:
T_assum = 50; %°F

% Hydrate Formation Temperature
[T] = fun_T(y,T_assum,P);

```